GIARLÃ CUNHA DA SILVA

MOBILOME-ASSOCIATED RESISTOME IN THE Pasteurellaceae FAMILY AND CHARACTERIZATION OF SMALL RNAS TRANSPORTED BY EXTRACELLULAR VESICLES PRODUCED BY *Actinobacillus pleuropneumoniae*

Thesis submitted to the Agricultural Microbiology's Graduate Program of the Universidade Federal de Viçosa in partial fulfillment of the requirements for the degree of *Doctor Scientiae*.

Adviser: Denise Mara Soares Bazzolli

Co-advisers: Hilário Cuquetto Mantovani
Tiago Antônio de Oliveira Mendes

VIÇOSA - MINAS GERAIS
2022

Ficha catalográfica elaborada pela Biblioteca Central da Universidade Federal de Viçosa - Campus Viçosa

T
S586m
2022

Silva, Giarlã Cunha da, 1993-
Mobilome-associated resistome in the Pasteurellaceae family and characterization of small RNAs transported by extracellular vesicles produced by *Actinobacillus pleuropneumoniae* / Giarlã Cunha da Silva. – Viçosa, MG, 2022.
1 tese eletrônica (143 f.): il. (algumas color.).

Texto em inglês.
Orientador: Denise Mara Soares Bazzolli.
Tese (doutorado) - Universidade Federal de Viçosa, Departamento de Microbiologia, 2022.
Inclui bibliografia.
DOI: https://doi.org/10.47328/ufvbbt.2022.335
Modo de acesso: World Wide Web.

1. Suíno - Doenças. 2. Pleuropneumonia. 3. Marcadores genéticos. 4. DNA. 5. RNA. 6. *Pasteurellaceae*. 7. *Actinobacillus pleuropneumoniae*. I. Bazzolli, Denise Mara Soares, 1974-. II. Universidade Federal de Viçosa. Departamento de Microbiologia. Programa de Pós-Graduação em Microbiologia Agrícola. III. Título.

CDD 22. ed. 636.4089692

Bibliotecário(a) responsável: Euzebio Luiz Pinto CRB 6/3317

GIARLÃ CUNHA DA SILVA

MOBILOME-ASSOCIATED RESISTOME IN THE Pasteurellaceae FAMILY AND CHARACTERIZATION OF SMALL RNAS TRANSPORTED BY EXTRACELLULAR VESICLES PRODUCED BY *Actinobacillus pleuropneumoniae*

Thesis submitted to the Agricultural Microbiology's Graduate Program of the Universidade Federal de Viçosa in partial fulfillment of the requirements for the degree of *Doctor Scientiae*.

APPROVED: April 29, 2022.

Assent:

Giarlã C. da Silva

Giarlã Cunha da Silva
Author

Denise Mara Soares Bazzolli
Adviser

ACKNOWLEDGEMENTS

Primeiramente eu agradeço a minha família por toda a força, incentivo, paciência, e por sempre acreditar em mim e estar presente em todos os momentos. Jamais teria chegado tão longe sem o apoio incondicional de todos eles.

À professora Denise por todos esses anos de orientação. Sempre serei grato pela oportunidade, por todos os ensinamentos e toda sua preocupação comigo, não só profissionalmente como pessoalmente.

À equipe da Imperial College London, Paul, Janine, e Yanwen por toda ajuda, pela parceria e pelos ensinamentos durante esses anos.

O presente trabalho foi realizado com apoio da Coordenação de Aperfeiçoamento de Pessoal de Nível Superior – Brasil (CAPES) – Código de Financiamento 001.

Ao Conselho Nacional de Desenvolvimento Científico e Tecnológico (CNPq), pela concessão da bolsa de estudos.

À Fundação de Amparo à Pesquisa do Estado de Minas Gerais (FAPEMIG), pela concessão da bolsa de estudos.

Ao Biotechnology and Biological Sciences Research Council (BBSRC) por todo o suporte financeiro que me permitiu o desenvolvimento deste trabalho.

À Universidade Federal de Viçosa, ao Departamento de Microbiologia e ao programa de pós-graduação em Microbiologia Agrícola por todo o suporte durante esses anos.

Aos professores do Departamento de Microbiologia que em algum momento da minha trajetória me ajudaram de alguma forma.

Aos funcionários do Departamento de Microbiologia e do Bioagro, por terem sido tão solícitos sempre que precisei.

Agradeço ao NEMA por toda a experiência, pelos ótimos momentos em equipe, aprendi muito trabalhando neste grupo.

E finalmente, gostaria agradecer aos meus amigos. Desde o início da minha jornada no LGMB, lá em 2013, tive a felicidade de poder contar com diversas pessoas que me ensinaram tanto e me deram a base pra crescer e chegar até aqui. Durante esses mais de oito anos, tive a honra de conhecer muitas pessoas e aprender um pouquinho com cada uma delas. Não agradeço somente aos meus amigos de trabalho, mas também a todos os outros fora do meio acadêmico, que por mais que

não compartilhassem da mesma vivência que eu, sempre foram muito especiais em minha vida. É muito difícil dizer o quanto todos representam para mim. Por várias vezes em que me ajudaram, dentro e fora do laboratório. Pelas palavras e gestos gentis, pelo carinho, paciência, compreensão e pela troca de conhecimento. Vocês são, para mim, uma das maiores conquistas. É uma honra e um orgulho poder dizer que tenho amigos tão incríveis.

Eu aprendi muito com a Graduação e a Pós-graduação, porém nem sempre da maneira mais fácil. Foram muitos percalços, escolhas difíceis, contratempos e frustrações. Mas foram muitos momentos incríveis, muitas conquistas, além do crescimento pessoal e profissional. O caminho percorrido para chegar até aqui não é fácil para ninguém, mas poder dividir isso com as pessoas próximas tornou tudo mais possível. E hoje, posso dizer com toda certeza, jamais teria conseguido sozinho.

A todos vocês, muito obrigado!

ABSTRACT

DA SILVA, Giarlã Cunha, D.Sc., Universidade Federal de Viçosa, April, 2022. **Mobilome-associated resistome in the Pasteurellaceae family and characterization of small RNAs transported by extracellular vesicles produced by *Actinobacillus pleuropneumoniae***. Adviser: Denise Mara Soares Bazzolli. Co-advisers: Hilario Cuquetto Mantovani and Tiago Antônio de Oliveira Mendes.

The Pasteurellaceae family comprises several species of Gram-negative, commensal or pathogenic bacteria of human and animal hosts. Some members of the Pasteurellaceae family are responsible for causing diseases of economic impact in food-producing animals, such as swine. In this sector, significant expenses are associated with the use of antimicrobials for the treatment of infections caused by species of the Pasteurellaceae family, which are often persistent and multidrug-resistant. *Actinobacillus pleuropneumoniae* (App) is a member of the Pasteurellaceae family and causes porcine pleuropneumonia, responsible for important economic losses in pig farming worldwide. *A. pleuropneumoniae* is a primary pathogen and has several virulence factors such as: capsule, LPS, iron siderophores and Apx exotoxins. In addition, they are capable of producing extracellular vesicles (BEVs – Bacterial Extracellular Vesicles), which represents another associated virulence factor, given the involvement in the dissemination of mobile genetic elements (MGEs) and antimicrobial resistance genes (AMR) and innovative abilities that leverage the virulence of App. Thus, the objectives of this work were: *i*. to evaluate the representativeness of MGEs associated with AMR in members of the Pasteurellaceae family, including App and *ii*. characterize the BEVs produced by App and their nucleic acid content, focusing on RNA and virulence. The investigation of the resistome associated with the mobilome in Pasteurellaceae was carried out from *in silico* analysis using complete genomes available in databases in order to identify and characterize MGEs with emphasis on the presence of resistance genes associated with these elements. Through these analyzes, 20 novel integrative and conjugative elements (ICEs) and 23 novel prophages were found, in addition to expanding the characterization of elements previously described for the family. From the results obtained, it was found that MGEs are responsible for carrying most of the resistance genes identified in bacteria of the Pasteurellaceae family, and can be disseminated by different mechanisms of horizontal gene transfer (HGT), such as vesiduction (via BEVs). Thus, in the second

part of the work, the BEVs of App were obtained, characterized and the DNA and RNA content investigated under different conditions. Vesicles were investigated for size, protein and lipid content, including LPS type, and nucleic acid content. The characterization of the BEVs revealed a protein profile similar to that found in the outer membrane of App, highlighting the lipid profile, not investigated so far for this specie. The results revealed that the condition of anaerobic growth affects several aspects of BEV production, such as quantity and relative size. The BEVs carry as nucleic acid content, DNA and RNA, the latter being the most abundant and therefore characterized in this work. Transcriptome analysis of the BEVs produced by App revealed that these vesicles carry several types of RNAs, such as tRNAs and small (sRNAs), the latter of which have already been described for App. In this work, 13 new sRNAs for App were described, 12 of which are present in BEVs. Some sRNAs found in BEVs are enriched in vesicles in relation to cells and are present in the intravesicular portion, protected from the action of nucleases. Among the sRNAs found in the BEVs of App, Rna01, previously identified by our group, was selected for further analysis. Target analysis of this sRNA revealed that it is associated with the regulation of several genes encoding membrane proteins, mainly in response to stress conditions, which was confirmed through quantitative expression analyses. Through analyzes carried out with mutant strains for Rna01, it was observed that the production of BEVs was also affected, revealing the participation of this sRNA in this process in App. This work provides a complete characterization of MGEs and AMR in the Pasteurellaceae family and is also the first work to perform a complete characterization of BEVs produced by App under different conditions, in addition to confirming the presence and functionality of sRNAs in BEVs produced by App. Thus, several unpublished information and guidelines for actions aimed at controlling porcine pleuropneumonia.

Keywords: Pasteurellaceae. *Actinobacillus pleuropneumoniae*. Pleuropneumonia. Mobile genetic elements. Antimicrobial resistance. Bacterial extracellular vesicles. Nucleic acids. small RNAs.

RESUMO

DA SILVA, Giarlã Cunha, D.Sc., Universidade Federal de Viçosa, abril de 2022. **Resistoma associado ao mobiloma na família Pasteurellaceae e caracterização de RNAs pequenos transportados por vesículas extracelulares produzidas por *Actinobacillus pleuropneumoniae***. Orientadora: Denise Mara Soares Bazzolli. Coorientadores: Hilario Cuquetto Mantovani e Tiago Antônio de Oliveira Mendes.

A família Pasteurellaceae compreende diversas espécies de bactérias Gram-negativas, comensais ou patogênicas de hospedeiros humanos e animais. Alguns membros da família Pasteurellaceae são responsáveis por causar doenças de impacto econômico em animais de produção, como suínos. Neste setor, gasto expressivos estão associados ao uso de antimicrobianos para o tratamento de infecções causadas por espécies da família Pasteurellaceae, muitas vezes persistentes e multirresistentes a drogas. *Actinobacillus pleuropneumoniae* (App) é um membro da família Pasteurellaceae e causa a pleuropneumonia suína, responsável por prejuízos econômicos importantes na suinocultura em escala global. *A. pleuropneumoniae* é um patógeno primário e apresenta diversos fatores de virulência como: cápsula, LPS, sideróforos para ferro e exotoxinas Apx. Além disso, são capazes de produzir vesículas extracelulares (BEVs – Bacterial Extracellular Vesicles), o que representa mais um fator de virulência associado, visto o envolvimento na disseminação de elementos genéticos móveis (EGMs) e genes de resistência a antimicrobianos (AMR) e habilidades inovadoras que potencializam a virulência de App. Assim, os objetivos deste trabalho foram: *i*. avaliar a representatividade de EGMs associados com AMR em membros da família Pasteurellaceae, incluindo App e *ii*. caracterizar as BEVs produzidas por App e seu conteúdo de ácidos nucleicos, com foco em RNA e virulência. A investigação do resistoma associado ao mobiloma em Pasteurellaceae foi realizada a partir de análises *in silico* utilizando genomas completos disponíveis em bancos de dados com o intuito de identificar e caracterizar EGMs com ênfase na presença de genes de resistência associados a esses elementos. Através dessas análises foram encontrados 20 novos elementos integrativos e conjugativos (ICEs) e 23 novos profagos, além de ampliação da caracterização de elementos previamente descritos para a família. A partir dos resultados obtidos foi constatado que EGMs são responsáveis por carrear a maioria dos genes de resistência identificados nas

bactérias da família Pasteurellaceae, podendo serem disseminados por diferentes mecanismos de transferência horizontal de genes (THG), como a vesidução (via BEVs). Assim, na segunda parte do trabalho, as BEVs de App foram obtidas, caracterizadas e o conteúdo de DNA e RNA investigado em diferentes de condições. As vesículas foram investigadas quanto ao tamanho, conteúdo proteico e lipídico, incluindo tipo de LPS, e conteúdo de ácidos nucleicos. A caracterização das BEVs revelou um perfil de proteínas semelhante ao encontrado na membrana externa de App, destacando o perfil dos lipídeos, não abordado até então para essa espécie. Os resultados revelaram que a condição de crescimento em anaerobiose afeta diversos aspectos da produção das BEVs, como quantidade e tamanho relativo. As BEVs apresentam como conteúdo de ácidos nucleicos, DNA e RNA, sendo o último mais abundante e por isso caracterizado neste trabalho. Análises de transcriptoma das BEVs produzidas por App revelou que essas vesículas transportam diversos tipos de RNAs, como tRNAs e small RNAs (sRNAs), sendo os últimos já descritos para App. Neste trabalho foram descritos 13 novos sRNAs para App, sendo 12 deles presentes em BEVs. Alguns sRNAs encontrados nas BEVs estão enriquecidos nas vesículas em relação às células e estão presentes na porção intravesicular, protegido da ação de nucleases. Dentre os sRNAs encontrados nas BEVs de App, o Rna01, previamente identificado por nosso grupo, foi selecionado para análises posteriores. Análises de alvos desse sRNA revelaram que ele está associado com a regulação de diversos genes que codificam proteínas de membrana, principalmente em resposta a condições de estresse, que foi confirmado através de análises de expressão quantitativa. Através de análises desenvolvidas com linhagens mutantes para Rna01, foi observado que a produção de BEVs também foi afetada, revelando a participação desse sRNA nesse processo em App. Esse trabalho traz uma completa caracterização de EGMs e AMR na família Pasteurellaceae e é também o primeiro trabalho a realizar uma caracterização completa das BEVs produzidas por App em diferentes condições, além de confirmar a presença e a funcionalidade de sRNAs em BEVs produzidas por App. Assim, várias informações inéditas e norteadoras de ações que visam o controle da pleuropneumonia suína.

Palavras-chave: Pasteurellaceae. *Actinobacillus pleuropneumoniae*. Pleuropneumonia. Elementos genéticos móveis. Resistência antimicrobiana. Vesículas extracelulares bacterianas. Ácidos nucleicos. RNAs pequenos.

SUMMARY

GENERAL INTRODUCTION

Pork is one of the most consumed meats worldwide, appearing in second place, behind only the consumption of poultry consumption (OECD 2022). The Covid-19 pandemic affected the growth of pig farming in many countries, most in the year 2020, however, world production has been recovering (USDA, 2022). Besides that, Brazil kept growing even during the COVID-19 pandemic and maintained the position as the fourth largest producer and exporter of pork in the world. Nationally, the state of Minas Gerais is considered the fourth largest producer of pork (ABPA, 2022).

In this sector, bacterial pathogens of the Pasteurellaceae family are considered important and have an economic impact on pork productivity (Bethe et al., 2009; Christensen et al., 2014; Sassu et al., 2018; Costa-Hurtado et al., 2020). Thus, studies involving swine pathogens with current approaches represent gain of information for the development of new therapeutic approaches based on the study of the population of the pathogens and on the genetic information that they carry on, in addition to the factors that they can produce and disperse, such as BEVs and resistance genes, respectively.

Pasteurellaceae are Gram-negative bacteria and is composed of commensals and pathogens from human and animal, such as *Haemophilus influenzae*, *Aggregatibacter actinomycetemcomitans*, *Mannheimia haemolytica*, *Glaesserella parasuis*, *Pasteurella multocida, Actinobacillus pleuropneumoniae* and others (Michael et al., 2018). These bacteria are part of the normal microbiota of several animals and humans (Christensen et al., 2014). In general, Pasteurellaceae is recognized for comprise species that cause a number of economically important diseases in food-producing animals, as pig (Michael et al., 2018).

Porcine pleuropneumonia (PPS) is one of the most important respiratory diseases in pig farming, it presents a contagious disease causing economic losses in several producing countries (Gottschalk, 2012; Helke et al., 2015). The PPS´s agent causative is the bacterium *Actinobacillus pleuropneumoniae* (named here as App).

Actinobacillus pleuropneumoniae is a Gram-negative, facultative anaerobic and encapsulated coccobacillus (Pattison et al., 1957). Different App isolates can be grouped into two biotypes, according to the NAD (nicotinamide adenine dinucleotide) requirement, NAD dependent as Biotype 1 and NAD independent as biotype 2 (Niven & Lévesque, 1988). Currently, there are nineteen serotypes of this specie described,

which are defined according to the organization of the genes involved in the production of the capsule and, consequently, with the antigenic properties of the capsule polysaccharides (Stringer et al., 2021). Of these serotypes, the serotype 8 is the most widespread in the state of Minas Gerais as well as in United Kingdom (Rossi et al., 2013; Sassu et al., 2018). All App serotypes are capable of causing disease, although some are more virulent than others (Frey, 2011). The virulence of *A. pleuropneumoniae* is multifaceted and involves several factors such as: capsule polysaccharides, lipopolysaccharide layer (LPS), transferrin-binding proteins (siderophores), Apx exotoxins (RTX family - Repeats-in-toxin) such as ApxI, ApxII and ApxIII, in addition to the production of extracellular vesicles (BEVs) (Negrete-Abascal et al., 2000; Bossé et al., 2002; Chiers et al., 2010; Frey, 2011).

Antimicrobial resistance (AMR), corresponds to a huge global threat to health and food safety, which is commonly associate to the misuse of antimicrobials in humans and animals (Ventola, 2015). The acquisition of AMR by bacteria is commonly associated with genes carried on mobile genetic elements (MGEs), that can lead to the establishment of multidrug resistance (MDR) strains (Nikaido, 2009). The collection of all AMR genes is known as the resistome (Wright, 2007) and the entire set of MGEs in a genome defines the mobilome (Siefert, 2009).

MGEs correspond to an essential weapon in microbial ecology because of their capacity to transfer genes with different roles throughout microbial populations (Rankin et al., 2011). MGEs includes Insertion sequences (IS) and transposons (Tn), plasmids, integrative and conjugative elements (ICEs) and prophages (Partridge et al., 2018). MGEs can be spread among bacteria by different mechanisms of horizontal gene transfer (HGT), i.e., conjugation, mobilization, transduction, transformation, and vesiduction (Ramsay & Firth, 2017; Soler & Forterre, 2020). The introduction of foreign sequences into novel genomic locations can alter phenotypes and lead to bacterial evolution (Frost et al., 2005; Carr et al., 2021).

Studies focused on microbial resistance in food food-producing animals revealed a great increase in the identification of resistant strains in animals worldwide, with a great increase in the number of publications in the last 20 years (Torres et al., 2021). The transmission of antimicrobial resistance based on AMR transported by MGEs among bacteria by HGT may represent a considerable public health threat (Vidovic & Vidovic, 2020). This transmission of AMR genes by MGEs, which can often happen among different ecosystems and increasing concern about the dissemination

of resistant pathogens, is directly related to the One Health concept (Hernando-Amado et al., 2019).

The dissemination of AMR genes via MGEs can be interpreted as an ability of bacterial species to stand out in a microbial community, favoring colonization in the host (Bottery et al., 2021). The repertoire of AMR genes, and in some cases, MDR found in the Pasteurellaceae, mediates resistance to important antimicrobials for human and animal treatments (aminoglycosides, beta-lactams, phenicols, sulfonamides, tetracyclines, and lincosamides) (Archambault et al., 2011; OIE, 2017; Michael et al., 2018; Woolums et al., 2018; WHO, 2019; Van Driessche et al., 2020).

Addressing the problematic of AMR genes associated to MGEs in Pasteurellaceae, some studies have been reported that Integrative Conjugative Elements (ICEs) and plasmids are responsible for carrying AMR and providing antimicrobial resistance for diverse pathogens in the family (Michael et al., 2018). However, most studies are focused on understanding the epidemiology of MDR strains rather than mechanisms of dissemination of the AMR genes by MGEs. Thus, leaving a gap on this information in Pasteurellaceae.

The use of antimicrobials is a common practice in livestock, for both growth promotion and treatment of infections (Boeckel et al 2015). Despite suitable management attempts, when this is done, including biosecurity, the use of antimicrobial agents to control infections caused by pathogenic Pasteurellaceae continues to be widely used (Michael et al., 2018). However, the emergence of multidrug-resistant bacteria increasingly makes the use of antimicrobials problematic (Freire-Moran et al., 2011). Based on this concern, efforts on studies focusing on AMR surveillance are of high importance not only for Pasteurellaceae, allowing the elaboration of better landscape of situation and map possible strategies for antimicrobial use in bacteria.

Bacterial extracellular vesicles (BEVs) correspond to a process for molecules transport by bacteria. Although the first report of BEVs have been in 60's years (Knox et al., 1966), most knowledge regarding these vesicles have available in recently years. BEVs production is documented in the three domains of life and that has aroused a lot of interest today (Deatherage and Cookson 2012; Gill et al., 2019).

Although the BEVs have great biological importance, so far there is no consensus on the mechanism of biogenesis of these vesicles. After several genetic analysis and biochemical factors, some mechanisms have been proposed for different

bacteria. Three models proposed that lipoproteins, LPS and peptidoglycan may be involved with BEVs production. The first model propose that the vesicles are produced by reduction of the lipoprotein quantity attached to the peptidoglycan. The second model propose that the vesicles are produced in response to an accumulation of peptidoglycan during the synthesis of peptidoglycan layer. The third model suggests that negatively charged LPS in the membrane causes the vesicles production during growth (Jan, 2017; Avila-Calderón et al., 2021). However, although tons of studies with mutant strains for diverse genes show some effect and a possibility of involvement with the process of vesicles production, a consensus for this process seems to be far from being full elucidated.

In general, BEVs show a circular structure, with a size ranging between 20-400 nm, an important factor that allows the cell to go beyond the wall limits to an unreachable place by the vesicles (Toyofuku et al., 2019). Moreover, BEVs shows a miscellaneous composition, mostly constituted of lipopolysaccharides and proteins, also carrying toxins, nucleic acids, and other molecules (Gill et al., 2019).

The BEVs may be constituted by phospholipids, outer membrane, inner membrane, cytoplasmic and periplasmic proteins and lipopolysaccharides or lipooligosaccharides (Roier et al., 2015). In addition, BEVs may also contain DNA, RNA, ions, metabolites, and signaling molecules (Pathirana & Kaparakis-Liaskos, 2016; Roier et al., 2015).

The studies developed so far have shown a plethora of functions assigned to BEVs, including cell to cell communication; as a new mechanism for gene horizontal transfer (vesiduction); predatory mechanism, biofilm formation; stress response; antimicrobial resistance and delivery of toxins, hydrolytic enzymes and secondary metabolites (Schwechheimer & Kuehn, 2015; Gill et al., 2019; Soler & Forterre, 2020). However, much remains to be elucidated, mostly regarding its content in contribution to microbial communities and host-pathogen interaction. Beyond functions, due to its composition and ability to generate an immune response, efforts have been done to use BEVs as platform for vaccine development (Micoli & MacLennan, 2020) as vaccine already done for *Neisseria meningitidis* serogroup B (Sierra et al., 1991) and in progress for other species (Micoli & MacLennan, 2020).

Previous reports already show the importance of the BEVs regarding diverse aspects of cell physiology and vaccine candidate to the Pasteurellaceae family, as seen for *Haemophilus influenzae*, *Pasteurella multocida*, *Mannheimia haemolytica*,

Avibacterium paragallinarum, *Galibacterium anatis* and *Aggregatibacter actinomycetemcomitans* (Roier et al., 2013, 2015; Pors et al., 2016; Choi et al., 2017; Mei et al., 2020).

The studies of BEVs developed with *A. pleuropneumoniae* are most focused on proteins characterization and mutant strains for vaccine development (Antenucci et al., 2017, 2018, 2019). However, attempts made so far have not been successful. Although studies of sRNAs had been done for this specie (Rossi et al., 2016; Su et al., 2016), there is no information of sRNAs and BEVs.

Regarding on sRNA cargo and transport by BEVs, previous reports had already shown the transport of this molecule by BEVs and interaction with host-cells (Badi et al., 2020; Lécrivain & Beckmann, 2020). Much is already known about sRNA contribution to bacterial fitness in response to different physiological and environmental conditions by distinct mechanisms of regulation (Gripenland et al., 2010; Michaux et al., 2014; Westermann et al., 2016; Hör et al., 2020).

Nevertheless, its interaction with host cells mediated by extracellular vesicles is poorly understood. Reports to BEV-derived sRNAs have already been made for some species as *Escherichia coli, Vibrio cholerae, Streptococcus mutans, Pseudomonas aeruginosa, Aggregatibacter actinomycetemcomitans, Porphyromonas gingivalis, Treponema denticola, Salmonella enterica* serovar Typhimurium and others (Badi et al., 2020; Lécrivain & Beckmann, 2020). Noteworthy, a sRNA carried by BEVs for *P. aeruginosa* showed important role in regulation of immune response of human airway cells (Koeppen et al., 2016). Cases of enrichment sRNAs sequences in vesicles cargo had already been reported, as described to Group A *Streptococcus* BEVs in comparison to the cell (Ulrike et al., 2016). Moreover, the sorting mechanism of sRNAs package in BEVs and how it can participate in the interaction with host cells remains to be elucidated.

The sRNAs represent an important class of post-transcriptional regulators of gene expression which are around 50-200 nucleotide in length (Choi et al., 2017). sRNAs are present in all domains of life and are considered an important class of gene expression regulators. The post-transcriptional control performed by sRNAs represents an important mechanism for regulating gene expression in bacteria (Wagner & Romby, 2015). The mechanism of action by which most sRNAs exert their function is through base pairing with their target messenger RNA (mRNA), which can

affect the translation, stability and/or processing of this target (Storz et al., 2011; Wagner & Romby, 2015).

Small regulatory RNAs are generally classified into four classes: RNAs modulating of protein activity, *cis-acting* sRNAs, *trans-acting* sRNAs, and CRISPRs (Storz et al., 2011). *trans-acting* sRNAs are distributed in bacterial genomes and encoded in different regions of the targets, showing partial complementarity to their target (Melamed et al., 2016). As a result of this characteristic, a single *trans-acting* sRNAs has a wide repertoire of targets (Villa et al., 2018). The trans-acting sRNAs are commonly transcribed from intergenic regions, however some sRNAs are prevenient from the 3' untranslated region of the gene (3' UTR). These sRNAs may be expressed by its specific promoter, which is inside the 3' UTR of the gene, or the sRNA may product of the mRNA processing (Miyakoshi et al., 2015).

The interaction of these sRNAs with the targets may be mediated by RNA chaperones, such as the Hfq protein (Sledjeski et al., 2001).Small RNAs have several functions that involve regulation of cell growth, adaptation to stress conditions, regulation of metabolism (Wagner & Romby, 2015). In addition, they play an important role in the pathogenicity of different microorganisms (Gong et al., 2011; Koo et al., 2011; Westermann et al., 2016).

The Hfq protein was discovered in the mid-1960 in a study analyzing proteins required for replication of Q-beta bacteriophage in *Escherichia coli*. The Hfq protein shows a hexameric structure (Franze de Fernandez et al., 1968, 1972). The role of Hfq in bacteria was only discovery in the 1990s when became clear the importance of this protein in the regulation of gene expression by interacting with small RNAs. Hfq facilitates the interaction of *trans-acting* sRNAs and their respective mRNAs targets by facilitating the base-pairing between them and leading up or down regulation of translation or sRNA stability (Storz et al., 2011; Vogel & Luisi, 2011).

Based on this information, our hypothesis is that mobile genetic elements (i.e., plasmid and ICEs), in Pasteurellaceae carry AMR and other important genes among species that may contribute to the success in the environment; BEVs produced by App are affected by growth conditions and transport nucleic acids in its cargo, that may participate in the host-cell or cell-cell communication. Also, sRNAs of *A. pleuropneumoniae*, besides it is transported by BEVs, are involved with regulation of diverse physiological response in the bacterium.

References

Associação Brasileira de Proteína Animal. Relatório anual 2022. Disponível em: https://abpa-br.org/relatorios/

Antenucci, F., Fougeroux, C., Bossé, J. T., Magnowska, Z., Roesch, C., Langford, P., Holst, P. J., & Bojesen, A. M. (2017). Identification and characterization of serovar-independent immunogens in *Actinobacillus pleuropneumoniae*. *Veterinary Research*, *48*(1), 74. https://doi.org/10.1186/s13567-017-0479-5

Antenucci, F., Fougeroux, C., Deeney, A., Ørskov, C., Rycroft, A., Holst, P. J., & Bojesen, A. M. (2018). In vivo testing of novel vaccine prototypes against *Actinobacillus pleuropneumoniae*. *Veterinary Research*, *49*(1), 4. https://doi.org/10.1186/s13567-017-0502-x

Antenucci, F., Magnowska, Z., Nimtz, M., Roesch, C., Jänsch, L., & Bojesen, A. M. (2019). Immunoproteomic characterization of outer membrane vesicles from hyper-vesiculating *Actinobacillus pleuropneumoniae*. *Veterinary Microbiology*, *235*, 188–194. https://doi.org/10.1016/j.vetmic.2019.07.001

Archambault, M., Harel, J., Gouré, J., Tremblay, Y. D. N., & Jacques, M. (2011). Antimicrobial Susceptibilities and Resistance Genes of Canadian Isolates of *Actinobacillus pleuropneumoniae*. *Microbial Drug Resistance*, *18*(2), 198–206. https://doi.org/10.1089/mdr.2011.0150

Avila-Calderón, E. D., Ruiz-Palma, M. del S., Aguilera-Arreola, M. G., Velázquez-Guadarrama, N., Ruiz, E. A., Gomez-Lunar, Z., Witonsky, S., & Contreras-Rodríguez, A. (2021). Outer membrane vesicles of Gram-negative bacteria: an outlook on biogenesis. *Frontiers in Microbiology*, *12*. https://doi.org/10.3389/fmicb.2021.557902

Badi, S. A., Bruno, S. P., Moshiri, A., Tarashi, S., Siadat, S. D., & Masotti, A. (2020). Small RNAs in Outer membrane vesicles and their function in host-microbe interactions. *Frontiers in Microbiology*, *11*, 1209. https://doi.org/10.3389/fmicb.2020.01209

Bethe, Astrid, Lothar H Wieler, Hans-J. Selbitz, and Christa Ewers. (2009). Genetic diversity of porcine *Pasteurella multocida* strains from the respiratory tract of healthy and diseased swine. Veterinary Microbiology 139(1): 97–105. https://www.sciencedirect.com/science/article/pii/S0378113509002156.

Boeckel, T.P. Van, Brower, C., Gilbert, M., Grenfell, B.T., Levin, S.A., Robinson, T.P., Teillant, A., Laxminarayan, R. (2015). Global trends in antimicrobial use in food animals. Proc. Natl. Acad. Sci. 112, 5649–5654. doi:10.1073/pnas.1503141112

Bossé, J. T., Janson, H., Sheehan, B. J., Beddek, A. J., Rycroft, A. N., Simon Kroll, J., & Langford, P. R. (2002). *Actinobacillus pleuropneumoniae*: pathobiology and pathogenesis of infection. *Microbes and Infection*, *4*(2), 225–235. https://doi.org/10.1016/S1286-4579(01)01534-9

Bottery, M. J., Pitchford, J. W., & Friman, V.-P. (2021). Ecology and evolution of antimicrobial resistance in bacterial communities. *The ISME Journal*, *15*(4), 939–948. https://doi.org/10.1038/s41396-020-00832-7

Carr, V. R., Shkoporov, A., Hill, C., Mullany, P., & Moyes, D. L. (2021). Probing the

Mobilome: Discoveries in the Dynamic Microbiome. *Trends in Microbiology*, *29*(2), 158–170. https://doi.org/10.1016/j.tim.2020.05.003

Chiers, K., De Waele, T., Pasmans, F., Ducatelle, R., & Haesebrouck, F. (2010). Virulence factors of *Actinobacillus pleuropneumoniae* involved in colonization, persistence and induction of lesions in its porcine host. *Veterinary Research*, *41*(5), 65. https://doi.org/10.1051/vetres/2010037

Choi, J.-W., Kim, S.-C., Hong, S.-H., & Lee, H.-J. (2017). Secretable small rnas via outer membrane vesicles in periodontal pathogens. *Journal of Dental Research*, *96*(4), 458–466. https://doi.org/10.1177/0022034516685071

Choi, Ji-Woong, Um, J.-H., Cho, J.-H., & Lee, H.-J. (2017). Tiny RNAs and their voyage via extracellular vesicles: Secretion of bacterial small RNA and eukaryotic microRNA. *Experimental Biology and Medicine*, *242*(15), 1475–1481. https://doi.org/10.1177/1535370217723166

Christensen, H., Kuhnert, P., Nørskov-Lauritsen, N., Planet, P. J., & Bisgaard, M. (2014). *The Family* Pasteurellaceae *BT - The Prokaryotes: Gammaproteobacteria* (E. Rosenberg, E. F. DeLong, S. Lory, E. Stackebrandt, & F. Thompson (eds.); pp. 535–564). Springer Berlin Heidelberg. https://doi.org/10.1007/978-3-642-38922-1_224

Costa-Hurtado, Mar, Emili Barba-Vidal, Jaime Maldonado, and Virginia Aragon. (2020). Update on Glässer's disease: How to control the disease under restrictive Use of Antimicrobials. Veterinary Microbiology 242: 108595. https://www.sciencedirect.com/science/article/pii/S0378113519314713.

Crispim, J. S., da Silva, T. F., Sanches, N. M., da Silva, G. C., Pereira, M. F., Rossi, C. C., Li, Y., Terra, V. S., Vohra, P., Wren, B. W., Langford, P. R., Bossé, J. T., & Bazzolli, D. M. S. (2020). Serovar-dependent differences in Hfq-regulated phenotypes in *Actinobacillus pleuropneumoniae*. *Pathogens and Disease*, *78*(9). https://doi.org/10.1093/femspd/ftaa066

Deatherage, B. L., & Cookson, B. T. (2012). Membrane Vesicle Release in Bacteria, Eukaryotes, and Archaea: a Conserved yet Underappreciated Aspect of Microbial Life. *Infection and Immunity*, *80*(6), 1948–1957. https://doi.org/10.1128/IAI.06014-11

Franze de Fernandez, M. T., Eoyang, L., & August, J. T. (1968). Factor fraction required for the synthesis of bacteriophage Qβ-RNA. *Nature*, *219*(5154), 588–590. https://doi.org/10.1038/219588a0

Franze de Fernandez, M. T., Hayward, W. S., & August, J. T. (1972). Bacterial proteins required for replication of phage Q ribonucleic acid. Pruification and properties of host factor I, a ribonucleic acid-binding protein. *The Journal of Biological Chemistry*, *247*(3), 824–831.

Freire-Moran, L., Aronsson, B., Manz, C., Gyssens, I. C., So, A. D., Monnet, D. L., & Cars, O. (2011). Critical shortage of new antibiotics in development against multidrug-resistant bacteria—Time to react is now. *Drug Resistance Updates*, *14*(2), 118–124. https://doi.org/https://doi.org/10.1016/j.drup.2011.02.003

Frey, J. (2011). The role of RTX toxins in host specificity of animal pathogenic Pasteurellaceae. *Veterinary Microbiology*, *153*(1), 51–58.

https://doi.org/https://doi.org/10.1016/j.vetmic.2011.05.018

Frost, L. S., Leplae, R., Summers, A. O., & Toussaint, A. (2005). Mobile genetic elements: the agents of open source evolution. *Nature Reviews Microbiology*, *3*(9), 722–732. https://doi.org/10.1038/nrmicro1235

Gill, S., Catchpole, R., & Forterre, P. (2019). Extracellular membrane vesicles in the three domains of life and beyond. *FEMS Microbiology Reviews*, *43*(3), 273–303. https://doi.org/10.1093/femsre/fuy042

Gong, H., Vu, G.-P., Bai, Y., Chan, E., Wu, R., Yang, E., Liu, F., & Lu, S. (2011). A Salmonella small non-coding RNA Facilitates bacterial invasion and intracellular replication by modulating the expression of virulence factors. *PLOS Pathogens*, *7*(9), e1002120. https://doi.org/10.1371/journal.ppat.1002120

Gottschalk, M. (2012). Actinobacillosis. In: Zimmerman, J.J. et al (Eds). Diseases of swine. *Chichester: Wiley-Blackwell*, *10*, 653–669.

Gripenland, J., Netterling, S., Loh, E., Tiensuu, T., Toledo-Arana, A., & Johansson, J. (2010). RNAs: regulators of bacterial virulence. *Nature Reviews Microbiology*, *8*(12), 857–866. https://doi.org/10.1038/nrmicro2457

Helke, K. L., Ezell, P. C., Duran-Struuck, R., & Swindle, M. M. (2015). Chapter 16 - Biology and Diseases of Swine. In J. G. Fox, L. C. Anderson, G. M. Otto, K. R. Pritchett-Corning, & M. T. B. T.-L. A. M. (Third E. Whary (Eds.), *American College of Laboratory Animal Medicine* (pp. 695–769). Academic Press. https://doi.org/https://doi.org/10.1016/B978-0-12-409527-4.00016-X

Hernando-Amado, S., Coque, T. M., Baquero, F., and Martínez, J. L. (2019). Defining and combating antibiotic resistance from One Health and Global Health perspectives. Nat. Microbiol. 4, 1432–1442. doi: 10.1038/s41564-019- 0503-9

Hör, J., Matera, G., Vogel, J., Gottesman, S., & Storz, G. (2020). Trans-acting small RNAs and their effects on gene expression in *Escherichia coli* and *Salmonella enterica*. *EcoSal Plus*, *9*(1). https://doi.org/10.1128/ecosalplus.ESP-0030-2019

Jan, A. T. (2017). Outer Membrane Vesicles (OMVs) of Gram-negative Bacteria: A Perspective Update. *Frontiers in Microbiology*, *8*, 1053. https://doi.org/10.3389/fmicb.2017.01053

Knox, K. W., Vesk, M., & Work, E. (1966). Relation between excreted lipopolysaccharide complexes and surface structures of a lysine-limited culture of *Escherichia coli*. *Journal of Bacteriology*, *92*(4), 1206–1217. https://doi.org/10.1128/jb.92.4.1206-1217.1966

Koeppen, K., Hampton, T. H., Jarek, M., Scharfe, M., Gerber, S. A., Mielcarz, D. W., Demers, E. G., Dolben, E. L., Hammond, J. H., Hogan, D. A., & Stanton, B. A. (2016). A novel mechanism of host-pathogen interaction through sRNA in bacterial outer membrane vesicles. *PLOS Pathogens*, *12*(6), e1005672. https://doi.org/10.1371/journal.ppat.1005672

Koo, J. T., Alleyne, T. M., Schiano, C. A., Jafari, N., & Lathem, W. W. (2011). Global discovery of small RNAs in *Yersinia pseudotuberculosis* identifies Yersinia-specific small, noncoding RNAs required for virulence. *Proceedings of the National Academy of Sciences of the United States of America*, *108*(37), E709-

17. https://doi.org/10.1073/pnas.1101655108

Lécrivain, A.-L., & Beckmann, B. M. (2020). Bacterial RNA in extracellular vesicles: A new regulator of host-pathogen interactions? *Biochimica et Biophysica Acta (BBA) - Gene Regulatory Mechanisms*, *1863*(7), 194519. https://doi.org/https://doi.org/10.1016/j.bbagrm.2020.194519

Mei, C., Sun, A., Blackall, P. J., Xian, H., Li, S., Gong, Y., & Wang, H. (2020). Component identification and functional analysis of outer membrane vesicles released by *Avibacterium paragallinarum*. *Frontiers in Microbiology*, *11*, 2313. https://doi.org/10.3389/fmicb.2020.518060

Melamed, S., Peer, A., Faigenbaum-Romm, R., Gatt, Y. E., Reiss, N., Bar, A., Altuvia, Y., Argaman, L., & Margalit, H. (2016). Global mapping of small RNA-target interactions in Bacteria. *Molecular Cell*, *63*(5), 884–897. https://doi.org/10.1016/j.molcel.2016.07.026

Michael, G. B., Bossé, J. T., & Schwarz, S. (2018). Antimicrobial resistance in Pasteurellaceae of veterinary origin. *Microbiology Spectrum*, *6*(3). https://www.asmscience.org/content/journal/microbiolspec/10.1128/microbiolspec.ARBA-0022-2017

Michaux, C., Verneuil, N., Hartke, A., & Giard, J.-C. (2014). Physiological roles of small RNA molecules. *Microbiology*, *160*(6), 1007–1019. https://doi.org/https://doi.org/10.1099/mic.0.076208-0

Micoli, F., & MacLennan, C. A. (2020). Outer membrane vesicle vaccines. *Seminars in Immunology*, *50*, 101433. https://doi.org/10.1016/j.smim.2020.101433

Miyakoshi, M., Chao, Y., & Vogel, J. (2015). Regulatory small RNAs from the 3′ regions of bacterial mRNAs. *Current Opinion in Microbiology*, *24*, 132–139. https://doi.org/https://doi.org/10.1016/j.mib.2015.01.013

Negrete-Abascal, E., García, R. M., Reyes, M. E., Godínez, D., & de la Garza, M. (2000). Membrane vesicles released by *Actinobacillus pleuropneumoniae* contain proteases and Apx toxins. *FEMS Microbiology Letters*, *191*(1), 109–113. https://doi.org/10.1111/j.1574-6968.2000.tb09326.x

Nikaido, H. (2009). Multidrug resistance in bacteria. *Annual Review of Biochemistry*, *78*, 119–146. https://doi.org/10.1146/annurev.biochem.78.082907.145923

Niven, D. F., & Lévesque, M. (1988). V-Factor-Dependent Growth of *Actinobacillus pleuropneumoniae* Biotype 2 (Bertschinger 2008/76). *International Journal of Systematic and Evolutionary Microbiology*, *38*(3), 319–320. https://doi.org/https://doi.org/10.1099/00207713-38-3-319

OECD (2022), "Meat consumption" (indicator), https://doi.org/10.1787/fa290fd0-en (accessed on 17 May 2022).

OIE. (2017). OIE annual report on antimicrobial agents intended for use in animals: better understanding of the global situation, second report.

Partridge, S. R., Kwong, S. M., Firth, N., & Jensen, S. O. (2018). Mobile genetic elements associated with antimicrobial resistance. *Clinical Microbiology Reviews*, *31*(4), e00088-17. https://doi.org/10.1128/CMR.00088-17

Pathirana, R. D., & Kaparakis-Liaskos, M. (2016). Bacterial membrane vesicles: Biogenesis, immune regulation and pathogenesis. *Cellular Microbiology*, *18*(11), 1518–1524. https://doi.org/https://doi.org/10.1111/cmi.12658

Pattison, I. H., Howell, D. G., & Elliot, J. (1957). A haemophilus-like organism isolated from pig lung and the associated pneumonic lesions. *Journal of Comparative Pathology and Therapeutics*, *67*, 320-IN37. https://doi.org/https://doi.org/10.1016/S0368-1742(57)80031-9

Pors, S. E., Pedersen, I. J., Skjerning, R. B., Thøfner, I. C. N., Persson, G., & Bojesen, A. M. (2016). Outer membrane vesicles of *Gallibacterium anatis* induce protective immunity in egg-laying hens. *Veterinary Microbiology*, *195*, 123–127. https://doi.org/https://doi.org/10.1016/j.vetmic.2016.09.021

Ramsay, Joshua P, and Neville Firth. (2017). Diverse mobilization strategies facilitate transfer of non-conjugative mobile genetic elements. Current Opinion in Microbiology 38: 1–9. https://www.sciencedirect.com/science/article/pii/S1369527416301680.

Rankin, D. J., Rocha, E. P. C., & Brown, S. P. (2011). What traits are carried on mobile genetic elements, and why? *Heredity*, *106*(1), 1–10. https://doi.org/10.1038/hdy.2010.24

Roier, S., Blume, T., Klug, L., Wagner, G. E., Elhenawy, W., Zangger, K., Prassl, R., Reidl, J., Daum, G., Feldman, M. F., & Schild, S. (2015). A basis for vaccine development: Comparative characterization of *Haemophilus influenzae* outer membrane vesicles. *International Journal of Medical Microbiology*, *305*(3), 298–309. https://doi.org/https://doi.org/10.1016/j.ijmm.2014.12.005

Roier, S., Fenninger, J. C., Leitner, D. R., Rechberger, G. N., Reidl, J., & Schild, S. (2013). Immunogenicity of *Pasteurella multocida* and *Mannheimia haemolytica* outer membrane vesicles. *International Journal of Medical Microbiology*, *303*(5), 247–256. https://doi.org/https://doi.org/10.1016/j.ijmm.2013.05.001

Rossi, C.C., Bossé, J.T., Li, Y., Witney, A.A., Gould, K.A., Langford, P.R., Bazzolli, D. M. S. (2016). A computational strategy for the search of regulatory small RNAs in *Actinobacillus pleuropneumoniae*. *RNA*, *Sep*; *22(9)*, 1373–1385.

Rossi, C. C., de Araújo, E. F., Queiroz, M. V. de, & Bazzolli, D. M. S. (2013). Characterization of the *omlA* gene from different serotypes of *Actinobacillus pleuropneumoniae*: A new insight into an old approach. *Genetics and Molecular Biology*, *36*(2), 243–251. https://doi.org/10.1590/S1415-47572013005000012

Sassu, E. L., Bossé, J. T., Tobias, T. J., Gottschalk, M., Langford, P. R., & Hennig-Pauka, I. (2018). Update on *Actinobacillus pleuropneumoniae*—knowledge, gaps and challenges. Transboundary and Emerging Diseases, 65(S1), 72–90. https://doi.org/https://doi.org/10.1111/tbed.12739

Schwechheimer, C., & Kuehn, M. J. (2015). Outer-membrane vesicles from Gram-negative bacteria: biogenesis and functions. *Nature Reviews Microbiology*, *13*(10), 605–619. https://doi.org/10.1038/nrmicro3525

Siefert, J. L. (2009). *Defining the Mobilome BT - Horizontal Gene Transfer: Genomes in Flux* (M. B. Gogarten, J. P. Gogarten, & L. C. Olendzenski (eds.); pp. 13–27). Humana Press. https://doi.org/10.1007/978-1-60327-853-9_2

Sierra, G. V, Campa, H. C., Varcacel, N. M., Garcia, I. L., Izquierdo, P. L., Sotolongo, P. F., Casanueva, G. V, Rico, C. O., Rodriguez, C. R., & Terry, M. H. (1991). Vaccine against group B *Neisseria meningitidis*: protection trial and mass vaccination results in Cuba. *NIPH Annals*, *14*(2), 110–195. http://europepmc.org/abstract/MED/1812432

Sledjeski, D. D., Whitman, C., & Zhang, A. (2001). Hfq is necessary for regulation by the untranslated RNA DsrA. *Journal of Bacteriology*, *183*(6), 1997–2005. https://doi.org/10.1128/JB.183.6.1997-2005.2001

Soler, N., & Forterre, P. (2020). Vesiduction: the fourth way of HGT. *Environmental Microbiology*, *22*(7), 2457–2460. https://doi.org/https://doi.org/10.1111/1462-2920.15056

Storz, G., Vogel, J., & Wassarman, K. M. (2011). Regulation by small RNAs in bacteria: expanding frontiers. *Molecular Cell*, *43*(6), 880–891. https://doi.org/10.1016/j.molcel.2011.08.022

Stringer, O. W., Bossé, J. T., Lacouture, S., Gottschalk, M., Fodor, L., Angen, Ø., Velazquez, E., Penny, P., Lei, L., Langford, P. R., & Li, Y. (2021). Proposal of *Actinobacillus pleuropneumoniae* serovar 19, and reformulation of previous multiplex PCRs for capsule-specific typing of all known serovars. *Veterinary Microbiology*, *255*, 109021. https://doi.org/https://doi.org/10.1016/j.vetmic.2021.109021

Su, Z., Zhu, J., Xu, Z., Xiao, R., Zhou, R., Li, L., & Chen, H. (2016). A transcriptome map of *Actinobacillus pleuropneumoniae* at single-nucleotide resolution using deep RNA-Seq. *PLOS ONE*, *11*(3), e0152363. https://doi.org/10.1371/journal.pone.0152363

Subashchandrabose, S., Leveque, R. M., Kirkwood, R. N., Kiupel, M., & Mulks, M. H. (2013). The RNA Chaperone Hfq Promotes Fitness of *Actinobacillus pleuropneumoniae* during Porcine Pleuropneumonia. Infection and Immunity, 81(8), 2952–2961. https://doi.org/10.1128/IAI.00392-13

Torres, R. T., Carvalho, J., Fernandes, J., Palmeira, J. D., Cunha, M. V, & Fonseca, C. (2021). Mapping the scientific knowledge of antimicrobial resistance in food-producing animals. *One Health*, *13*, 100324. https://doi.org/https://doi.org/10.1016/j.onehlt.2021.100324

Toyofuku, M., Nomura, N., & Eberl, L. (2019). Types and origins of bacterial membrane vesicles. *Nature Reviews Microbiology*, *17*(1), 13–24. https://doi.org/10.1038/s41579-018-0112-2

Ulrike, R., Anthony, T. J., Anaïs, L. R., Gerald, S., Manfred, R., Sergo, K., Susanne, H., Philip, T., Nyunt, W. S., Emmanuelle, C., & Peter, G. E. (2016). A two-component regulatory system impacts extracellular membrane-derived vesicle production in group A *Streptococcus*. *MBio*, *7*(6), e00207-16. https://doi.org/10.1128/mBio.00207-16

Van Driessche, L., Vanneste, K., Bogaerts, B., De Keersmaecker, S. C. J., Roosens, N., Haesebrouck, F., De Cremer, L., Deprez, P., Pardon, B., & Boyen, F. (2020). Isolation of drug-resistant *Gallibacterium anatis* from calves with unresponsive bronchopneumonia, Belgium. *Emerging Infectious Disease Journal*, *26*(4), 721.

https://doi.org/10.3201/eid2604.190962

Ventola, C. L. (2015). The antibiotic resistance crisis: part 1: causes and threats. *P & T : A Peer-Reviewed Journal for Formulary Management*, *40*(4), 277–283. https://pubmed.ncbi.nlm.nih.gov/25859123

Vidovic, N., & Vidovic, S. (2020). Antimicrobial resistance and food animals: influence of livestock environment on the emergence and dissemination of antimicrobial resistance. *Antibiotics (Basel, Switzerland)*, *9*(2), 52. https://doi.org/10.3390/antibiotics9020052

Villa, J. K., Su, Y., Contreras, L. M., & Hammond, M. C. (2018). Synthetic biology of small RNAs and riboswitches. *Microbiology Spectrum*, *6*(3). https://doi.org/10.1128/microbiolspec.RWR-0007-2017

Vogel, J., & Luisi, B. F. (2011). Hfq and its constellation of RNA. *Nature Reviews Microbiology*, *9*(8), 578–589. https://doi.org/10.1038/nrmicro2615

Wagner, E. G. H., & Romby, P. (2015). Small RNAs in bacteria and archaea: who they are, what they do, and how they do it. *Advances in Genetics*, *90*, 133–208. https://doi.org/10.1016/bs.adgen.2015.05.001

Westermann, A. J., Förstner, K. U., Amman, F., Barquist, L., Chao, Y., Schulte, L. N., Müller, L., Reinhardt, R., Stadler, P. F., & Vogel, J. (2016). Dual RNA-seq unveils noncoding RNA functions in host–pathogen interactions. *Nature*, *529*(7587), 496–501. https://doi.org/10.1038/nature16547

WHO. (2019). *Critically important antimicrobials for human medicine* (6th revisi).

Woolums, A. R., Karisch, B. B., Frye, J. G., Epperson, W., Smith, D. R., Blanton, J., Austin, F., Kaplan, R., Hiott, L., Woodley, T., Gupta, S. K., Jackson, C. R., & McClelland, M. (2018). Multidrug resistant *Mannheimia haemolytica* isolated from high-risk beef stocker cattle after antimicrobial metaphylaxis and treatment for bovine respiratory disease. *Veterinary Microbiology*, *221*, 143–152. https://doi.org/https://doi.org/10.1016/j.vetmic.2018.06.005

Chapter 1

Mobile genetic elements drive antimicrobial resistance gene spread in Pasteurellaceae species

(Article published as original research in Frontiers in Microbiology, January 2022 | Volume 12 | Article 773284 | doi: 10.3389/fmicb.2021.773284)

Giarlã Cunha da Silva[1,†], Osiel Silva Gonçalves[2,†], Jéssica Nogueira Rosa[1], Kiara Campos França[2], Janine Thérèse Bossé[3], Paul Richard Langford [3,*], Mateus Ferreira Santana[2,*], Denise Mara Soares Bazzolli[1,*]

[1]Laboratório de Genética Molecular de Bactérias, Departamento de Microbiologia, Instituto de Biotecnologia Aplicada à Agropecuária, Universidade Federal de Viçosa, Viçosa, Minas Gerais, Brazil.
[2]Grupo de Genômica Evolutiva Microbiana, Laboratório de Genética Molecular de Microrganismos, Instituto de Biotecnologia Aplicada à Agropecuária, Universidade Federal de Viçosa, Minas Gerais, Brazil.
[3]Section of Paediatrics, Department of Medicine, Imperial College London, London, United Kingdom.
† Equal contribution

Abstract

Mobile genetic elements (MGEs) and antimicrobial resistance (AMR) drive important ecological relationships in microbial communities and pathogen-host interaction. In this study, we investigated the resistome-associated mobilome in 345 publicly available Pasteurellaceae genomes, a large family of Gram-negative bacteria including major human and animal pathogens. We generated a comprehensive dataset of the mobilome integrated into genomes, including 10,820 insertion sequences, 2,939 prophages, and 43 integrative and conjugative elements. Also, we assessed plasmid sequences of Pasteurellaceae. Our findings greatly expand the diversity of MGEs for the family, including a description of novel elements. We discovered that MGEs are comparable and dispersed across species and that they also co-occur in genomes, contributing to the family's ecology via gene transfer. In addition, we investigated the impact of these elements in the dissemination and shaping of AMR genes. A total of 55 different AMR genes were mapped to 721 locations in the dataset. MGEs are linked

with 77.6% of AMR genes discovered, indicating their important involvement in the acquisition and transmission of such genes. This study provides an uncharted view of the Pasteurellaceae by demonstrating the global distribution of resistance genes linked with MGEs.

Keywords: mobile DNA, bacterial resistance, gene transfer, genome evolution, one health

Introduction

Antimicrobial resistance (AMR), one of the biggest global threats to health and food safety, continues to be driven by misuse of antimicrobials in humans and animals. In bacteria, the acquisition of AMR genes carried on mobile genetic elements (MGEs) can lead to the establishment of multidrug resistance (MDR) (Nikaido, 2009). The collection of all AMR genes is known as the resistome (Wright, 2007) and the entire set of MGEs in a genome defines the mobilome (Siefert, 2009). MGEs are essential in microbial ecology because of their capacity to transfer genes with different roles throughout microbial populations (Rankin et al., 2011). Horizontal gene transfer (HGT) mechanisms, i.e., conjugation, transduction, transformation, and vesiduction (Soler and Forterre, 2020), mediate dispersion of MGEs, often leading to bacterial evolution, as the introduction of foreign sequences into novel genomic locations can alter phenotypes (Frost et al., 2005; Carr et al., 2021). Larger MGEs can carry AMR genes between microbes (Partridge et al., 2018; Carr et al., 2020), whereas further movement within a host (between co-resident large MGEs and/or chromosomes) can be facilitated by smaller elements (Che et al., 2021). Studies on the resistome-associated mobilome are required to elucidate the dispersion of AMR in bacteria, particularly for human and animal pathogens. The Pasteurellaceae family comprises mainly commensals and pathogens associated with mammalian hosts, including humans and food-production animals (Rosenberg et al., 2013; Michael et al., 2018) where infections have historically been/continue to be treated with antimicrobials, leading to significant problems with AMR (Michael et al., 2018). While MGEs have previously been reported in the Pasteurellaceae (Juhas et al., 2007; Moleres et al., 2015; Michael et al., 2018; Szafranski et al., 2019), several aspects of their contribution to MDR have not been addressed. Here, we performed the first large-scale genomic analysis of Pasteurellaceae in order to investigate the role of MGEs in the dissemination of AMR

genes in this family. We initially focused on the discovery and characterization of MGEs integrated into Pasteurellaceae genomes, which provided a substantial dataset to assess their role in the dissemination and shaping of AMR genes in this important family.

Materials and Methods

Genome Dataset, Data Processing, and Phylogenetic Analysis

The complete genomes of 345 Pasteurellaceae were retrieved from the National Center for Biotechnology Information (NCBI) non-redundant RefSeq database (last accessed in May 2020)[1] (Supplementary Table 1). Phylogenetic relationships between the genomes were determined using alignment of 16S rRNA sequences using ClustalW (Juraschek et al., 2019), and a maximum likelihood phylogenetic tree was constructed in MEGA X (Kumar et al., 2018), using the Generalized Time Reversible (GTR) and bootstrap confidence value of 1000. The phylogenetic tree was visualized with Interactive Tree of Life (iTOL) (Letunic and Bork, 2019), where the tree was edited and supplemented with genome information. The global distribution of genomes was determined using the ggmap R package version 3.0.0, a heatmap being plotted based on the number of genomes available for each region.

Identification and Analysis of Insertion Sequences

GenBank format (.gbk) of the genome dataset was used as input for insertion sequence (IS) prediction using ISsaga (Varani et al., 2011) with default parameters. In addition, the recommendations of the Everyman's Guide to Bacterial Insertion Sequences (Siguier et al., 2015) were used to identify partial elements and provide IS family features. Hierarchic organization of IS family distribution was visualized in the R environment using the ggplot2 circular package version 3.3.5. ISsaga was used to assess IS ORF genome context. Transposase and adjacent gene sequence were extracted and analyzed for conserved domains using CD-Search (Marchler-Bauer and Bryant, 2004) against the CDD v3.18 database with an expected value threshold of 0.01, and its gene product was inspected for gene ontology annotation through the QuickGO resource at EMBL-EBI (Binns et al., 2009). Next, we created a local database

[1] ftp.ncbi.nlm.nih.gov/genomes/refseq/

of genes flanking ISs (Supplementary Table 3) and divided them into four classes according to their function: stress response, AMR, adaptation, and virulence. Circular visualization of these classes was created in Circos Table Viewer (Krzywinski et al., 2009). The genome sequences (.gbk format) of *Mannheimia haemolytica* (strains M42548, USDA-ARS-USMARC-184, and NCTC10643) and Aggregatibacter actinomycetemcomitans (strains HK_907, KK1651, and VT1169) were selected as examples of genomes carrying many or few IS copies, and a multiple genome alignment was performed using progressive Mauve (Darling et al., 2004).

Identification and Analysis of Prophage Elements

We analyzed the prophage elements integrated into the genomes of Pasteurellaceae in three critical aspects: prophage-like elements, complete prophages, and novel putative prophage elements. First, we looked for prophage-like elements, i.e., candidate intact prophage that contained phage attachment sites, genes encoding structural phage proteins, genes coding for proteins involved in DNA regulation, insertion into the host genome, and lysis (Arndt et al., 2016; Czajkowski, 2019). We used PHASTER (Arndt et al., 2016) and Prophage Hunter (Song et al., 2019) to predict prophage-like elements. Raw data from the predictions were used for further analysis (Supplementary Tables 4, 5). Next, we screened for complete prophages and prophage-like elements in the classes of intact and active prophage-like elements from PHASTER and Prophage Hunter, respectively. Sequences were subject to BLASTN searches against reference viral genomes already described in the family (Supplementary Table 7) using MegaBLAST (Chen et al., 2015) alignment with a cut-off of 75% of cover and 85% identity, allowing identification of complete prophages found in the bacterial genomes (Supplementary Table 6). More than one complete prophage insertion into the genome was considered a poly-lysogenic event. Finally, we identified novel putative prophages considering the classes of incomplete, questionable, and ambiguous. We also manually inspected the results of mismatched prophage-like elements, according to our criteria, from previous analyses of complete prophages. We screened these sequences for phage-associated functions. Upper boundaries of the novel prophages were determined, wherever possible, by searching for phage integrases from the tyrosine recombinase family at the tRNAs. A sequence identity matrix was built using whole nucleotide sequences of putative novel prophages. These sequences were aligned by Clustal Omega (Sievers and Higgins,

2014) with the default parameters. To show that putative novel prophages were different from those previously reported in the family (Supplementary Table 7), a synteny analysis using clinker and clustermap.js (Gilchrist and Chooi, 2021) among phages classified by genus was performed. Additionally, we classified a prophage to a family belonging to the order Caudovirales using the occurrence of head-necktail module genes detected by the Virfam (Lopes et al., 2014). Phylogenomic analysis of the novel prophages was performed by the ViPTree (Nishimura et al., 2017) webserver. A MegaBLAST analysis against the novel prophages to evaluate their dispersion among Pasteurellaceae genomes, using a cutoff of 90% of cover and identity, was carried out. A bipartite network was constructed using vConTACT (Bolduc et al., 2017) to estimate the relationship and clustering of prophages belonging to the Pasteurellaceae family. A graphic representation of novel and previously reported prophages mapped onto the genomes of the family (grouped by genus), based on size, GC content, and number of ORFs was carried out. The annotation of protein sequences was done using GeneMarkS (Besemer et al., 2001) version 4.28 with the sequence type of the phage marked. BLASTP (McGinnis and Madden, 2004) was used to build a local database of the protein sequences, which provided a homologous protein cluster (HPC) with sequences > 30% amino acid identity, > 80% alignment coverage, and clustering E-value < 1E-5. Next, the functional annotation of HPC was done using HMMER69 v3.b2 searches with default parameters to the PFAM (Finn et al., 2014). We also analyzed the lifestyle of prophages using the phage Classification Tool Set (PHACTS) (McNair et al., 2012).

Detection, Delimitation, and Comparative Analysis of Integrative and Conjugative Elements

To identify integrative and conjugative elements (ICEs) in the genomes of the Pasteurellaceae, the genomes were inspected for MGE-encoding relaxases, type-IV coupling proteins (T4CP), and the type-IV secretion system (T4SS) gene cluster using the oriTfinder (Li et al., 2018) (Supplementary Table 9). ICE sequences experimentally validated for the family were retrieved from the ICEberg (Liu et al., 2018) database version 2.0. Comparative analyses with the ICEberg data allowed the identification of novel putative ICE elements within the Pasteurellaceae family (Supplementary Table 11). An element was considered as conjugative when it contained a relaxase, a T4CP, a T4SS gene cluster, and type-specific genes related to mating pair formation (Cury et

al., 2017). We inspected attachment sites located between the tRNA and the integrase gene using Repeat Finder plugins on Geneious PrimeR version 2020. The opposite boundary of the element was delimited by BLASTN searching, and alignment of the ICE and attachment site sequences using minimum general parameters and filter low complexity region marking. The integrase family was classified by conserved domain searches using CD-Search (Marchler-Bauer and Bryant, 2004), tRNAscan-SE (Chan and Lowe, 2019) and MOBscan (Garcillán-Barcia et al., 2020) were used to identify tRNA genes and classify relaxase families, respectively. We built a sequence identity matrix using whole nucleotide sequences of putative novel ICEs. These sequences were aligned by Clustal Omega (Sievers and Higgins, 2014) with the default parameters, and a heatmap was generated using the ggplot2 R package. To show that putative novel ICEs were different from those previously reported in the family (Supplementary Table 7), a synteny analysis using clinker and clustermap.js (Gilchrist and Chooi, 2021) among groups of ICEs classified by genus was performed. Next, we performed a global analysis of ICEs mapped onto the genomes, based on size, GC content, and number of ORFs. GeneMarkS (Besemer et al., 2001) was used to annotate predicted protein sequences. A BLASTP alignment to obtain HPC with sequences > 30% protein identity, > 80% alignment coverage, and clustering E-value < 1E-5 was done. Next, the functional annotation of HPC was done using HMMER (Wheeler and Eddy, 2013) v3.b2 searches with default parameters to the Pfam (Finn et al., 2014). Key ICE genes were used for tracking the evolutionary history of these elements. The integrase (*int*), topoisomerase (*parA*), and coupling protein (*traD*) genes were found in almost all ICE sequences. Nucleotide sequences of these genes were aligned using ClustalW to construct maximum likelihood phylogenetic trees. The GTR model and a bootstrap confidence value of 1,000 were applied to each tree. The alignment and phylogenetic analysis were done using MEGA X (Kumar et al., 2018) and edited using iTOL (Letunic and Bork, 2019). Finally, we constructed a network to evaluate the dispersion of the ICEs among the Pasteurellaceae host genomes. A local database with nucleotide sequences of the ICEs was created and MegaBLAST alignments were done, with a cut-off of 75% of cover and identity to consider the interaction between individual ICE and the host genomes, and a tabular representation of this interaction was constructed. The network was visualized using Cytoscape (Shannon et al., 2003).

Plasmid Dataset and Clustering Plasmid Type

A total of 162 plasmid sequences from the Pasteurellaceae were retrieved from the NCBI RefSeq database (last accessed on Nov 2020)[2] (Supplementary Table 12). We manually curated the plasmid database, eliminating partial plasmid DNA sequences, redundant nomenclature, and unassignable hosts. Relaxases were classified using MOBscan (Garcillán-Barcia et al., 2020), and the nucleotide sequence of mob genes was aligned using ClustalW to construct a maximum likelihood phylogenetic tree. The Tamura- Nei (TN) model and a bootstrap confidence value of 1,000 were applied. Alignment and phylogenetic analyses were done using MEGA X and edited using iTOL. To analyze potentially non-mobilizable plasmids, amino acid sequences were aligned using Muscle (Madeira et al., 2019) with the output format adjusted to Phylip sequential. A distant matrix was constructed using the output file through EMBOSS (Madeira et al., 2019). A multi-dimensional graph was created in R. Lastly, to correlate the redundant nomenclature plasmids mentioned above with the One-health concept, an arc diagram was created using the common plasmids found in different species/genomes.

Resistome Profile Associated with the Mobile Genetic Elements

AMR genes were identified by ResFinder 4.0 (Bortolaia et al., 2020) and the Comprehensive Antibiotic Resistance Database (CARD 2020) (Alcock et al., 2020). The latter was also used to identify any synonymous AMR genes indicated in different published elements using different names. Firstly, we used the context genes associated with AMR provided by ISsaga analysis (Supplementary Table 3) to investigate the association of transposable elements (TEs) with AMR genes. Subsequently, the impact of IS elements in three classes (upstream, downstream, and interruption of AMR gene) according to the transposase position in relation to the AMR genes, was classified. Sequences were extracted from transposons associated with ICEs to analyze the possible transfer of AMR gene sequences. Individual transposases were aligned using the ISfinder database (Siguier et al., 2006), using default parameters (E-value ≤ 10-5), and a minimum alignment coverage of 50% and with at least 70% identity was considered. The direct repeat and terminal inverted repeats

[2] https://ftp.ncbi.nih.gov/refseq/release/plasmid/

were manually identified and annotated using Geneious PrimeR based BLASTn searches against ISfinder to identify known IS elements. Fasta sequences of all genomes and MGEs of the Pasteurellaceae were used as input for the AMR gene predictions. To show the contribution of the MGEs in carrying AMR genes, we compared the content of AMR genes of these elements to the total number of AMR genes in their respective genomes. For comparison, we used localization of the ICE in the genomes and verified whether the genes were located within the element, and also looked for AMR genes in plasmids belonging to isolates from our genome dataset. Also, individual plasmid and prophage sequences were inspected for AMR genes. The distribution of AMR genes and classes among ICEs and plasmids was represented using the Sankey diagram[3]. Finally, sequences of the most prevalent AMR genes detected in MGEs were evaluated for selective pressure. AMR gene sequences were aligned in MEGAX (Kumar et al., 2018) and exported in meg format. The program DnaSP v6 (Rozas et al., 2017) was used to carry out Tajima (1989) and Fu and Li (1993) tests.

Results

Our Dataset Comprises Highly Diverse and Globally Widespread Genomes

We surveyed 345 publicly available Pasteurellaceae complete genomes, spanning 34 species belonging to 14 genera (Figure 1A). Our genome dataset contains representatives from diverse veterinary species (212), humans (119), and unknown sources (14) (Figure 1A, Supplementary Figure 1, and Supplementary Table 1). Genome sizes ranged from 1.5 Mb in *Haemophilus* spp. to 2.8 Mb in *Mannheimia* spp. (Figure 1A and Supplementary Table 1). We inferred an evolutionary tree using 16S rRNA (Figure 1A). Similar to previous studies (Naushad et al., 2015), our phylogeny indicates that many Pasteurellaceae genera have different paraphyletic clades and tend to form different separated clusters, which may reflect misclassifications awaiting resolution. Four different species were assigned to the genus Mannheimia (i.e., *Mannheimia granulomatis*, *M. haemolytica*, *Mannheimia varigena*, and *Mannheimia succiniciproducens*), and eight different species have names indicating they are members of the genus *Actinobacillus* [i.e., (*Actinobacillus*) *delphinicola*, *Actinobacillus*

[3] http://sankeymatic.com/

equuli, (*Actinobacillus*) *indolicus*, *Actinobacillus lignieresii*, *Actinobacillus pleuropneumoniae*, (*Actinobacillus*) *porcitonsillarum*, (*Actinobacillus*) *succinogenes*, and *Actinobacillus suis*], though square brackets around the genus names indicate species that require reclassification, as they are not *Actinobacillus* sensu stricto (Blackall and Turni, 2020). Our dataset shows a global distribution of sources, though America, Europe and Asia are more highly represented (Figure 1B). *H. influenzae*, *Pasteurella multocida*, *A. pleuropneumoniae*, and *A. actinomycetemcomitans* had the most genomes available per species, presumably reflecting their importance for human and veterinary health.

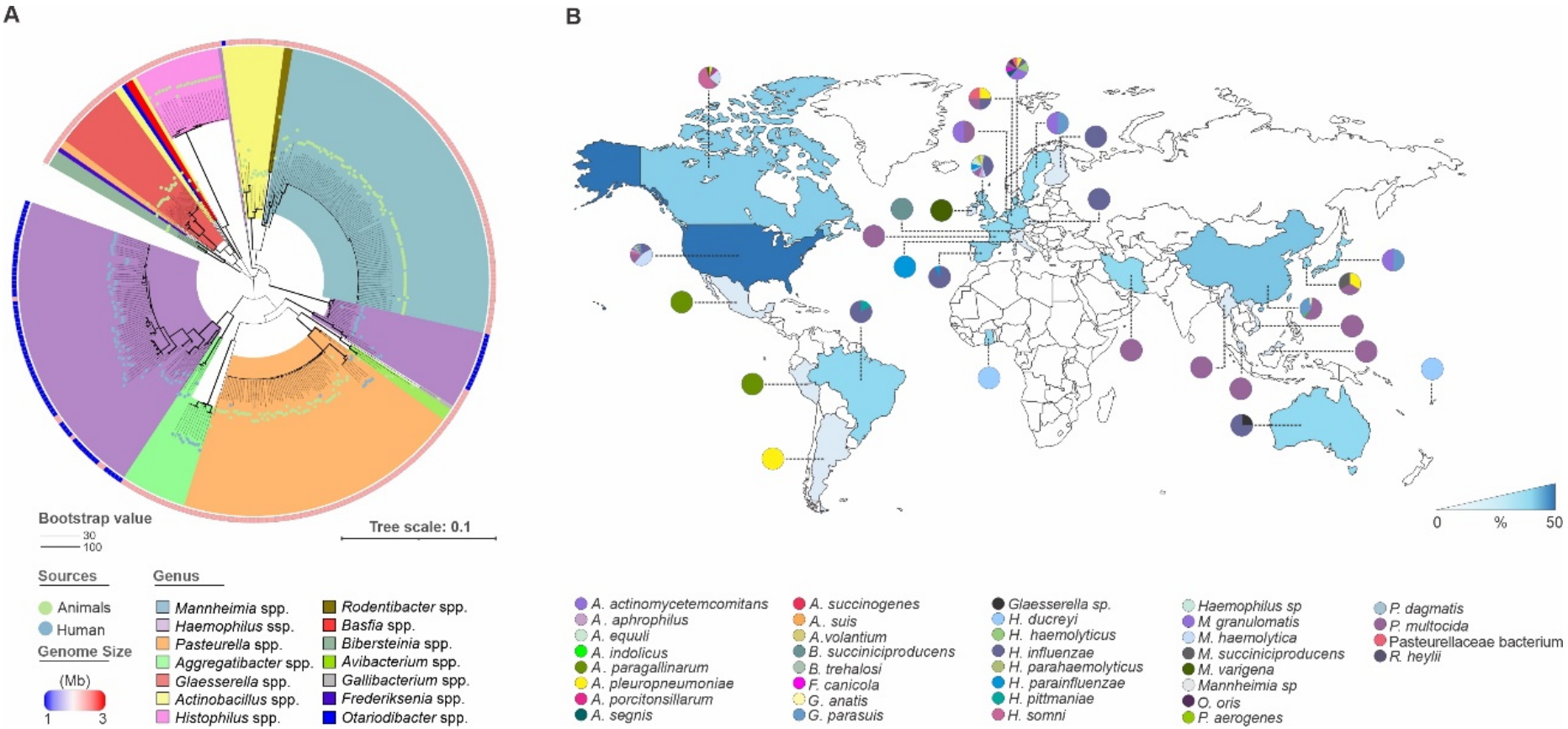

Figure 1 | The whole dataset comprises highly diverse and globally widespread genomes. (A) Phylogenetic tree of 16S rRNA genes from 345 complete genomes of Pasteurellaceae species. From the inside to the outside: the 14 main groups according to genus cluster, the size of the genomes (see legend), and the source of each genome (color dots). The evolutionary history was inferred by using the Maximum Likelihood method based on the General Time Reversible model. The tree is drawn to scale, with branch lengths in the same units as those of the evolutionary distances used to infer the phylogenetic tree. (B) Global distribution of publicly available Pasteurellaceae genomes by country. The heatmap below the map was plotted based on the number of genomes among the countries. Species distribution by country is represented by pie charts color-code as indicated in the legend.

Insertion Sequences Are Broadly Disseminated Affecting Genome Size and Organization

We used ISsaga to predict, map and annotate a total of 10,820 ISs, belonging to 19 different families and divided into 12 subgroups (ssgr), in our genome dataset (Supplementary Table 2 and Supplementary Figure 2A). Of the known elements, 37.8% (4,016) were intact and 62.2% (6,611) were partial. The most frequent IS families found were: IS*481*, IS*L3* and IS*1595* ssgr IS*1016* with 2,802 (25.9%), 1,588 (14.67%), 1,211 (11.2%) occurrences, respectively. These elements were broadly disseminated among the Pasteurellaceae genomes, with a higher diversity of IS families and an average number of 53, 23, and 94 ISs per genome in *Mannheimia*, *Haemophilus*, and *Glaesserella* genera, respectively (Supplementary Table 2 and Supplementary Figure 2B). Despite the majority of ISs belonging to IS*481*, this family was only found in eight genera, whereas IS*L3*, IS*1595*, and IS*3* were the most widespread within the Pasteurellaceae (Figure 2A). Mapping of ISs with regards to genomic locations (Supplementary Table 3) identified 14 IS families inserted within/adjacent to 337 genes associated with stress responses (n D 145), AMR (n D 89), adaptation (n D 42), and virulence (n D 61), with IS481 and ISL3 being the most represented families (Figure 2C). The abundance of IS elements was positively correlated with genome size for *Mannheimia* spp., *Haemophilus* spp., and *Histophilus* spp., but not for *Glaesserella* spp., *Actinobacillus* spp., *Aggregatibacter* spp., and *Pasteurella* spp. (Figure 2B). Alignment of *M. haemolytica* genomes (species with many ISs) compared to alignment of *A. actinomycetemcomitans* genomes (species with few ISs) revealed, based on synteny analysis, numerous internal rearrangements in genomes possessing a higher number of IS copies compared with those with a lower number of ISs (Supplementary Figure 3), which might have an impact on the genetic organization of these species.

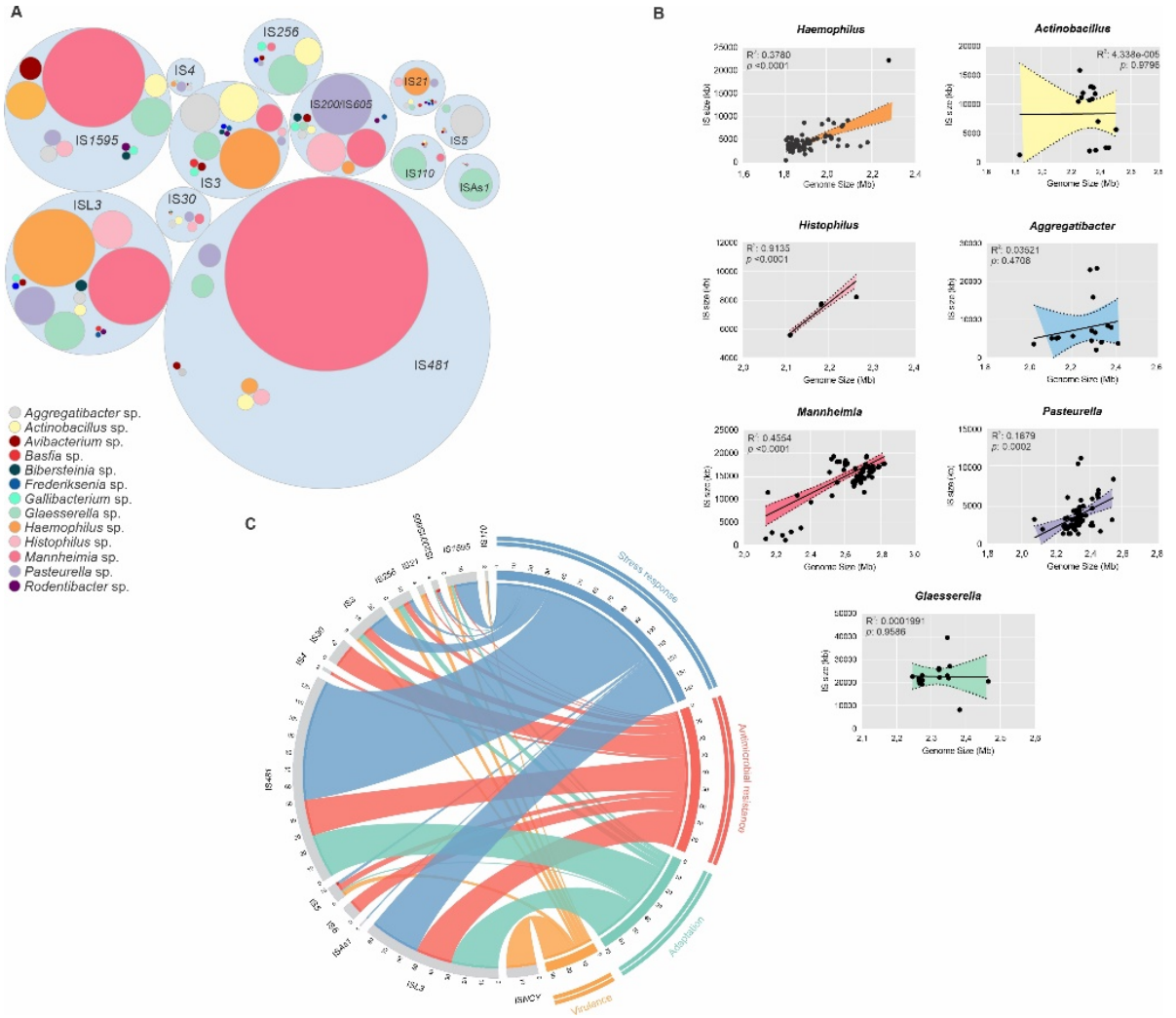

Figure 2 | Dissemination, impact in genome size and genetic context of insertion sequences (ISs). (A) Hierarchic organization of ISs distribution around the Pasteurellaceae species, colored by genus as shown in the legend. (B) Correlation graph between genome sizes and ISs grouped by genus. The x-axis indicates the genome size and the y-axis indicates the IS size in kilobases. Shaded regions indicate the 95% confidence interval according to the Pearson correlation coefficient. (C) Circular visualization of ISs context in four classes according to their flanking genes: Stress response, antimicrobial resistance, adaptation, and virulence (Clockwise direction). Inner connections represent the connection between IS families (anti-clockwise direction) and the function of the flanking genes. Values outside of the ring represent the total number of the IS elements from the respective connection.

Comparative Analysis Reveals High Diversity of Prophages in the Pasteurellaceae

Using PHASTER and Prophage Hunter, we mapped 2,939 prophage-like elements within our genome dataset (Supplementary Table 4, 5). Of these, 1,398 were classified as intact, questionable, or incomplete by PHASTER, and 1,541 were classified as active or ambiguous using Prophage Hunter (Supplementary Figure 4A). For prophage-like elements classified as intact and active from PHASTER and Prophage Hunter, respectively, we delimited complete prophages comprising eleven different viral species, identified in 193 insertions in 91 Pasteurellaceae genomes (Supplementary Table 6 and Supplementary Figure 4B). Manual inspection of sequences identified by PHASTER and Prophage Hunter as

incomplete/questionable/ambiguous, as well as complete prophages not matching any reported phage for the family, further identified possible novel prophage species, beyond those previously reported in the Pasteurellaceae (Supplementary Table 7). This approach identified 23 putative novel prophages in ten different genera (Supplementary Table 8), which exhibit the potential to encode proteins (Open Reading Frames- ORFs) necessary for their assembly and replication (Figure 3A). Whole-sequence alignment and synteny analysis using known Pasteurellaceae phages demonstrated that the predicted novel phages are new for this family (Supplementary Figures 4C, 5). These novel phages, predicted to belong to the *Myoviridae* (69%) and *Syphoviridae* (31%) families (Supplementary Table 8), are disseminated in different genomes in our dataset (Supplementary Figure 4D), with the most common being those designated here as *Haemophilus* phage GHA9 and *Mannheimia* phage 38599, and several representing the first report of phage in some of the Pasteurellaceae species (Supplementary Figure 4E). In some *M. haemolytica* and *A. actinomycetemcomitans* genomes, poly- insertions were noted (Supplementary Figure 6). Combining our predicted novel prophage sequences with those previously reported for the Pasteurellaceae, overview analysis of the complete dataset revealed that the average size ranged from 31 kb (in *Bibersteinia* spp.) to 47 kb (in *Haemophilus* spp.), with between 30 and 136 ORFs and GC contents of 38– 44% (Figure 3B). The average GC contents were similar to those of the genomes (40% _ 2) and the encoded proteins were predicted to be primarily involved in structure/assembly, transcriptional regulation, and recombination/replication, as well as some unknown function (Figure 3B). All prophages belonged to either the *Myoviridae* (73.8%) or *Syphoviridae* (26.2%) family (Supplementary Figure 4F). By comparison to closely related prophages, 83.3% are predicted to be temperate and 16.7% lytic (Figure 3C). Phylogenomic analysis revealed two distant clades, both containing monophyletic groups. None of the putative novel prophages grouped with previously reported Pasteurellaceae phages (cluster with 100% identity), confirming the novelty of our findings (Figure 3D). Results of VConTACT analysis further support the viral relationships among the published Pasteurellaceae phages, indicating four different clusters (according to the viral family), with homogeneous groups, found for *Aggregatibacter* and *Mannheimia*, and heterogeneous groups for *Haemophilus*, *Mannheimia*, and *Pasteurella* (Supplementary Figure 6). These results agree with the phylogenomic analysis, suggesting a strong evolutionary relationship amongst Pasteurellaceae phages

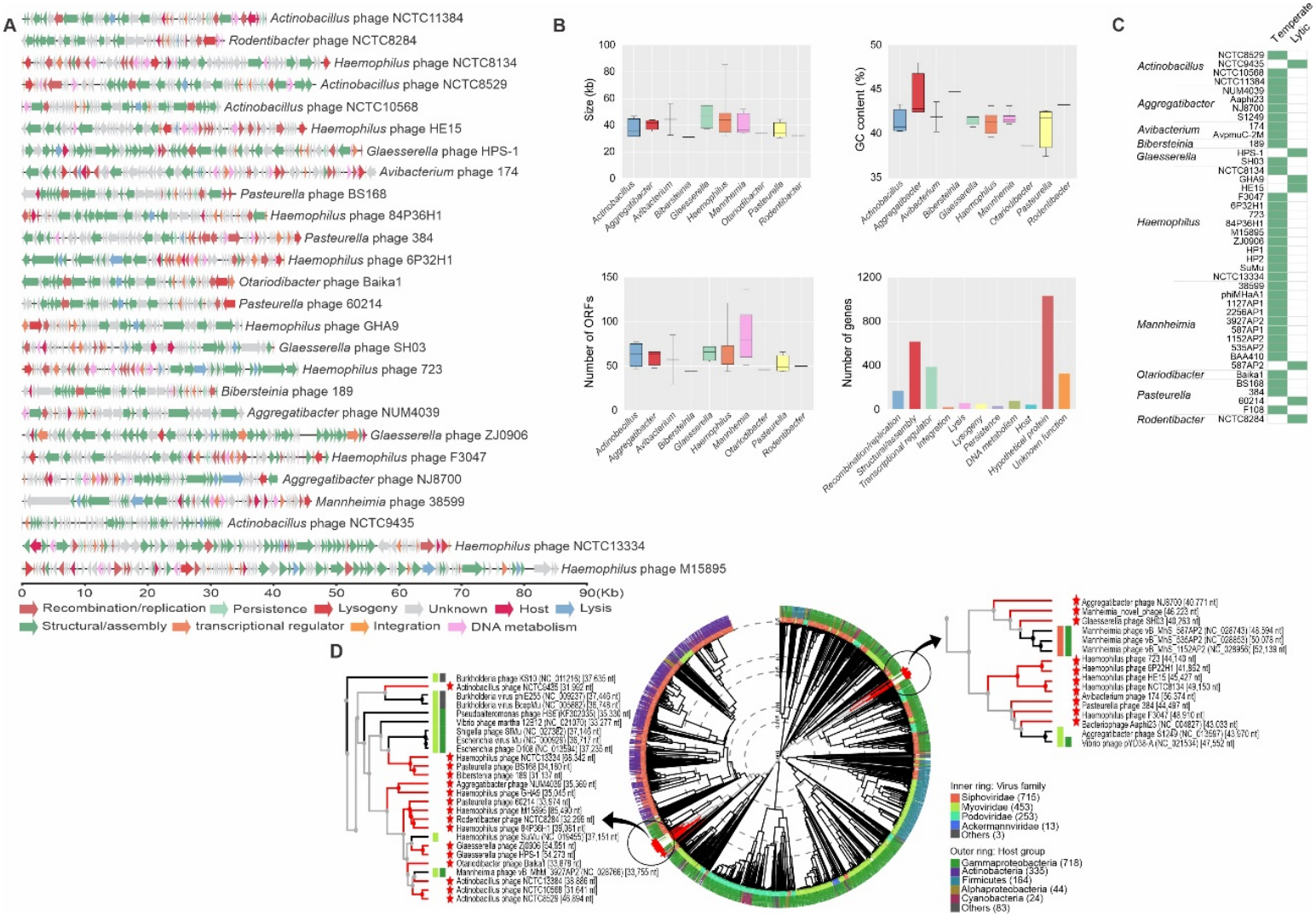

Figure 3 | The diversity of prophage elements integrated into Pasteurellaceae genomes. (A) Representation of novel prophage elements found integrated into Pasteurellaceae genomes. Prophage size is indicated in the scale bar (in kilobases) and ORF function is represented by arrows colored below the figure. (B) General overview of complete and novel prophages grouped by genus according to phage size (top-left graph), GC content (top-right graph), ORF content (bottom-left graph), and gene function (bottom-right graph). (C) Lifestyle classification (temperate or lytic) of complete and novel prophages are shown for all of the prophages in this study. (D) Phylogenomic tree analysis of novel prophages and references phages for Pasteurellaceae generated on the VipTree website. Colored rings show the families of viruses (inner rings) and host groups (outer rings). The length of the branch is log-scaled. The red stars represent the novel prophages found in this study.

Pasteurellaceae Genomes Contain Heterogeneous Groups of Disseminated Integrative and Conjugative Elements

OriTFinder analysis identified possible ICEs in our dataset. Results indicated several regions with high potential for self-transferability in 126 genomes comprising ten genera (Supplementary Table 9 and Supplementary Figure 8A). Using ICEfinder and MegaBLAST against known Pasteurellaceae ICEs (Supplementary Table 10), we identified nine previously reported ICEs in the genomes. We additionally found evidence of 20 putative novel ICEs (Supplementary Table 11), which exhibit typical modular structures, with blocs of core genes related to ICE replication and dissemination interspersed with cargo genes encoding functions that may benefit the host bacterium (such as resistance or virulence-related genes) (Figure 4A). Most ICEs are preferentially integrated into tRNA sites and encode an integrase belonging to the Xer family and a MOB_H relaxase (Supplementary Table 11 and Supplementary Figure 8B). Whole sequence alignment and synteny analysis with previously reported Pasteurellaceae ICEs demonstrated the novelty of the 20 putative ICEs (Supplementary Figures 8C, 9). Collective analysis of the previously reported and novel ICEs indicated that they ranged from 16 to 78 kb, encoding 23– 107 ORFs with GC contents from 37 to 41% (averaging 40%, similar to the genomes). Most of the encoded proteins have predicted functions related to ICE replication/dissemination, as well as antimicrobial and/or heavy-metal resistance, however, few virulence genes were found (Figure 4B). Using the key genes *int*, *parA*, and *traD* (where present), we generated phylogenies to determine evolutionary relationships between the various ICE and identified conserved clusters within some genera which encompasses species that may cohabit in the host, such as Pasteurella spp., *Mannheimia* spp. and *Histophilus* spp., and other groups in *Haemophilus* spp. and *Aggregatibacter* spp. (Figure 4C). The *parA* gene was the most informative for tracing the evolutionary history of these ICEs. Results also indicate the presence of putative novel ICEs in seven of the Pasteurellaceae species (Supplementary Figure 8D). Network analysis revealed that some related ICEs found in the Pasteurellaceae are heterogeneous and widespread among species, e.g., the cluster of ICEs (not yet assigned an ICE family designation) found in *M. haemolytica*, *P. multocida*, and *H. somni*, and the ICE*Hin1056* family of ICEs found in *H. influenzae*, *Haemophilus parainfluenzae*, *A. pleuropneumoniae*, and *Haemophilus ducreyi*. By contrast, some ICEs were found exclusively in *A. actinomycetemcomitans* genomes and do not connect with any other

group (Figure 4D). In several *H. ducreyi* isolates (GHA3, GHA5, GHA8, and GHA9), two coexisting ICEs (ICE*Hdu2* and ICE*Hin1056*) were identified (data not shown).

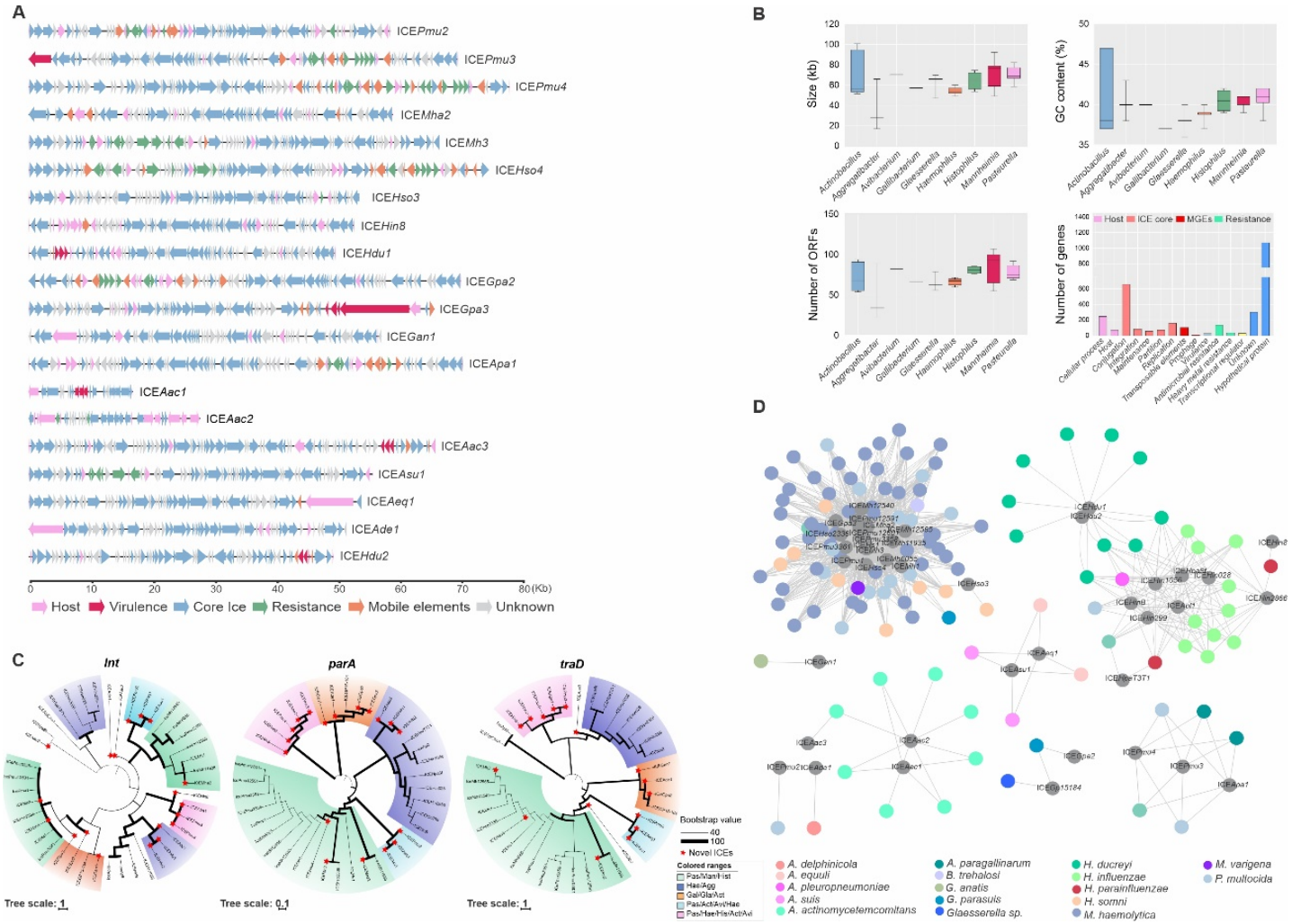

Figure 4 | Heterogeneous groups of integrative and conjugative elements (ICEs). (A) Representation of novel ICEs found integrated into Pasteurellaceae genomes. ICE size is indicated in the scale bar (in kilobases) and ORF functions are represented by arrows colored below the figure. (B) General overview of reported and novel ICEs of the family grouped by genus according to ICE size (top-left graph), GC content (top-right graph), ORF content (bottom-left graph), and gene function (bottom-right graph). (C) The evolutionary history of integrase (*int*), topoisomerase (*parA*), and coupling protein (*traD*) genes from ICEs inferred by using the Maximum Likelihood method based on the General Time Reversible model. The tree is drawn to scale, with branch lengths in the same units as those of the evolutionary distances used to infer the phylogenetic tree. Colored clusters represent conserved species groups among the trees. Bootstrap values are represented by the line thickness (see legend in the figure). (D) Network dispersion analysis of the ICEs among the Pasteurellaceae species (host genomes) represented in the species group. ICEs are displayed in dark gray circles with respective names.

Plasmids Are a Miscellaneous Class of Mobile Genetic Element in Pasteurellaceae

Plasmids are extrachromosomal MGEs that contribute significantly to AMR gene dissemination by HGT (Rodríguez- Beltrán et al., 2021). For our analysis, we retrieved 162 complete Pasteurellaceae plasmid sequences from the NCBI RefSeq database (Supplementary Table 12), comprising plasmids from worldwide representatives of 22 species, with *Glaesserella parasuis*, *P. multocida*, and *A. pleuropneumoniae* having the most entries (Supplementary Figure 10). Although all available plasmids are listed in Supplementary Table 12, where different accession numbers exist for the same plasmid, only one representative sequence of each was included in our analysis to avoid bias. Of the 151 different plasmids analyzed, the smallest was 1 kb and the largest 325 kb. The number of ORFs ranged from 1 to 353, with GC contents from 31 to 61% (average of 41%). Using MOBscan, plasmids were classified according to the type of relaxase encoded, with most assigned to the MOB_P, MOB_Q, MOB_V, and MOB_F families (Figure 5A), whereas 52 were designated as potentially non-mobilizable. Results of phylogenetic analysis of the different MOB genes revealed that, even within families, there are polyphyletic clusters, indicating the wide diversity of these sequences (Smillie et al., 2010) (Figure 5B and Supplementary Figure 11). Whole-sequence alignments of the potentially non-mobilizable plasmids revealed four clusters of related, but not identical, plasmids present in multiple species (Figure 5C), possibly indicating host-specific divergence following the loss of mobilization function. Notably, four particular plasmids were present in multiple Pasteurellaceae species known to infect different animal hosts, i.e., pIG1 (Wright et al., 1997), pB1002 (San Millan et al., 2010), pB1001/p780 (San Millan et al., 2010; Li Y. et al., 2018), and pB1000 (San Millan et al., 2010; Gangaiah et al., 2016; Bossé et al., 2017), the last of which is found in five species including the human pathogens *H. influenzae* and *H. ducreyi*, indicating a One Health concern (Figure 5D).

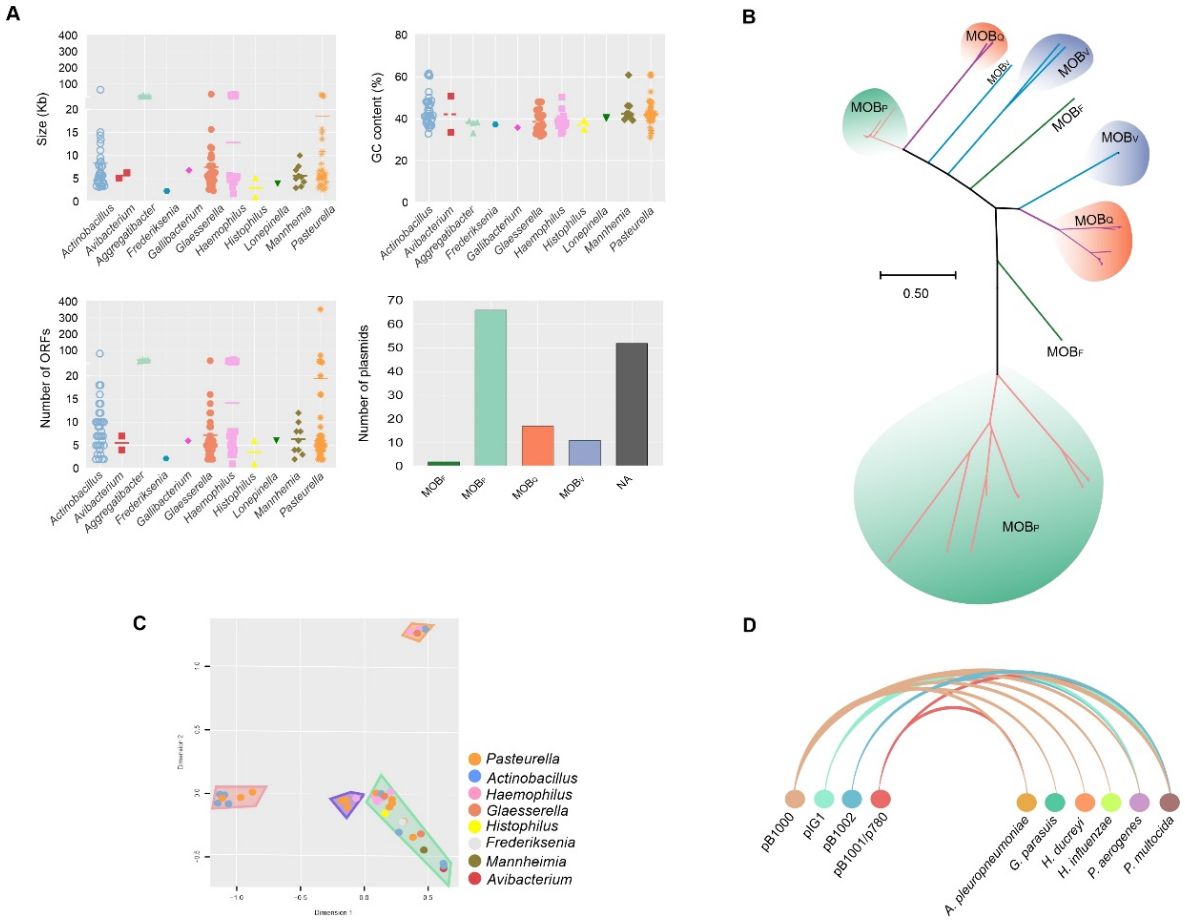

Figure 5 | General characteristics and clustering of plasmids found in the Pasteurellaceae family. (A) A general overview of plasmids in the Pasteurellaceae family grouped by genera according to plasmid size (top-left graph), GC content (top-right graph), ORF content (bottom-left graph), and relaxase family (bottom-right graph). (B) Evolutionary history of mob genes from plasmids inferred by using the Maximum Likelihood method based on the General Time Reversible model. The tree is drawn to scale, with branch lengths measured in the number of substitutions per site. (C) A multidimensional graph for analysis of the potentially non-mobilizable plasmid by sequence comparison. Clusters are highlighted in the graph in color-codes that represent the taxonomic group present in that taxon of plasmids. (D) Arc diagram representing four plasmids identified in different species/genomes, pB1000, pIG1, pB1002, and pB1001/pB780 (there is no deposit of the plasmid pB1000 identified in *A. pleuropneumoniae*, however, this has already been previously reported (Bossé et al., 2017).

The Role of Mobile Genetic Elements in the Dissemination and Acquisition of Antimicrobial Resistance Genes in the Pasteurellaceae

Comprehensive analysis of all Pasteurellaceae chromosome and plasmid sequences in our datasets revealed a total of 33 different AMR genes were mapped to 478 locations onto 131 genomes from 10 genera (Supplementary Figure 12A). Genes encoding resistance to aminoglycosides, tetracyclines, and sulfonamides were the most represented classes identified (Supplementary Figure 12B). Multiple AMR genes were found in many genomes, and 371 of the 478 AMR genes were associated with MGEs (Supplementary Figure 12C). Also, a wide diversity of AMR genes has been found in species from animal reservoirs such as *P. multocida*, *M. haemolytica* and *Bibersteinia trehalosi*. However, the same was not observed for human pathogens. Determination of TE genetic context with regards position upstream, downstream, or

interrupting ORFs mediating AMR (using the dataset shown in Figure 2C and Supplementary Table 3), we identified ten IS families (ISL3, IS481 and IS30 being most prevalent) mapping to such sites (Figure 6A). In some *M. haemolytica* genomes, IS*481* interrupts and potentially impacts the macrolide-resistance gene *macB* and the fluoroquinolone (norfloxacin and enoxacin) resistance gene *mdtH*. IS30 in *B. trehalose* interrupts *marB*, a repressor of the *marRAB* operon involved in activation of AMR and oxidative stress genes (Ariza et al., 1994) (Figure 6A). Members of the Tn*3*, Tn*5*, and Tn*10* transposon families were mapped to ICEs carrying sulfonamide, phenicol, and aminoglycoside resistance genes (Figure 6B). Although we found prophage-like elements carrying AMR genes in the genomes of *H. influenzae* and *A. indolicus*, no AMR genes were found in our dataset of complete prophages (Supplementary Table 13). In contrast, a total of 33 different AMR genes were mapped to 195 locations onto 103 plasmids (68% of the plasmids), and a total of 26 different AMR genes were mapped to 126 locations onto 28 ICEs (65% of the ICEs), including ICEs disseminated among different species of the family, with genes encoding resistance to 10 and 8 classes of antimicrobials, respectively (Supplementary Figures 13A, B and Supplementary Table 13). In plasmids, genes for resistance to aminoglycosides and sulfonamides were most prevalent, whereas genes for resistance to aminoglycosides and tetracyclines were the most common in ICEs (Supplementary Table 13). We assessed the contribution of the ICEs and plasmids carrying AMR genes compared to their respective chromosome, and we found that the majority of AMR genes are exclusively associated with ICEs (Figure 6C). Some classes of AMR genes were exclusively associated with specific elements, e.g., genes for resistance to rifamycin, lincosamide, and N-glycosides were only found in plasmids, and fluoroquinolone resistance genes only in ICEs (Figure 6D). But most classes of AMR genes were distributed among both ICEs and plasmids (Figure 6D) and several plasmids and ICEs encoded multiple AMR genes (Supplementary Figure 13C). Copies of the chromosomally encoded *kpnH* gene, mediating resistance to various antimicrobials such as azithromycin, ertapenem, imipenem, norfloxacin, and polymyxin B (colistin) (Srinivasan et al., 2014), found in human and animal pathogens share 75% nucleotide identity. Whereas, some plasmid and ICE-encoded resistance genes, such as *tetB*, *catII*, and $bla_{ROB\text{-}1}$, show > 99% nucleotide identity between human and animal pathogens. However, only the pB1000 plasmid (carrying $bla_{ROB\text{-}1}$) shows clear evidence of transfer, with identical sequences found in pathogens from five different

host species, including humans (Figure 5D). In contrast, many AMR genes were found exclusively in human pathogens (e.g., *hmrM*, *catS*, *lpsA*, and bla_{TEM-1}) or animal pathogens (e.g., *floR*, *strA*, *strB dfrA*, *ermF*, and bla_{OXA}), despite being MGE-associated. In total, 87.24% (n = 629) of AMR genes were found in animal and 12.76% (n = 92) in human pathogens. Some AMR genes associated with MGEs were more globally distributed than others in our dataset, e.g., the bla_{ROB-1}, *floR*, *strA*, *sul2*, and *tetB* genes were more abundant in isolates from Europe and Asia (Figure 6E). In contrast, 28 AMR genes were associated with specific localities (Supplementary Figure 13D). Neutrality analysis of the most prevalent MGE associated AMR genes per geographic location indicated possible recent selection for resistance to sulfonamides (*sul2*) in Europe (Tajima's D –2.54153, p < 0,001; Fu and Li D_: –4.3437, p < 0.02; Fu and Li's F_ test statistic: –4.43062, p < 0.02) and tetracyclines (*tetB*) in Asia (Tajima's D: –1.27745; Fu and Li's D_: –1.27336, P < 0.02; Fu and Li's F_ test statistic: –1.38944, P < 0.02).

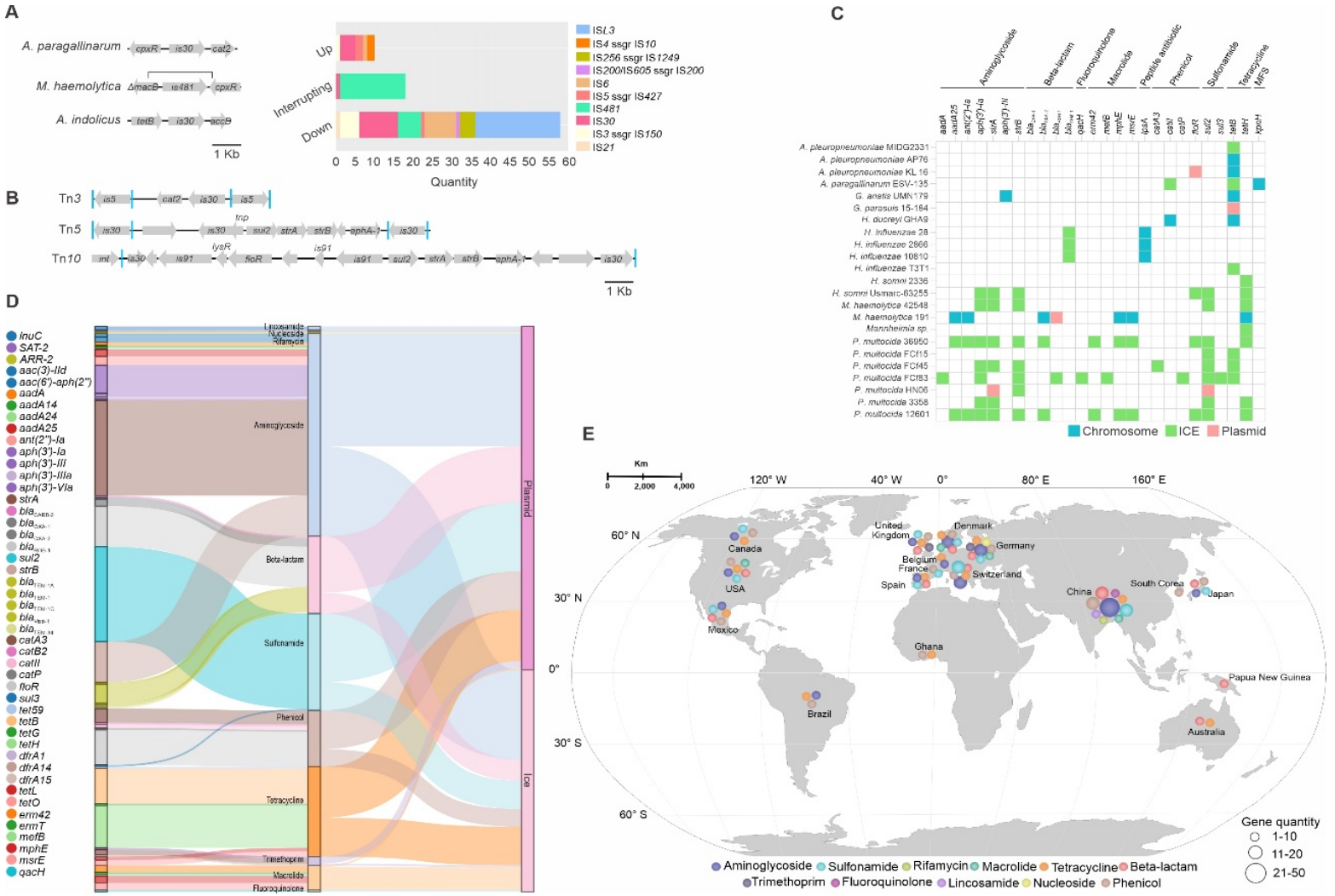

Figure 6 | Mobile genetic elements (MGEs) role in dissemination of antimicrobial resistance (AMR) genes. (A) Three representative ISs and AMR gene contexts found in this study. Figure highlights, in order, ISs from three different species (genomes) upstream, interrupting, and downstream of AMR genes. The bar graph (top-left graph) shows the values from the previous context for ten IS families. (B) Representation of the Tn*3*, Tn*5*, and Tn*10* transposon families carrying AMR genes. Squares in blue identify direct repeats of the IS elements. The name of the AMR gene is shown inside the arrows. (C) Comparison of MGEs (green and pink) and their host genomes (in blue) carrying AMR genes. The name of AMR genes and their classes are shown at the top of the table. (D) Sankey diagram representing the diversity of AMR genes and their classes; the distribution of these genes between plasmids and ICEs. (E) Geographic distribution of AMR classes found within MGEs, color-coded as to their AMR classes. The scale below the map indicates the quantity of AMR genes found for each class.

Discussion

The Pasteurellaceae family is composed of a diverse group of Gram-negative bacteria comprising commensals and pathogens of human and animal hosts. These bacteria are part of the normal microbiota of several animals, including humans (Wang et al., 2010; Wilson and Ho, 2013) and can mediate HGT via conjugative mobile elements, with some species also competent for natural transformation (Sinha et al., 2008). The dissemination of microbial MDR determinants represents an increasingly significant problem. However, most efforts are focused on understanding the epidemiology of MDR strains rather than mechanisms of dissemination of the AMR genes by MGEs. In our investigation of the mobilome, we discovered a vast repertoire of MGEs in Pasteurellaceae, some of which were quite similar and distributed across taxa. Our analyses also indicated that the co-occurrence of several types of MGEs (prophages, ICEs, and ISs) is frequent, as shown in some *M. haemolytica*, *H. ducreyi*, *H. influenzae*, *A. actinomycetemcomitans*, and *Avibacterium paragallinarum* strains. All of these discoveries, based on the existence of key genes carried by these elements, highlight the relevance of MGEs in the evolution, diversity, and ecology of Pasteurellaceae. By systematically investigating the resistome-associated mobilome in publicly available complete Pasteurellaceae genomes and plasmids, our study reveals the importance of MGEs in the dispersion of AMR genes within this family. We recognize that due to the type of genomes considered, we did not capture the whole diversity of MGEs and AMR genes, though many efforts have shown the limitation of the characterization/discovery of MGEs in draft genomes (Gonçalves et al., 2020a, b). However, we have presented the most comprehensive and curated dataset of the mobilome found within 345 complete genomes of the Pasteurellaceae, comprised of 10,820 IS elements, 43 complete prophages, 43 ICEs, and 162 plasmid sequences. Our findings expand the diversity of MGEs for the family, including the first report of prophages and ICEs for some species. We identified diverse groups of MGEs, both adapted to the host bacterial genome and highly disseminated throughout the family. Importantly, we demonstrated the role of ICEs, plasmids, prophages, and transposons in the dissemination of AMR genes in members of the Pasteurellaceae family. The occurrence of AMR and in some cases MDR has been documented in the Pasteurellaceae (Archambault et al., 2011; Woolums et al., 2018; Van Driessche et al., 2020) but the association of AMR genes with MGEs has received comparatively little attention. Despite suitable management, including biosecurity and vaccines, the use

of antimicrobial agents to control infections caused by pathogenic Pasteurellaceae is widespread (Michael et al., 2018). However, the emergence of multidrug-resistant bacteria increasingly makes the use of antimicrobials problematic. We discovered that most AMR genes found in Pasteurellaceae genomes are associated with ICEs and plasmids since few AMR genes were found in genomes lacking these MGEs. Furthermore, most Pasteurellaceae ICEs and plasmids have one or more AMR genes, and these MGEs are, in most cases, responsible for the observed MDR phenotypes, which have a direct influence on the fitness of the species in this family in their environment. Antimicrobial resistance might be regarded as a colonization factor in the presence of drugs. The dissemination of AMR genes via MGEs in Pasteurellaceae might be interpreted as a mechanism by bacterial species to stand out in a microbial community and become more effective during host colonization (Martínez and Baquero, 2002). The repertoire of AMR gene found in the Pasteurellaceae mediates resistance to highly important antimicrobials for human and animal treatments (aminoglycosides, beta-lactams, phenicols, sulfonamides, tetracyclines, and lincosamides) (OIE, 2017; WHO, 2019). The gene diversity in pathogens from animal reservoirs was higher than that seen in human pathogens, which is consistent with the dispersion of MGEs among bacterial species. Although our results have shown that most AMR genes are associated with MGEs, dissemination of these elements from veterinary to human pathogens, a concern that is directly related to the One Health concept (Hernando-Amado et al., 2019), does not appear to be common within the Pasteurellaceae, although our analyzes have shown that some ICEs are widely disseminated among Pasteurellaceae species. One example, noted previously by others (Alvaro et al., 2009; San Millan et al., 2010; Bossé et al., 2017) and seen again in this study, is for the beta-lactam resistance plasmid, pB1000. This plasmid has been identified in both human and veterinary Pasteurellaceae pathogens, including *P. multocida*, one of the few members of this family capable of infecting a range of animals, including humans. It should be noted that our results do not preclude the possibility of transfer of MGE-associated AMR determinants from members of the Pasteurellaceae to other co-resident bacterial species found within the same animal host, some of which may be zoonotic and therefore present a greater threat to human health (Köck et al., 2021). The use of genomic data to track global AMR has revolutionized diagnostic microbiology, mostly due to improvements in sequencing technologies and increasing numbers of publicly available genomes, providing an

opportunity to expand and align with a One Health surveillance framework (Hendriksen et al., 2019). For AMR surveillance purposes, draft genome sequences have been shown to be sufficient for the identification of genes conferring resistance to a number of antimicrobials, including for members of the Pasteurellaceae (Bossé et al., 2017). However, short-read sequencing is not capable of assembling across repeat regions, common in MGEs, and does not give an overall picture of the abundance of these elements within genomes.

Conclusion

In conclusion, the MGEs described in this study reveal the significance of these elements in the ecology of Pasteurellaceae species, mostly regarding the dissemination of AMR genes. To our knowledge, the resistome-associated mobilome data generated in our study represents the most comprehensive description of MGE-associated AMR genes for the Pasteurellaceae, providing a valuable resource for future research. Such knowledge is critical for the effective design and interpretation of experimental data to elucidate mechanisms of AMR and to facilitate the development of effective strategies to control resistant bacteria. Lastly, we reinforce that similar approaches, as employed here, can be used to inform future decisions toward the surveillance of AMR genes and to gain insights into their microbial ecology and evolution.

Data availability statement

The datasets presented in this study can be found in online repositories. The names of the repository/repositories and accession number(s) can be found in the Supplementary Material for this manuscript which is online available at: https: //doi.org/10.6084/m9.figshare.c.5538240.v2.

Funding

This work was supported by the Conselho Nacional de Desenvolvimento Científico e Tecnológico-CNPq (Process Nos. 141328/2018-5 and 143132/2019-9), Coordenacão de Aperfeiçoamento de Pessoal de Nível Superior/Programa de Excelência Acadêmica-Finance Code 001 (CAPES ProEx grant 23038.019105/2016-86) and Fundação de Amparo à Pesquisa do Estado de Minas Gerais—FAPEMIG for the

financial support. This work was also supported by the UK Biotechnology and Biological Sciences Research Council (Grants BB/S002103/1 and BB/S020543/1).

References

Alcock, B. P., Raphenya, A. R., Lau, T. T. Y., Tsang, K. K., Bouchard, M., Edalatmand, A., et al. (2020). CARD 2020: antibiotic resistome surveillance with the comprehensive antibiotic resistance database. Nucleic Acids Res. 48, D517–D525. doi: 10.1093/nar/gkz935

Alvaro, S. M., Antonio, E. J., Belen, G., Laura, H., Nerea, G., Montserrat, L., et al. (2009). Multiresistance in *Pasteurella multocida* is mediated by coexistence of small plasmids. Antimicrob. Agents Chemother. 53, 3399–3404. doi: 10.1128/ AAC.01522-08

Archambault, M., Harel, J., Gouré, J., Tremblay, Y. D. N., and Jacques, M. (2011). Antimicrobial susceptibilities and resistance genes of canadian isolates of *Actinobacillus pleuropneumoniae*. Microb. Drug Resist. 18, 198–206. doi: 10.1089/mdr.2011.0150

Ariza, R. R., Cohen, S. P., Bachhawat, N., Levy, S. B., and Demple, B. (1994). Repressor mutations in the *marRAB* operon that activate oxidative stress genes and multiple antibiotic resistance in *Escherichia coli*. J. Bacteriol. 176, 143L–148. doi: 10.1128/jb.176.1.143-148.1994

Arndt, D., Grant, J. R., Marcu, A., Sajed, T., Pon, A., Liang, Y., et al. (2016). PHASTER: a better, faster version of the PHAST phage search tool. Nucleic Acids Res. 44, W16–W21. doi: 10.1093/nar/gkw387

Besemer, J., Lomsadze, A., and Borodovsky, M. (2001). GeneMarkS: a self-training method for prediction of gene starts in microbial genomes. Implications for finding sequence motifs in regulatory regions. Nucleic Acids Res. 29, 2607–2618. doi: 10.1093/nar/29.12.2607

Binns, D., Dimmer, E., Huntley, R., Barrell, D., O'Donovan, C., and Apweiler, R. (2009). QuickGO: a web-based tool for Gene Ontology searching. Bioinformatics 25, 3045–3046. doi: 10.1093/bioinformatics/btp536

Blackall, P. J., and Turni, C. (2020). *Actinobacillus*. Bergey's Man. Syst. Archaea Bact. 2020, 1–14. doi: 10.1002/9781118960608.gbm01197.pub2

Bolduc, B., Jang, H., Bin, Doulcier, G., You, Z.-Q., Roux, S., et al. (2017). vConTACT: an iVirus tool to classify double-stranded DNA viruses that infect Archaea and Bacteria. PeerJ. 5, e3243–e3243. doi: 10.7717/peer j.3243

Bortolaia, V., Kaas, R. S., Ruppe, E., Roberts, M. C., Schwarz, S., Cattoir, V., et al. (2020). ResFinder 4.0 for predictions of phenotypes from genotypes. J. Antimicrob. Chemother. 75, 3491–3500. doi: 10.1093/jac/dkaa345

Bossé, J. T., Li, Y., Rogers, J., Fernandez Crespo, R., Li, Y., Chaudhuri, R. R., et al. (2017). Whole genome sequencing for surveillance of antimicrobial resistance in *Actinobacillus pleuropneumoniae*. Front. Microbiol. 8:311. doi: 10.3389/ fmicb.2017.00311

Carr, V. R., Shkoporov, A., Hill, C., Mullany, P., and Moyes, D. L. (2021). Probing the mobilome: discoveries in the dynamic microbiome. Trends Microbiol. 29, 158–170. doi: 10.1016/j.tim.2020.05.003

Carr, V. R., Witherden, E. A., Lee, S., Shoaie, S., Mullany, P., Proctor, G. B., et al. (2020). Abundance and diversity of resistomes differ between healthy human oral cavities and gut. Nat. Commun. 11:693. doi: 10.1038/s41467-020-14422-w

Chan, P. P., and Lowe, T. M. (2019). tRNAscan-SE: Searching for tRNA Genes in Genomic Sequences. Methods Mol. Biol. 1962, 1–14. doi: 10.1007/978-1-4939-9173-0_1

Che, Y., Yang, Y., Xu, X., Bˇrinda, K., Polz, M. F., Hanage, W. P., et al. (2021). Conjugative plasmids interact with insertion sequences to shape the horizontal transfer of antimicrobial resistance genes. Proc. Natl. Acad. Sci. 118:e2008731118. doi: 10.1073/pnas.2008731118

Chen, Y., Ye, W., Zhang, Y., and Xu, Y. (2015). High speed BLASTN: an accelerated MegaBLAST search tool. Nucleic Acids Res. 43, 7762–7768. doi: 10.1093/nar/ gkv784

Cury, J., Touchon, M., and Rocha, E. P. C. (2017). Integrative and conjugative elements and their hosts: composition, distribution and organization. Nucleic Acids Res. 45, 8943–8956. doi: 10.1093/nar/gkx607

Czajkowski, R. (2019). May the Phage be With You? prophage-like elements in the genomes of soft rot Pectobacteriaceae: *Pectobacterium* spp. and *Dickeya* spp. Front. Microbiol. 10:138. doi: 10.3389/fmicb.2019.00138

Darling, A. C. E.,Mau, B., Blattner, F. R., and Perna, N. T. (2004).Mauve: Multiple Alignment of Conserved Genomic Sequence With Rearrangements. Genome Res. 14, 1394–1403. doi: 10.1101/gr.2289704

Finn, R. D., Bateman, A., Clements, J., Coggill, P., Eberhardt, R. Y., Eddy, S. R., et al. (2014). Pfam: the protein families database. Nucleic Acids Res. 42, D222–D230. doi: 10.1093/nar/gkt1223

Frost, L. S., Leplae, R., Summers, A. O., and Toussaint, A. (2005). Mobile genetic elements: the agents of open source evolution. Nat. Rev. Microbiol. 3:722. doi: 10.1038/nrmicro1235

Fu, Y. X., and Li, W. H. (1993). Statistical tests of neutrality of mutations. Genetics 133, 693L–709.

Gangaiah, D., Marinov, G. K., Roberts, S. A., Robson, J., and Spinola, S. M. (2016). Draft whole-genome sequence of *Haemophilus ducreyi* strain AUSPNG1, isolated from a cutaneous ulcer of a child from papua New Guinea. Genome Announc. 4, e1661–e1615. doi: 10.1128/genomeA.01661-15

Garcillán-Barcia, M. P., Redondo-Salvo, S., Vielva, L., and de la Cruz, F. (2020). MOBscan: Automated Annotation of MOB Relaxases BT - Horizontal Gene Transfer: Methods and Protocols. Methods Mol. Biol. 2020, 295–308. doi: 10. 1007/978-1-4939-9877-7_21

Gilchrist, C. L. M., and Chooi, Y.-H. (2021). clinker & clustermap.js: automatic generation of gene cluster comparison figures. Bioinformatics 2021:7. doi: 10. 1093/bioinformatics/btab007

Gonçalves, O. S., Campos, K. F., de Assis, J. C. S., Fernandes, A. S., Souza, T. S., do Carmo, et al. (2020a). Transposable elements contribute to the genome plasticity of *Ralstonia solanacearum* species complex. Microb. Genomics 2020:mgen000374. doi: 10.1099/mgen.0.000374

Gonçalves, O. S., de Queiroz, M. V., and Santana, M. F. (2020b). Potential evolutionary impact of integrative and conjugative elements (ICEs) and genomic islands in the *Ralstonia solanacearum* species complex. Sci. Rep. 10:12498. doi: 10.1038/s41598-020-69490-1

Hendriksen, R. S., Bortolaia, V., Tate, H., Tyson, G. H., Aarestrup, F. M., and McDermott, P. F. (2019). Using genomics to track global antimicrobial resistance. Front. Public Heal. 7:242. doi: 10.3389/fpubh.2019.00242

Hernando-Amado, S., Coque, T. M., Baquero, F., and Martínez, J. L. (2019). Defining and combating antibiotic resistance from One Health and Global Health perspectives. Nat. Microbiol. 4, 1432–1442. doi: 10.1038/s41564-019- 0503-9

Juhas, M., Power, P. M., Harding, R. M., Ferguson, D. J. P., Dimopoulou, I. D., Elamin, A. R. E., et al. (2007). Sequence and functional analyses of *Haemophilus* spp. genomic islands. Genome Biol. 8:R237. doi: 10.1186/gb-2007-8-11-r237

Juraschek, K., Borowiak, M., Tausch, S. H., Malorny, B., Käsbohrer, A., Otani, S., et al. (2019). CLUSTAL W: improving the sensitivity of progressive multiple sequence alignment through sequence weighting, position-specific gap penalties and weight matrix choice. Nucleic Acids Res. 5, 102. doi: 10.3390/ microorganisms9030598

Köck, R., Herr, C., Kreienbrock, L., Schwarz, S., Tenhagen, B.-A., and Walther, B. (2021). Multiresistant Gram-negative pathogens-a zoonotic problem. Dtsch. Arztebl. Int. 118:184. doi: 10.3238/arztebl.m2021.0184

Krzywinski, M., Schein, J., Birol, I., Connors, J., Gascoyne, R., Horsman, D., et al. (2009). Circos: an information aesthetic for comparative genomics. Genome Res. 19, 1639–1645. doi: 10.1101/gr.092759.109

Kumar, S., Stecher, G., Li, M., Knyaz, C., and Tamura, K. (2018). MEGA X: Molecular Evolutionary Genetics Analysis across Computing Platforms. Mol. Biol. Evol. 35, 1547–1549. doi: 10.1093/molbev/msy096

Letunic, I., and Bork, P. (2019). Interactive Tree Of Life (iTOL) v4: recent updates and new developments. Nucleic Acids Res. 2019:239. doi: 10.1093/nar/gkz239

Li, X., Xie, Y., Liu, M., Tai, C., Sun, J., Deng, Z., et al. (2018). oriTfinder: a webbased tool for the identification of origin of transfers in DNA sequences of bacterial mobile genetic elements. Nucleic Acids Res. 46, W229–W234. doi: 10.1093/nar/gky352

Li, Y., da Silva, G. C., Li, Y., Rossi, C. C., Fernandez Crespo, R., Williamson, S. M., et al. (2018). Evidence of illegitimate recombination between two Pasteurellaceae plasmids resulting in a novel multi-resistance replicon, pM3362MDR, in *Actinobacillus pleuropneumoniae*. Front. Microbiol. 9:2489. doi: 10.3389/fmicb.2018.02489

Liu, M., Li, X., Xie, Y., Bi, D., Sun, J., Li, J., et al. (2018). ICEberg 2.0: an updated database of bacterial integrative and conjugative elements. Nucleic Acids Res. 47, D660–D665. doi: 10.1093/nar/gky1123

Lopes, A., Tavares, P., Petit, M.-A., Guérois, R., and Zinn-Justin, S. (2014). Automated classification of tailed bacteriophages according to their neck organization. BMC Genomics 15:1027. doi: 10.1186/1471-2164-15-1027

Madeira, F., Park, Y. M., Lee, J., Buso, N., Gur, T., Madhusoodanan, N., et al. (2019). The EMBL-EBI search and sequence analysis tools APIs in 2019. Nucleic Acids Res. 47, W636–W641. doi: 10.1093/nar/gkz268

Marchler-Bauer, A., and Bryant, S. H. (2004). CD-Search: protein domain annotations on the fly. Nucleic Acids Res. 32, W327–W331. doi: 10.1093/nar/ gkh454

Martínez, J. L., and Baquero, F. (2002). Interactions among strategies associated with bacterial infection: pathogenicity, epidemicity, and antibiotic resistance. Clin. Microbiol. Rev. 15, 647–679. doi: 10.1128/CMR.15.4.647-679.2002

McGinnis, S., and Madden, T. L. (2004). BLAST: at the core of a powerful and diverse set of sequence analysis tools. Nucleic Acids Res. 32, W20–W25. doi: 10.1093/nar/gkh435

McNair, K., Bailey, B. A., and Edwards, R. A. (2012). PHACTS, a computational approach to classifying the lifestyle of phages. Bioinformatics 28, 614–618. doi: 10.1093/bioinformatics/bts014

Michael, G. B., Bossé, J. T., and Schwarz, S. (2018). Antimicrobial Resistance in Pasteurellaceae of Veterinary Origin. Microbiol. Spectr. 6:2017. doi: 10.1128/

microbiolspec. ARBA-0022-2017

Moleres, J., Santos-López, A., Lázaro, I., Labairu, J., Prat, C., Ardanuy, C., et al. (2015). Novel *bla*$_{ROB-1}$-bearing plasmid conferring resistance to β-Lactams in *Haemophilus parasuis* isolates from healthy weaning pigs. Appl. Environ. Microbiol. 81, 3255L–3267. doi: 10.1128/AEM.03865-14

Naushad, S., Adeolu, M., Goel, N., Khadka, B., Al-Dahwi, A., and Gupta, R. S. (2015). Phylogenomic and molecular demarcation of the core members of the polyphyletic Pasteurellaceae genera *Actinobacillus*, *Haemophilus*, and *Pasteurella*. Int. J. Genomics 2015:198560. doi: 10.1155/2015/198560

Nikaido, H. (2009). Multidrug resistance in bacteria. Annu. Rev. Biochem. 78, 119–146. doi: 10.1146/annurev.biochem.78.082907.145923

Nishimura, Y., Yoshida, T., Kuronishi, M., Uehara, H., Ogata, H., and Goto, S. (2017). ViPTree: the viral proteomic tree server. Bioinformatics 33, 2379–2380. doi: 10.1093/bioinformatics/btx157

OIE (2017). OIE annual report on antimicrobial agents intended for use in animals: better understanding of the global situation, second report. Paris. Available online at: http://www.oie.int/fileadmin/Home/eng/Our_scientific_ expertise/docs/pdf/AMR/Annual_Report_AMR_2.pdf (accessed March, 2021).

Partridge, S. R., Kwong, S. M., Firth, N., and Jensen, S. O. (2018). Mobile genetic elements associated with antimicrobial resistance. Clin. Microbiol. Rev. 31, e88–e17. doi: 10.1128/CMR.00088-17

Rankin, D. J., Rocha, E. P. C., and Brown, S. P. (2011). What traits are carried on mobile genetic elements, and why? Heredity 106, 1–10. doi: 10.1038/hdy.2 010.24

Rodríguez-Beltrán, J., DelaFuente, J., León-Sampedro, R., MacLean, R. C., and San Millán, A. (2021). Beyond horizontal gene transfer: the role of plasmids in bacterial evolution. Nat. Rev. Microbiol. 2021:1. doi: 10.1038/s41579-020- 00497-1

Rosenberg, E., DeLong, E. F., Lory, S., Stackebrandt, E., and Thompson, F. (2013). The prokaryotes: Gammaproteobacteria. Prokaryotes: Gammaproteobacteria 2013, 1–768. doi: 10.1007/978-3-642-38922-1

Rozas, J., Ferrer-Mata, A., Sánchez-DelBarrio, J. C., Guirao-Rico, S., Librado, P., Ramos-Onsins, S. E., et al. (2017). DnaSP 6: DNA Sequence Polymorphism Analysis of Large Data Sets. Mol. Biol. Evol. 34, 3299–3302. doi: 10.1093/ molbev/msx248

San Millan, A., Garcia-Cobos, S., Escudero, J. A., Hidalgo, L., Gutierrez, B., Carrilero, L., et al. (2010). *Haemophilus influenzae* clinical isolates with plasmid pB1000 bearing *bla*$_{ROB-1}$: fitness cost and interspecies dissemination. Antimicrob. Agents Chemother. 54, 1506L–1511. doi: 10.1128/AAC.01489-09

Shannon, P., Markiel, A., Ozier, O., Baliga, N. S., Wang, J. T., Ramage, D., et al.

(2003). Cytoscape: a software environment for integrated models of biomolecular interaction networks. Genome Res. 13, 2498–2504. doi: 10.1101/ gr.1239303

Siefert, J. L. (2009). Defining the Mobilome BT - Horizontal Gene Transfer: Genomes in Flux. Totowa, NJ: Humana Press, 13–27. doi: 10.1007/978-1-60327- 853-9_2

Sievers, F., and Higgins, D. G. (2014). in Clustal Omega, Accurate Alignment of Very Large Numbers of Sequences BT - Multiple Sequence Alignment Methods, ed. D. J. Russell (Totowa, NJ: Humana Press), 105–116. doi: 10.1007/978-1-62703-646-7_6

Siguier, P., Gourbeyre, E., Varani, A., and Bao Ton-Hoang, M. C. (2015). Everyman's Guide to Bacterial Insertion Sequences. Microbiol. Spectr. 3, 550– 590. doi: 10.1128/microbiolspec.MDNA3-0030-2014

Siguier, P., Perochon, J., Lestrade, L., Mahillon, J., and Chandler, M. (2006). ISfinder: the reference centre for bacterial insertion sequences. Nucleic Acids Res. 34, D32–D36. doi: 10.1093/nar/gkj014

Sinha, S., Maughan, H. L. W., and Redfield, R. (2008). "Competence, DNA Uptake and Transformation in the Pasteurellaceae," in Pasteurellaceae: Biology, Genomics and Molecular Aspects, eds P. Kuhnert and H. Christensen (Norfolk: Caister Academic Press).

Smillie, C., Garcillán-Barcia, M. P., Francia, M. V., Rocha, E. P. C., and de la Cruz, F. (2010). Mobility of plasmids. Microbiol. Mol. Biol. Rev. 74, 434L–452. doi: 10.1128/MMBR.00020-10

Soler, N., and Forterre, P. (2020). Vesiduction: the fourth way of HGT. Environ. Microbiol. 22, 2457–2460. doi: 10.1111/1462-2920.15056

Song, W., Sun, H.-X., Zhang, C., Cheng, L., Peng, Y., Deng, Z., et al. (2019). Prophage Hunter: an integrative hunting tool for active prophages. Nucleic Acids Res. 47, W74–W80. doi: 10.1093/nar/gkz380

Srinivasan, V. B., Singh, B. B., Priyadarshi, N., Chauhan, N. K., and Rajamohan, G. (2014). Role of novel multidrug efflux pump involved in drug resistance in *Klebsiella pneumoniae*. PLoS One 9:e96288. doi: 10.1371/journal.pone.0096288

Szafranski, S. P., Kilian, M., Yang, I., Bei der Wieden, G., Winkel, A., Hegermann, J., et al. (2019). Diversity patterns of bacteriophages infecting *Aggregatibacter* and *Haemophilus* species across clades and niches. ISME J. 13, 2500–2522. doi: 10.1038/s41396-019-0450-8

Tajima, F. (1989). Statistical method for testing the neutral mutation hypothesis by DNA polymorphism. Genetics 123, 585–595.

Van Driessche, L., Vanneste, K., Bogaerts, B., De Keersmaecker, S. C. J., Roosens, N., Haesebrouck, F., et al. (2020). Isolation of drug-resistant *Gallibacterium anatis* from calves with unresponsive bronchopneumonia, Belgium. Emerg. Infect. Dis.

J. 26:721. doi: 10.3201/eid2604.190962

Varani, A. M., Siguier, P., Gourbeyre, E., Charneau, V., and Chandler, M. (2011). ISsaga is an ensemble of web-based methods for high throughput identification and semi-automatic annotation of insertion sequences in prokaryotic genomes. Genome Biol. 12, R30–R30. doi: 10.1186/gb-2011-12-3-r30

Wang, C.-Y., Wang, H.-C., Li, J.-M., Wang, J.-Y., Yang, K.-C., Ho, Y.- K., et al. (2010). Invasive Infections of *Aggregatibacter* (*Actinobacillus*) *actinomycetemcomitans*. J. Microbiol. Immunol. Infect. 43, 491–497. doi: 10. 1016/S1684-1182(10)60076-X

Wheeler, T. J., and Eddy, S. R. (2013). nhmmer: DNA homology search with profile HMMs. Bioinformatics 29, 2487–2489. doi: 10.1093/bioinformatics/btt403

WHO (2019). Critically important antimicrobials for human medicine, 6th revision. Geneva: WHO.

Wilson, B. A., and Ho, M. (2013). *Pasteurella multocida*: from zoonosis to cellular microbiology. Clin. Microbiol. Rev. 26, 631L–655. doi: 10.1128/CMR.00024-13

Woolums, A. R., Karisch, B. B., Frye, J. G., Epperson, W., Smith, D. R., Blanton, J., et al. (2018). Multidrug resistant *Mannheimia haemolytica* isolated from high-risk beef stocker cattle after antimicrobial metaphylaxis and treatment for bovine respiratory disease. Vet. Microbiol. 221, 143–152. doi: 10.1016/j.vetmic. 2018.06.005

Wright, C. L., Strugnell, R. A., and Hodgson, A. L. M. (1997). Characterization of *Pasteurella multocida* plasmid and its use to express recombinant proteins in *P. multocida*. Plasmid 37, 65–79. doi: 10.1006/plas.1996.1276

Wright, G. D. (2007). The antibiotic resistome: the nexus of chemical and genetic diversity. Nat. Rev. Microbiol. 5, 175–186. doi: 10.1038/nrmicro1614

Chapter 2

To infinity and beyond: the transport of small RNAs by extracellular vesicles produced by *Actinobacillus pleuropneumoniae*

(Manuscript written according to the guidelines of the Frontiers in Microbiology journal)

Giarlã Cunha da Silva[1], Jéssica Nogueira Rosa[1], Patrícia Pereira Fontes[2], Alex Gazolla de Castro[2], Everton de Almeida Alves Barbosa[3], Hilário Cuquetto Mantovani[2], Janine Thérèse Bossé[4], Paul Richard Langford[4*] and Denise Mara Soares Bazzolli[1*]

[1]Laboratório de Genética Molecular de Bactérias, Departamento de Microbiologia, Instituto de Biotecnologia Aplicada à Agropecuária - Bioagro, Universidade Federal de Viçosa, Viçosa, Brazil.

[2]Departamento de Microbiologia, Universidade Federal de Viçosa, Viçosa, Minas Gerais, Brasil.

[3]Departamento de Bioquímica e Biologia Molecular, Universidade Federal de Viçosa, Viçosa, Minas Gerais, Brasil.

[4]Section of Paediatrics, Department of Medicine, Imperial College London, London, United Kingdom.

Abstract

Bacterial extracellular vesicles (BEVs) are an important mechanism of microbial communication and host-pathogen interaction. BEVs play an important role in the current scenario of studies involving microbiota/pathogen/host and in the numerous possibilities of application. BEVs carry numerous components, such as proteins, lipids and nucleic acids, either intra or extravesicular. BEVs cargo is associated with cell's communication and its involvement with the environment. Previous reports for some species revealed the presence of nucleic acids in BEVs, however the role of small RNAs packaged in these vesicles is poorly understood so far. To contribute to this field, here we reported, for the first time, the RNA cargo of the BEVs produced by the pig pathogen *Actinobacillus pleuropneumoniae*, the causal agent of porcine pleuropneumonia, a disease which causes great economic losses worldwide to the pig industry. First, we focused on characterizing the production, size, composition and toxicity of the BEVs secreted by *A. pleuropneumoniae* in aerobic and anaerobic growth

conditions. Then, we investigated the RNA cargo of the vesicles produced in aerobiosis, by RNAseq. We observed that the BEVs presented similar profile of proteins and lipids when comparing with cells. Moreover, comparing BEVs from aerobiosis and anaerobiosis conditions, differences were found, mostly associated with size and quantity produced. The BEVs produced by *A. pleuropneumoniae* have specific RNA cargo, composed of tRNAs and small RNAs. We have identified thirteen novel small RNA candidates in *A. pleuropneumoniae*, which were confirmed by RT-PCR. Some small RNAs identified are enriched in the vesicles, and others are protected from nuclease degradation inside them. Altogether, we revealed novel aspects of EVs produced by *A. pleuropneumoniae*, bringing a new perspective for these vesicles to the pathogenesis of this species.

Key words: Pasteurellaceae; Non-coding small RNAs; Pathogenicity; Virulence.

Introduction

Actinobacillus pleuropneumoniae is a Gram-negative cocobacillus, facultative anaerobe and encapsulated member of Pasteurellaceae family and is the etiological agent of porcine pleuropneumonia, an important disease responsible for great economic losses worldwide (Pattison et al., 1957; Gottschalk, 2012).

Extracellular vesicles production is a natural process documented in the three domains of life (Deatherage and Cookson 2012; Gill et al., 2019). In general, EVs have a circular structure, with a size ranging between 20-400 nm (Toyofuku et al., 2019). EV production is an important factor that allows the cell to go beyond the wall limits to otherwise unreachable locations. EVs have a miscellaneous composition, mostly constituted of lipopolysaccharides and proteins, also carrying toxins, nucleic acids, and other molecules (Gill et al., 2019).

The studies developed so far have shown a plethora of functions assigned to EVs, including cell to cell communication; as a mechanism for horizontal gene transfer (vesiduction); predatory mechanisms, biofilm formation; stress response; antimicrobial resistance and delivery of toxins, hydrolytic enzymes and secondary metabolites (Schwechheimer & Kuehn, 2015; Gill et al., 2019; Soler & Forterre, 2020). However, much remains to be elucidated, mostly regarding its content in contribution to microbial communities and host-pathogen interaction. Due to its composition and ability to

generate an immune response, efforts have been done to use EVs as platforms for vaccine development (Micoli & MacLennan, 2020), such as the vaccine developed for *Neisseria meningitidis* serogroup B (Sierra et al., 1991) and in progress for other species (Micoli & MacLennan, 2020).

Bacterial extracellular vesicles (BEVs) correspond to a process for molecule transport by bacteria. Although the first report of these vesicles in bacteria was in the 60's on a study developed with *Escherichia coli* (Knox et al., 1966), most knowledge regarding these vesicles have emerged in recent years.

The BEVs are commonly constituted by phospholipids, outer membrane, inner membrane, cytoplasmic and periplasmic proteins and lipopolysaccharides or lipooligosaccharides (Roier et al., 2015). EVs may also contain DNA, RNA, ions, metabolites, and signaling molecules (Pathirana & Kaparakis-Liaskos, 2016; Roier et al., 2015). The sRNAs, which are around 50-200 nucleotide in length, represent an important class of post-transcriptional regulators of gene expression (Choi et al., 2017). Much is already known about its contribution to bacterial fitness in response to different physiological and environmental conditions by distinct mechanisms of regulation (Gripenland et al., 2010; Michaux et al., 2014; Westermann et al., 2016; Hör et al., 2020).

Reports to EV-derived sRNAs have already been made for some species, such as *E. coli, Vibrio cholerae, Streptococcus mutans, Pseudomonas aeruginosa, Aggregatibacter actinomycetemcomitans, Porphyromonas gingivalis, Treponema denticola, Salmonella enterica* serovar Typhimurium and others (Badi et al., 2020; Lécrivain and Beckmann, 2020). Moreover, the sorting mechanism of sRNAs package in EVs remains to be elucidated.

Previous reports have shown the importance of the EVs to cell physiology and as vaccine candidates to the Pasteurellaceae family, as seen for *Haemophilus influenzae*, *Pasteurella multocida*, *Mannheimia haemolytica*, *Avibacterium paragallinarum*, *Galibacterium anatis* and *Aggregatibacter actinomycetemcomitans* and *A. pleuropneumoniae* (Roier et al., 2013, 2015; Pors et al., 2016; Choi et al., 2017; Antenucci et al., 2018; Mei et al., 2020). However, reports contemplating RNAs in Pasteurellaceae were only described for *A. actinomycetemcomitans* (Choi et al., 2017). Although studies of sRNAs had been done for this specie (Rossi et al., 2016; Su et al., 2016), there is no information of sRNAs and BEVs, which makes providential the investigation of different aspects of the BEVs to this pathogen.

The mechanism that BEVs from *A. pleuropneumoniae* affect the host is unknown, so, the participation of sRNAs associated with BEVs in this interaction may be an important factor during pathogenesis process. Based on that, the aim of this study was to identify and characterize the nucleic acid content, focusing the sRNAs, of the BEVs produced by *A. pleuropneumoniae.* Here we report, for the first time, the identification and characterization of nucleic acids packaged into BEV produced by *A. pleuropneumoniae.*

Material and methods

Bacterial strains and maintenance conditions

The *A. pleuropneumoniae* genetically treatable isolate MIDG2331 from United Kingdom, 1995 (Bossé et al., 2016), which belongs to serotype 8, was utilized in this study. The bacterium was grown at 37 °C in a 5% CO_2 atmosphere in brain-heart infusion (BHI, BD - 237500) medium supplemented with NAD (10 $mg.mL^{-1}$) (Sigma-Aldrich, N0632-5G). For anaerobic growth, BHI broth was prepared with removal of oxygen and addition of N_2, according to Uchino & Ken-Ichiro (2011), with strains being cultivated in N_2 gas line without shaking at 37°C until they reached early stationary phase

Isolation and purification of BEVs

The BEVs were purified as described by Antenucci et al (2017). For aerobiosis condition, the strain was plated in BHI-NAD at 37° C and 5% CO_2 atmospheric for 24 hours. Few colonies were resuspended in 20 mL in BHI-NAD and incubated overnight at 37° C and 180 rpm. An aliquot from the overnight culture of *A. pleuropneumoniae* was transferred to 600 mL of a fresh broth adjusting the initial OD_{600} to 0.1 and cultivated until late exponential phase (OD_{600} ~2.5 and ~2,36 $x10^{13}$ CFU/mL). For anaerobiosis condition, the strain was plated in BHI-NAD at 37° C and 5% CO_2 atmospheric for 24 hours. Few colonies were resuspended in 1 mL of broth, which was transferred to 10 mL of O_2-free BHI-NAD in a Hungate tube and incubated overnight. An aliquot of the overnight culture was transferred to 100 mL of a new O_2 free BHI-NAD and incubated at 37 °C and cultivated overnight. The culture was transferred to 900 mL of a new O_2-free BHI-NAD broth (initial OD_{600} ~0.1) and cultivated until late exponential phase (OD_{600} ~1 and ~2,64 x 10^{10} CFU/mL). The following steps were the same for both conditions. The culture supernatants were obtained after centrifugation

(20 minutes at 5,000 *g* at 4 °C) and filtered through a 0.45 µm filter (Millipore, Billerica, MA, USA). The filtrated were loaded in the 1,000 kDa dialysis membrane (Biotech CE Tubing - Spectrumlabs) which was encased in a glass column sealed with transparent film and incubated overnight at 4 °C. The membrane was filled with 600 mL of Phosphate-Buffered Saline (PBS) (300 mL twice) to wash the filtrated and incubated overnight at 4 °C. The filtered was dialyzed in PBS overnight at 4 °C in low agitation to purify the sample. The samples were filtered in a 0.45 µm filter (Cole-Parmer), concentrated with a 100 kDa Amicon Ultra Centrifugal Filter Units (Millipore, Billerica, MA, USA) and stored at -20°C.

BEVs quantification

For BEVs quantification, samples were quantified by flow cytometry and abundance of protein, as described below. For flow cytometry quantification, a volume of 20 µL of BEVs were treated with proteinase K (20 µg/mL) (Promega) and DNase I (20 µg/mL) (Promega). A final volume of 200 µL of treated BEVs were stained with 10 µL of propidium lyodide (Live/DeadTM - Thermo Fisher Scientific) following the recommendations of the manufacturer. Finally, BEVs were quantified using the BD Accuri C6 flow cytometer. For quantification of BEVs based on the abundance of proteins, samples were quantified using the Bradford method (Sigma-Aldrich B6916) using a standard curve obtained with bovine serum albumin (BSA – Sigma-Aldrich).

Characterization of BEVs

After the purification of BEVs from both aerobic and anaerobic conditions, the analysis first performed was the transmission electron microscopy (TEM) to access the integrity of the vesicles and evaluation of the profiles found. For that, 10 µL containing ~0.3 µg of EV samples from aerobic and anaerobic conditions were placed on a formvar coated grids, stained with 3% uranyl acetate and analyzed under a Zeiss EM 109 transmission electron microscope at 80 kV at the Center of Microscopy and Microanalysis (NMM-UFV) at the Universidade Federal de Viçosa.

Estimative of BEVs Size

The size of the BEVs from aerobiosis and anaerobiosis was measured using the dynamic light scattering apparatus (DLS) (Zetasizer Nano ZS, Malvern Instruments, United Kingdom). The data were analyzed with malvern zetasizer

software version 7.11 to obtain the average hydrodynamic diameter of the particles in solution. The measurements were conducted at 25 ºC with three replicated runs of 5 min each, for each sample, and the average intensity weighted diameter was calculated. To measure these parameters, we used 300 µg of BEVs diluted with PBS 1X, pH 7, with a refractive index of 1.332 and a viscosity of 0.9043.

BEV´s Protein profile

For obtaining whole cell extract proteins from cells, *pellet* of cells from same BEVs purification assay was washed in PBS 1X and transferred to tubes containing Lysing Matrix B beads (MP Biomedicals, CA, USA). The lysis was conducted in the FastPrep-24™apparatus (MP Biomedicals, CA, USA). The lysate was centrifuged (10 min, 16000 x g at 4° C) and the supernatant was used. Outer membrane proteins fraction from cell cultivated in aerobiosis and anaerobiosis grown until late exponential phase (cells from same BEVs purification assay) was obtained as previously described (Thein et al., 2010) following the “method 1”. Aliquots containing 25 ug of BEVs samples, outer membrane proteins fraction from cells and samples of whole cell extract from both conditions were dissolved in lysis buffer (50 mM Tris-HCl (pH 6.8); 100 mM dithiothreitol; 2% SDS; 0.1% bromophenol blue; 10% glycerol) and heated for 10 minutes at 100 °C. The proteins were separated by 12% SDS-PAGE, followed by Coomassie blue staining (Green & Sambrook, 2012).

Total lipid composition analysis

For fatty acids analysis, 40 µg of pelleted cells from late exponential phase of aerobic and anaerobic growth (cells from same BEVs production assay stored at -80° C), and 200 µg of BEVs from aerobiosis and anaerobiosis growth were submitted to fatty acid methyl esters (FAME) analysis. The samples were submitted to saponification, extraction, derivatization, and clarification, according to the Sherlock Microbial Identification System (MIS, version 6.2; MIDI, Inc.). Samples were analyzed in an Agilent 7890 (Santa Clara, CA, USA) gas chromatograph coupled with an FID detector. The MIDI system was used to identification and quantification of FAMEs (the experiments were conducted in biological triplicate). The MIDI Sherlock® software (Sherlock Microbial Identification MIDI System of Inc. Newark, Delaware, USA) was used to adjust the equipment operational parameters and for recognition, quantification of obtained peaks, and comparison with ITSA 1.0 reference library.

LPS extraction was also done to compare the profiles of the BEVs and their respective cells. For this assay, 40 µg of pelleted *A. pleuropneumoniae* cells cultivated in aerobiosis and anaerobiosis until late exponential phase (cells from same BEVs production assay stored at -80° C), and 70 µg of BEVs from aerobiosis and anaerobiosis were used. The protocol was developed as described by Davis & Goldberg, (2012). 10 µl of each sample was applied in a 16 % SDS-PAGE and silver stained.

Toxicity of BEVs in *Galleria mellonella*

The toxicity of BEVs produced by *A. pleuropneumoniae* was assessed using the *Galleria mellonella* model, as previously described (Pereira et al., 2015). Last-instar larvae were injected into the first right pro-leg into the haemocoel using the SGE Syringe, 25-gauge microvolume (26248 - Sigma-Aldrich). For each experimental replicate were utilized 10 larvae, which was infected with 10 or 20 µg of BEVs from aerobiosis or anaerobiosis growth. As negative control, PBS solution 1x was injected in the larvae. The larvae were incubated at 37 °C and observed for 96 hours (the experiments were conducted in biological triplicate).

For melanin production evaluation, larvae were injected with 3 µg of App´s BEVs and quantified as described by (Jorjão et al., 2018), with modifications. Briefly, incisions were made in the larvae's prolegs with a micro scissor to allow the haemolymph to leak. Then, haemolymph was collected with a micropipette and transferred to microtubes and kept on ice. The microtubes were centrifuged at 9500 *g* for 10 min at 4ºC. The supernatant was diluted in anticoagulant solution (Mead et al., 1986), and the OD_{405} measured. Larvae injected with PBS solution 1x was used as negative control (the experiments were conducted in biological triplicate).

Nucleic acid extraction

Total RNA was extracted from *A. pleuropneumoniae* MIDG2331 cells and BEVs from late exponential phase from aerobic and anaerobic growth (cells from same BEVs production assay stored at -80° C) using the miRNeasy kit (Qiagen) according to manufacture instructions. RNA total obtained was evaluated for quantity (Nanodrop 2000c – Thermo Scientific), and for quality by electrophoresis in a 12% acrylamide:bis-acrylamide 29:1/8 M urea gel and the gel was stained with ethidium bromide as described by (Summer et al., 2009).

DNA extraction from BEVs was developed using a phenol:chloroform method and precipitated in one volume of isopropanol (Sigma-Aldrich) and a 1:4 volume of 10M ammonium acetate. After extraction, the DNA was treated with TURBO DNA-free kit™ DNAse (Ambion, Austin, TX) following the manufacturer's instructions, to validate the presence of DNA associated to the BEVs, and then the samples were visualized in a 0.8 % agarose gel.

Sequencing (RNA-seq) and bioinformatic analysis

Samples of RNA from cell and BEVs from aerobic growth were treated with TURBO DNA-free kit™ DNAse (Ambion, Austin, TX) following the manufacturer's instructions. The small RNA fraction (< 200 nt) was obtained from the total RNA samples using the RNeasy MinElute Cleanup kit (Qiagen). The NGS library pool was single-read sequenced on an Illumina NextSeq 500 system using 75 bp read length. The output sequences were trimmed with Trimmomatic (Bolger, Lohse, and Usadel 2014) (parameters: -phred33; ILLUMINACLIP:adapter:2:30:10; SLIDINGWINDOW :4:15; LEADING:3; TRAILING:3; MINLEN:30) version 0.36 and reads were mapped onto *A. pleuropneumoniae* MIDG2331 genome (access number LN908249) using Bowtie2 (Langmead and Salzberg 2012) version 2.3.4.3 (parameters - local). The resulting bam files were uploaded to NCBI's Short Read Archive (SRA, experiment PRJNA842076). Results were analyzed using the sequence viewer Artemis (Carver et al. 2012).

Identification of reported sRNAs for *A. pleuropneumoniae* in BEVs

Aiming to seek sRNAs previously reported for *A. pleuropneumoniae* (Rossi et al., 2016; Chapter 3) (Supplementary table S1), the ones confirmed sRNAs in these previously studies were searched in the RNAseq data of the BEVs and cells. Those sRNAs identified were analyzed to compare their presence in BEVs and their respective cell based by normalizing read counts as reads per kilobase million (RPKM).

Identification of novel sRNAs candidates

Using the RNAseq mapped data, we searched for putative novel sRNA candidates. For this purpose, first, we used the mapped data of the RNAseq from vesicles RNA using Artemis software. We looked for increased reads regions in the annotated genome of MIDG2331 (Genbank access LN908249) and these sequences

were manually delimited and compared in the mapped data of the RNAseq from cell RNA to improve the delimitation. Read coverage of the candidates were visualized using the integrative genome viewer (Robinson et al., 2020). The sRNAs candidates were analyzed to compare their presence in BEVs and their respective cell by normalizing read counts as reads per kilobase million (RPKM). Then the candidates were selected for RT-PCR confirmation and *in silico* analysis.

Confirmation of sRNAs by RT-PCR

The sRNAs from cells and BEVs from aerobiosis and anaerobiosis were extracted and treated with DNAse as described above prior to cDNA synthesis. The cDNA synthesis was done using the High-Capacity cDNA Reverse Transcription Kit (Thermo Fischer – Scientific) as suggested by the manufacturers. The PCR reactions were performed with 1 U of GoTaq DNA polymerase (Promega) in a final volume of 25 µL of enzyme buffer containing 1.5 mM MgCl2, 0.2 mM of each dNTP, and 0.2 µM of each primer. The samples were initially denatured at 95 °C for 2 min, followed by 35 reaction cycles (94° C for 45 seconds, 45 seconds to annealing (Tm° according with each primer pair; primers sequence are available in the Supplementary table S2), and 72°C for 30 sec) and a final extension step at 72°C for 5 min. As a negative control, cell and BEV DNAse-treated RNA was used. As positive controls, cDNA prepared from cell RNA and 50 ng of DNA from cells were used. The DNA from cells was extracted using the FastDNA SPIN Kit (MP Biomedicals). The confirmation of the sRNAs was done for the cells and BEVs from aerobic and anaerobic growth.

Identification of RNAs inside the BEVs

To seek the ability of the BEVs in protecting the sRNAs from degradation, we treated the vesicles with RNAse prior to RNA extraction as described by Koeppen et al, (2016). Briefly, BEVs samples were treated using 0.5 µg/mL of RNAse A (Qiagen) for 30 minutes at 37 °C. The BEVs were then washed with PBS in a 100 kDa Amicon Ultra Centrifugal Filter Units (Millipore, Billerica, MA, USA) to remove the RNAse. The small RNAs were extracted, and cDNA was obtained as described above. The sRNAs already confirmed in the total RNA of BEVs were inspected for their presence inside the BEVs and protected from RNAse degradation.

Characterization of sRNAs candidates confirmed by RT-PCR

The candidates confirmed by RT-PCR were evaluated regarding their novelty by searching in the Rfam database (version 14.7). The secondary structure and fre energy (∆G) of the candidates was predicted using RNAfold (Lorenz et al., 2011). Putative promoters of the sRNAs candidates were predicted using BProm, available at http://www.softberry.com, by analyzing up to 100 bp upstream the candidates' sequences. To investigate the putative association of the sRNAs candidates with the RNA chaperone Hfq, putative Hfq-binding sequence was manually inspected based on the sequence "GGGUUUUUUU" (Holmqvist et al., 2016). Then, the search for homologues was performed using BLASTn and PATRIC database with a cuttoff of 70 % for coverage and identity. Promoter and Hfq-binding sequence consensus using the homologue's sequence after alignment with ClustalW were visualized using WebLogo (Crooks et al., 2004). Dispersion of the novel sRNAs candidates among species were visualized in a network developed using Cytoscape (Shannon et al., 2003).

Statistical analysis

For toxicity in *G. mellonella* assay, survival curves were plotted using the Kaplan-Meier method (Kleinbaum & Klein, 2012), and differences in survival were estimated by using the log rank test using the software *R*, version 2.13.0, with *p* values <0.05 considered as statistically significant. For melanization analysis, the differences were analyzed using analysis of variance (ANOVA) followed by Tuckey test for multiple comparisons with *p* values <0.05 considered as statistically significant. For the vesicles production and fatty acid analysis, t-test was used considering *p* values <0.05 as statistically significant.

Results

Analysis of BEVs

BEVs production by App in different conditions

BEVs produced by App from aerobiosis and anaerobiosis were analyzed. Transmission electron microscopy showed the integrity of the vesicles and revealed different populations of vesicles with different sizes (Figure 1A). Also, TEM revealed different types of vesicles, most of them carrying a unique membrane and some carrying two membrane and an electron dense content (Figure 1A).

By DLS, was confirmed a heterogenous population of vesicles for both conditions. Among the population of the BEVs from aerobiosis, the most prominent range was around 44 nm (~23 %), with the particle's sizes ranging between 28 nm and 300 nm approximately (Figure 1B). For the vesicles produced in anaerobiosis, the prominent range was 24 nm (~28 %), with variation from 16 nm to 190 nm.

The BEVs production was higher in aerobiosis culture, being produced ~1.446 vesicles by mL of culture in aerobiosis and ~913 vesicles by mL in anaerobiosis (Supplementary Figure S1A), although statistical difference was not observed (p= 0,365). Considering the production of BEVs by protein abundance, cells growing in aerobiosis produced more vesicles than aerobiosis (p= 0.0002), being produced 2.570 µg and 0.72 µg of BEVs by mL of culture in aerobiosis and anaerobiosis, respectively (Supplementary Figure S1B). The ratio of BEVs (quantified flow cytometry or by protein amount) / CFU revealed more vesicles produced per cell in anaerobiosis growth than in aerobiosis (p= 0.001 for both methods) (Supplementary Figure S1C; S1D).

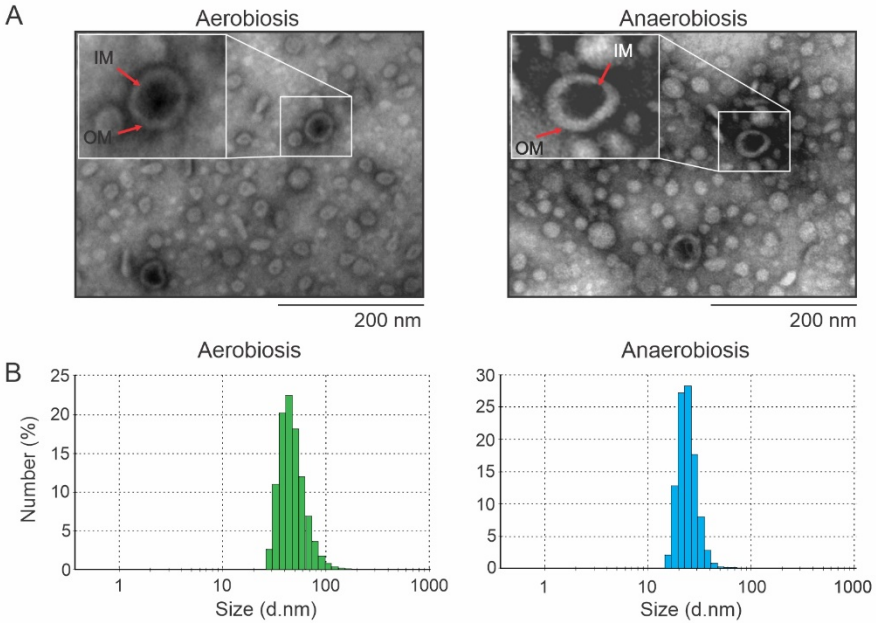

Condition	Particles size (diameter)		
	Minimum (nm)	Most present (nm)	Maximum (nm)
Aerobiosis	28.2	43.8	295
Anaerobiosis	15.7	24.36	190.1

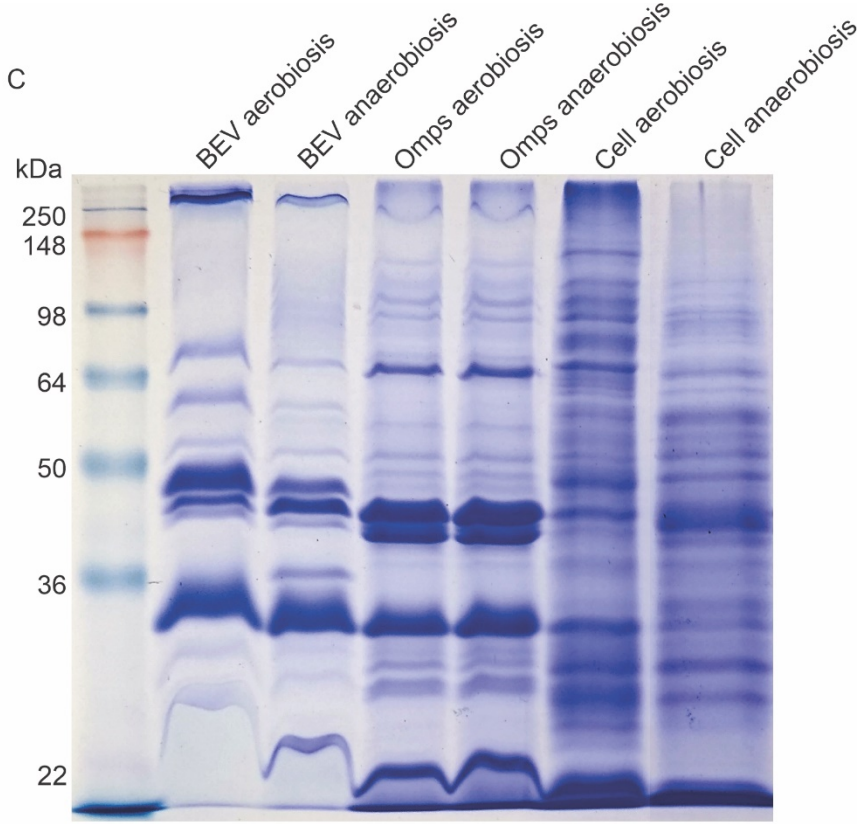

Figure 1 – Morphology, size measuring, and proteins profile of BEVs produced by *A. pleuropneumoniae*. (A) Transmission electron microscopy (TEM) of the vesicles from aerobiosis (left) and anaerobiosis (right). Both size and type are observed in BEV preparations. OM probably correspond to the outer membrane of the cell, and IM probably correspond to the inner membrane of the cell. The cytoplasmic portion is represented by electron dense material. (B) Vesicles size from aerobiosis (left) and anaerobiosis (right) BEVs. The BEVs were measured by Dynamic light scattering (DLS) and are represented in the graphs. The minimum, most present and maximum size of the vesicles are represented at the bottom of the figure. (C) Proteins profile of BEVs, outer membrane from cells and total protein extract from cells from aerobiosis and anaerobiosis.

Proteins and Lipids profiles in BEVs produced by App

Comparing the proteins profile between BEVs from both conditions, a similar protein profile was observed, with slight differences (Figure 1C). BEVs protein profile showed to be very different from the total proteins profile from cells in both aerobiosis and anaerobiosis conditions (Figure 1C). When comparing the proteins profile of BEVs to the outer membrane proteins from cells, it was possible to observe that, despite the intensity of some bands, the proteins profile of the BEVs is quite similar to the outer membrane from cells (Figure 1C).

The LPS profiles from BEVs were different from the cells, as we did not observe all the bands observed from cell in the BEVs (Figure 2A). The profile of fatty acid has few differences. For App cells grown in aerobic and anaerobic conditions were found as the most abundant the myristic acid (14:00), followed by palmitic acid (16:00), palmitoleic acid (16:1 w7c), stearic acid (18:00) and the tetradecanoic acid14:0 3OH (Figure 2B). Similar to the abundance observed to the cells, in the BEVs, 14:00, 14:0 3OH, 16:00 and 16:1 w7c were respectively the most abundant fatty acid observed (Figure 2B). In the cell's comparison, significative difference was observed only to the 16:00 and 18:1 w9c ($p= 0.08$ and $p= 0.00001$) (Figure 2B). For the BEVs comparison, significative difference was observed only to the 14:0 3OH, 18:1 w9c and 18:00 ($p= 0.011$, 0.014 and 0.03) (Figure 2B). Comparing BEVs and cells, for both aerobiosis and anaerobiosis, 14:00 ($p= 0.005$ for aerobiosis and $p= 0.008$ for anaerobiosis) and 14:0 3OH ($p= 0.001$ for aerobiosis and $p= 0.003$ for anaerobiosis) showed higher abundance in BEVs while 16:1 w7c ($p= 0.001$ for aerobiosis and $p= 0.001$ for anaerobiosis), 16:00 ($p= 0.006$ for aerobiosis and $p= 0.002$ for anaerobiosis) and 18:00 ($p= 0.017$ for aerobiosis and $p= 0.005$ for anaerobiosis) showed higher abundance in cell (Figure 2B). Also, the vesicles showed a higher amount of saturated fatty acids in comparison to the respective cells (~77% for cells and ~89% for BEVs).

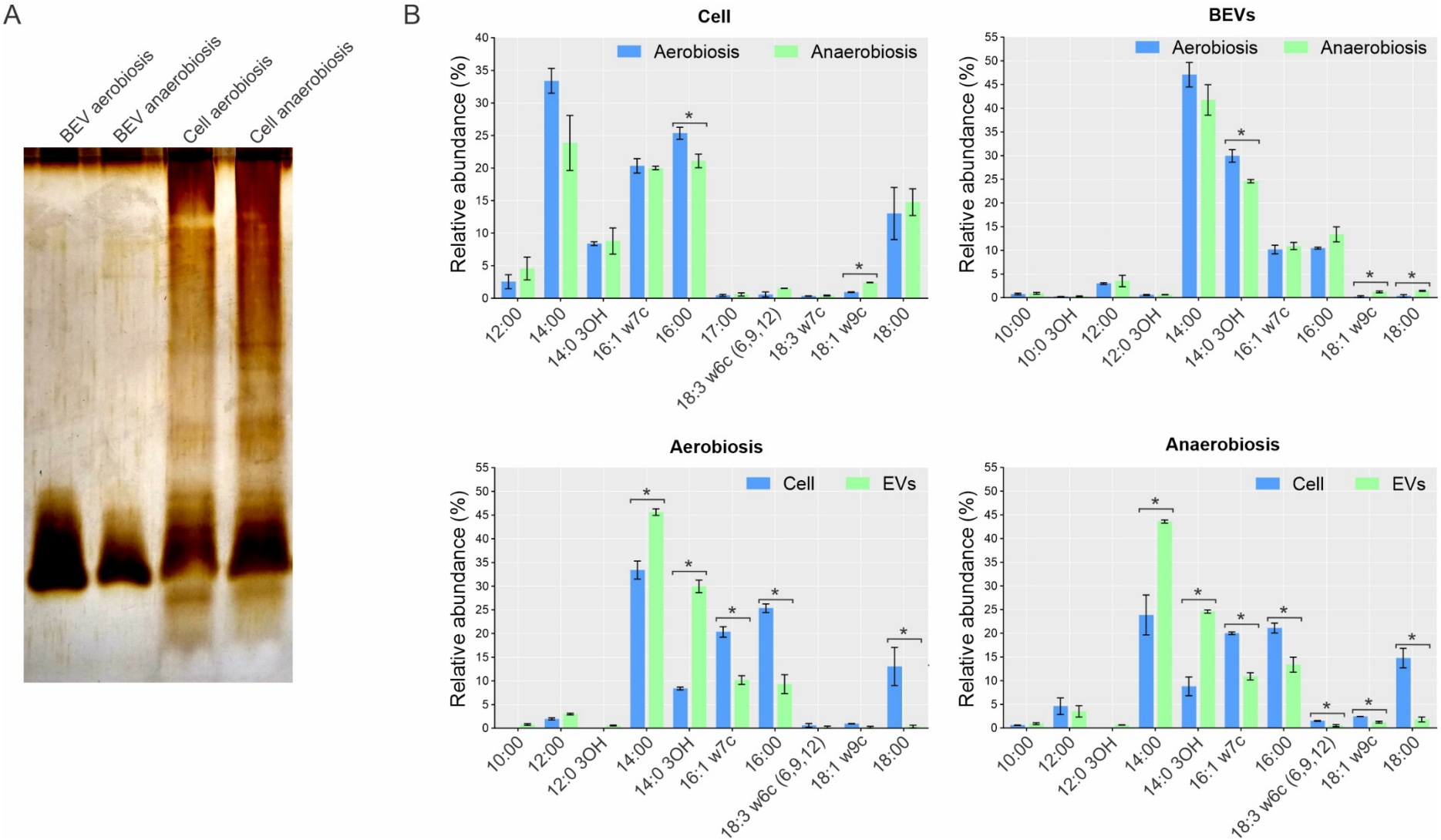

Figure 2 – LPS and Lipids profile from *A. pleuropneumoniae* cells and BEVs. (A) LPS profile of BEVs and respective cells. (B) Relative abundance and profile of fatty acids for BEVs and respective cells. Comparisons of fatty acids composition: Between cells from aerobiosis and anaerobiosis (Top-left); between BEVs from aerobiosis and anaerobiosis (Top-right); between cells and BEV from aerobiosis (Bottom-left); between cells and BEVs from anaerobiosis (Bottom-right). Significative difference is represented by "*" after comparisons by t-test ($p<0.05$).

BEVs produced by App and toxicity in *G. mellonella*

Only a few larvae were dead when infected with 10 µg of BEVs (~20 %), while the dosage of 20 µg killed more larvae (~50 %) (Supplementary Figure S2A). However, no statistical difference was seen for larvae infected with BEVs from aerobic or anaerobic conditions (p= 0,739 for 10 µg of BEVs and p= 0,817 for 20 µg of BEVs).

Melanization quantification showed slight difference only at 24 hours showing more melanization in larvae infected with BEVs from aerobiosis (p= 0.019), however no significative difference was observed until 96 hours, also revealing a reduction in the melanization during the experiment (Supplementary Figure S2B; S2C).

Nucleic acid cargo from App BEVs

The BEVs of App produced under aerobic conditions showed DNA and RNA, verified from the extraction and purification of these nucleic acids and analysis by electrophoresis in agarose (Supplementary Figure S3) and polyacrylamide gel (Figure 3). From the results obtained, a higher yield of RNA than DNA was evidenced, from the same amount of BEVs used in the extraction procedure. Therefore, the RNA content of the BEVs was chosen for further investigation.

Denaturing polyacrylamide urea gel showed a similar pattern of small RNAs between BEVs from aerobiosis and anaerobiosis, with slight differences. The same was observed for the total sRNAs from cell. The gel revealed sRNAs with a size around 300 bp, 100 bp and some smaller than 50 bp in the vesicles, while the cells showed a wide variety of sRNAs sizes (Figure 3A). As no significant differences were observed between BEVs produced by App in aerobic and anaerobic conditions, the identification and characterization analysis of RNAs carried by BEVs from App were conducted only with BEVs from App cultivated in aerobic conditions. After RNA sequencing from aerobiosis condition and mapping to the *A. pleuropneumoniae* MIDG2331 genome, it was obtained 13,462,604, 9,166,775 and 9,766,708 reads mapped to the total RNA from cell and 134,070, 686,819 and 152,393 reads mapped to RNA from BEVs. RNAseq from BEVs produced by *A. pleuropneumoniae* revealed that BEVs transport diverse classes of RNAs, including mRNAs, miscellaneous RNA (MiscRNAs), tmRNA, rRNA and tRNA, also intergenic RNAs were associated with BEVs (Figure 3B). Moreover, tRNAs and MiscRNAs were more abundant in BEVs than cell (Figure 3B). The profile of RNAs identified by RNAseq confirmed the profile obtained by denaturing polyacrylamide gel electrophoresis, revealing that BEVs transport small RNAs.

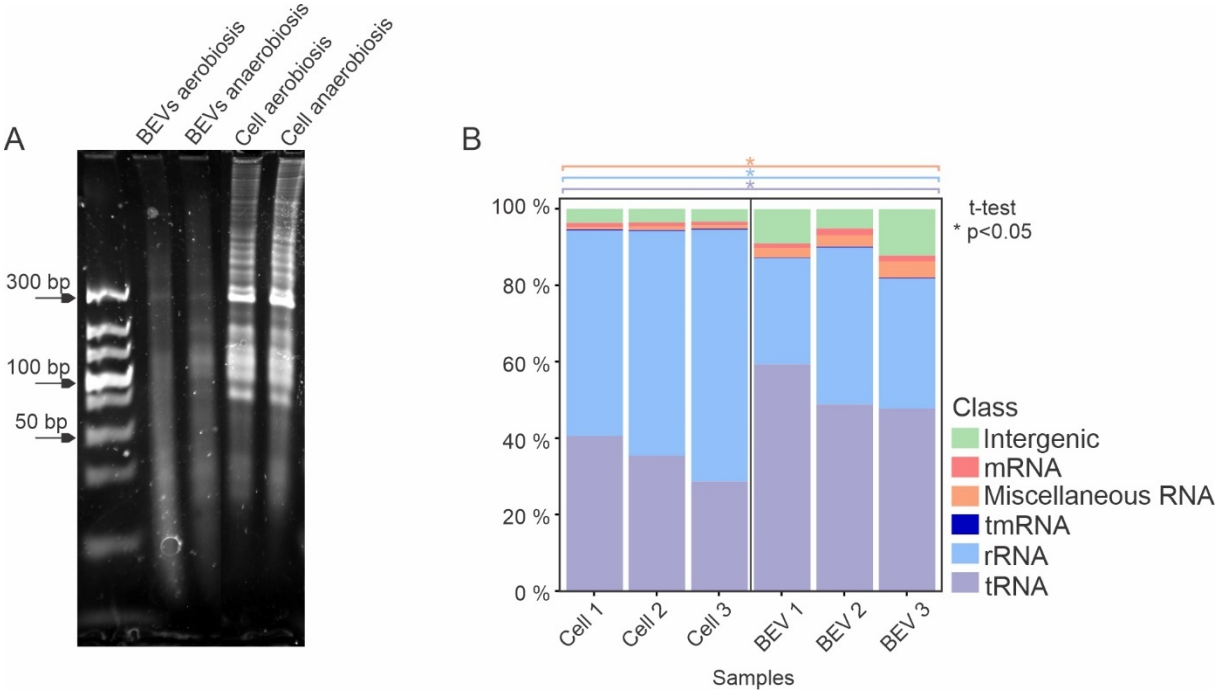

Figure 3 – BEVs from *A. pleuropneumoniae* carries a diverse RNA content. (A) 10 % denaturing urea gel of BEV RNA and cell RNA from aerobiosis and anaerobiosis growth. (B) RNA composition of cell and BEVs from aerobiosis growth. Significative difference between Cells group and BEVs group is represented by "*" for each class of RNA (following the color of each class) compared by t-test ($p<0.05$).

Among the housekeeping small RNAs transported by BEVs, many of them were more abundant in the vesicles than cells, as some tRNAs and 6S RNA (Figure 4). The search for previously described *A. pleuropneumoniae* sRNAs (Rossi et al., 2016; Chapter 3) (Supplementary table S1) in the RNAseq data showed the presence of twenty of them in the vesicles, being some more abundant in BEVs than the respective cells, as observed for Arrc05, 06, 07, 08, 10 (6S), 11, 15, 17, 21 and Rna10 (Figure 4B).

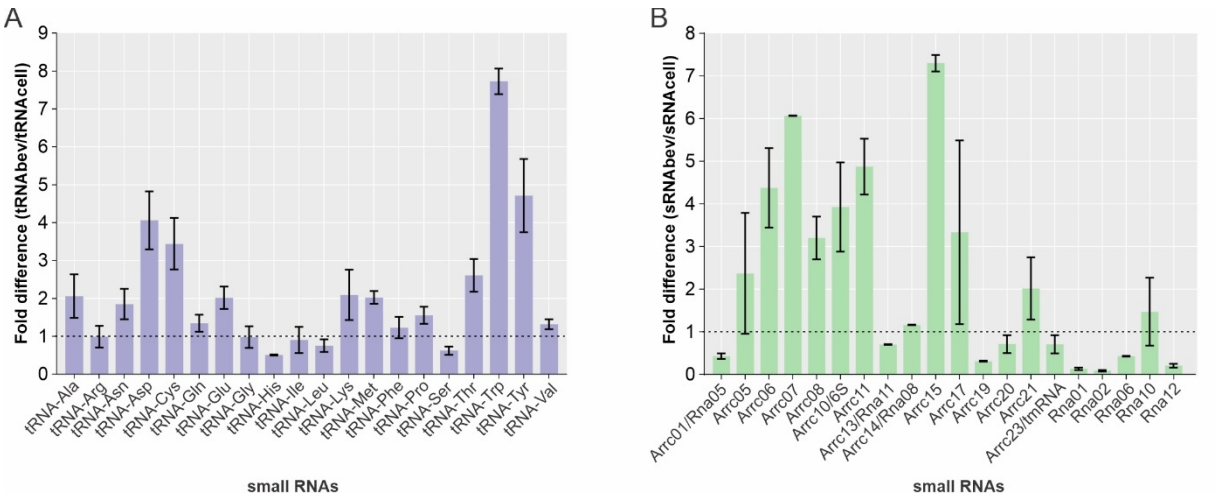

Figure 4 – Some small RNAs are enriched in BEVs produced by *A. pleuropneumoniae*. Fold difference (ratio of BEV/cell RNAs) of tRNAs (A) and small RNAs previously reported for *A. pleuropneumoniae* (B). The bars above the dotted line represent the RNAs enriched in the BEVs than cells. The bars below the dotted line represent the RNAs enriched in the cell than BEVs.

Identification of novel sRNAs candidates

Manual inspection for novel sRNAs candidates allowed us to identify 16 novel candidates, named as EVsRna1 to 16, all localized in intergenic regions (Table 1, Figure 5A). Predicting putative promotes for the novel sRNAs candidates, we found putative -35 and -10 for all excepted for EvsRna3 and EvsRna5 (Table 1). By manual identification, we found putative Hfq binding site in 11 candidates, EVsRna1, 2, 3, 4, 6, 7, 10, 11, 12, 13 and 16 (Table 1). Only the EVsRna14, identified as RNA-OUT, was previously described in Rfam, being all of the other considered as novel sRNAs candidates, no family found in the Rfam database. The novel sRNA candidates EVsRna5, 10 and 16 were more abundant in the vesicles than in the cells (Figure 5B).

Table 1 - Novel sRNAs candidates associated with BEVs from *A. pleuropneumoniae*

Candidate	Position	Size (bp)	Strand	Putative -35	Putative -10	Putative *Hfq- binding site*	*Upstream* gene	*Downstream* gene	Homologue in Pasteurellaceae/ other families*	Rfam classification
EvsRna1	217434..217566	133	-	TTGAAT	TGCGATAAT	UCGUUUUUUU	*mcrA*	*aroK*	Yes/No	No match
EvsRna2	324793..324857	65	-	TTGATC	CTGTAAAAT	UUCUUUUUUA	MIDG2331_00301	MIDG2331_00302	Yes/ Yes	No match
EvsRna3	351412..351530	119	+	-	-	GGUUUCUUUU	tRNA-Asn	*rumA*	Yes/No	No match
EvsRna4	755602..755733	132	-	TTGACT	GGCTAGAAT	AGGGAUUUUU	MIDG2331_00698	*mtfA*	Yes/No	No match
EvsRna5	848973..849047	75	-	-	-	No	MIDG2331_00786	*rec2*	Yes/No	No match
EvsRna6	896360..896467	108	-	TTGCAA	TAGAAT	UUUUUAAUUU	MIDG2331_01325	MIDG2331_01324	Yes/No	No match
EvsRna7	1039104..1039175	72	-	TTGCCG	CTAAATAAT	UCAACUUUUU	*iscU*	*iscA1*	Yes/ No	No match
EvsRna8	1322264..1322316	53	+	TTTCGT	GACTATCCT	No	*rpsF*	*purD*	Yes/ No	No match
EvsRna9	1432325..1432455	131	-	TTGAAA	TAAAAT	No	MIDG2331_01325	MIDG2331_01324	No/ No	No match
EvsRna10	1558709..1558900	192	-	ATGGCG	TATACT	CGGAUUUUUA	*topB2_2*	MIDG2331_01469	Yes/ No	No match
EvsRna11	1695309..1695397	89	-	TATACT	TGCTAAGG	CAGAUUUUUU	MIDG2331_01606	MIDG2331_01605	Yes/ Yes	No match
EvsRna12	1892321..1892453	133	-	GTGACC	ATAAAAATA	GCAAUUUUCU	*ureA*	*ureB*	Yes/ No	No match
EvsRna13	2021328..2021575	248	-	TTGAAA	ATAGTA	CGGUUUUUUU	*gloA2*	*sfsA*	Yes/ No	No match
EvsRna14	1546771..1546841	71	-	CAGAAT	TAAAAT	No	MIDG2331_01454	MIDG2331_01452	Yes/ Yes	RNA-OUT (RF00240)
EvsRna15	2035311..2035394	84	+	TTTACA	TAAGAT	No	MIDG2331_01951	tRNA-Asn	Yes/ No	No match
EvsRna16	2292439..2292513	75	+	TTGCAA	TATAAT	AGUUUUUUGA	*comF*	*rsmC*	Yes/ No	No match

* Homologues were considered by blastn against NCBI and PATRIC databases with a cuttoff of 70% for cover and ID.

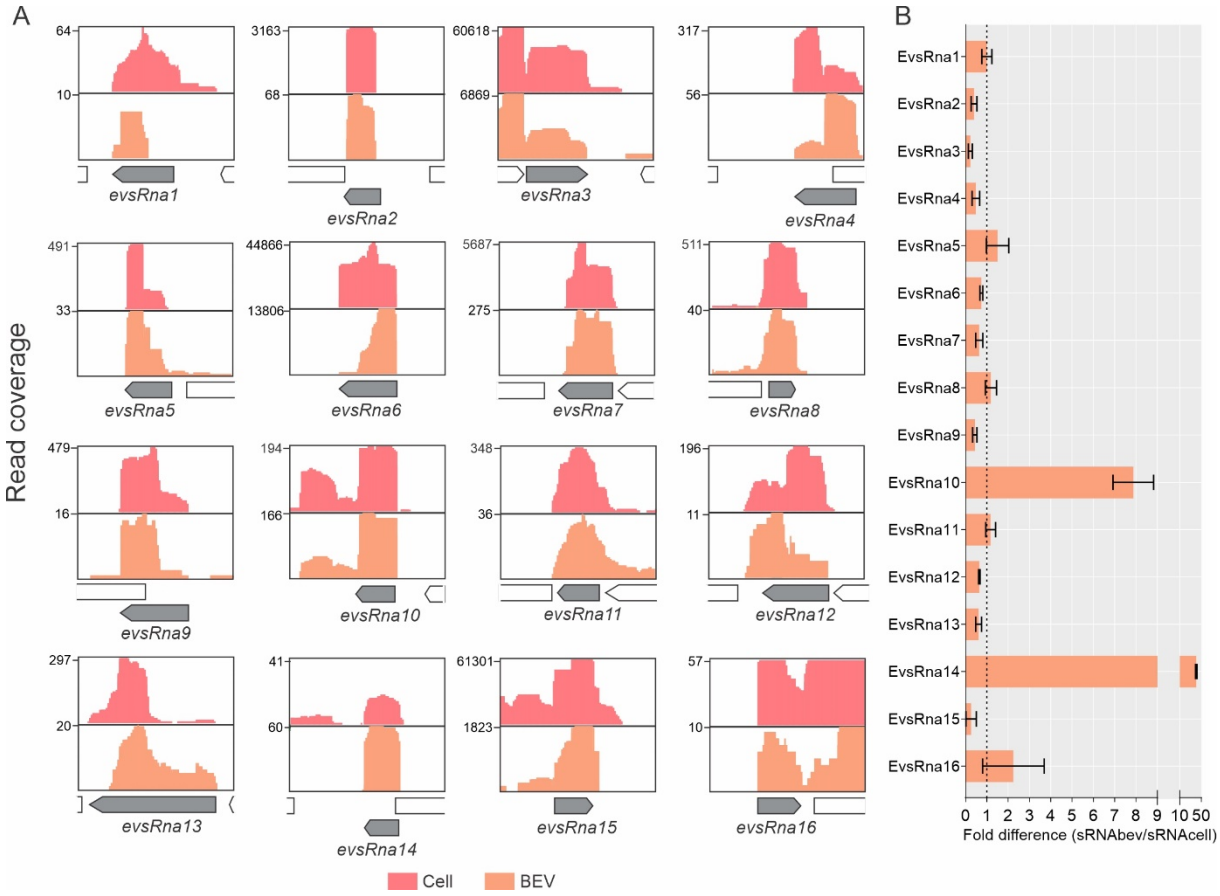

Figure 5 – Mapping regions of the novel small RNA candidates from the BEVs and respective cells of *A. pleuropneumoniae* and its relative abundance. (A) Increased reads on intergenic regions of RNAseq from cell and BEVs mapped in the MIDG2331 genome. The mapping was done using integrative genome viewer. (B) Fold difference of EV/cell novel small RNAs candidates.

sRNAs expression by RT- PCR

By RT-PCR analysis, the fifteen *trans-acting* sRNAs previously reported to *A. pleuropneumoniae* (Supplementary table S1) have expression confirmed in App cells growing aerobically. However, for the 16 novel sRNAs candidates, only EvsRna3 and EvsRna5 were not confirmed. Of the sRNAs confirmed in the cells, only Rna02, Rna09 and EvsRna14 were not found in BEVs (Table 2). For the intravesicular RNAs extracted from the BEVs, only EvsRna7, EvsRna11 and EvsRna12 were not found inside the vesicles from aerobiosis (Table 2). On expression of the sRNAs in App cells on anaerobiosis conditions, only Rna02, EsRNA3 and EvsRNA5 were not confirmed. Moreover, Arrc08, Rna10, EvsRna11 and EvsRna14 were not found associated with BEVs in anaerobiosis (Table 2).

Table 2- Expression of *trans* small RNAs caried by BEVs in *A. pleuropneumoniae* cells.

sRNA*	Confirmed in aerobiosis Cell/BEVs by RT-PCR	Confirmed inside aerobiosis BEVs by RT-PCR**	Confirmed in anaerobiosis Cell/BEVs by RT-PCR
Arrc01	Yes/ Yes	Yes	Yes/ Yes
Arrc05	Yes/ Yes	Yes	Yes/ Yes
Arrc07	Yes/ Yes	Yes	Yes / Yes
Arrc08	Yes/ Yes	Yes	Yes/ No
Arrc11	Yes/ Yes	Yes	Yes/ Yes
Arrc14	Yes/ Yes	Yes	Yes/ Yes
Arrc17	Yes/ Yes	Yes	Yes/ Yes
Arrc20	Yes/ Yes	Yes	Yes/ Yes
Arrc21	Yes/ Yes	Yes	Yes/Yes
Rna01	Yes/ Yes	Yes	Yes/ No
Rna02	Yes/ No	NA***	No/ No
Rna06	Yes/ Yes	Yes	Yes/ Yes
Rna09	Yes/ No	NA**	Yes/Yes
Rna10	Yes/ Yes	Yes	Yes/No
Rna12	Yes/ Yes	Yes	Yes/ Yes
EvsRna1	Yes/ Yes	Yes	Yes/Yes
EvsRna2	Yes/ Yes	Yes	Yes/Yes
EvsRna3	No/ No	NA***	No/ No
EvsRna4	Yes/ Yes	Yes	Yes/Yes
EvsRna5	No/ No	NA***	No/ No
EvsRna6	Yes/ Yes	Yes	Yes/Yes
EvsRna7	Yes/ Yes	No	Yes/Yes
EvsRna8	Yes/ Yes	Yes	Yes/Yes
EvsRna9	Yes/ Yes	Yes	Yes/Yes
EvsRna10	Yes/ Yes	Yes	Yes/Yes
EvsRna11	Yes/ Yes	No	Yes/No
EvsRna12	Yes/ Yes	No	Yes/Yes
EvsRna13	Yes/ Yes	Yes	Yes/Yes
EvsRna14	Yes/No	NA***	Yes/No
EvsRna15	Yes/ Yes	Yes	Yes/Yes
EvsRna16	Yes/ Yes	Yes	Yes/Yes

*Only *trans-acting* sRNAs previously described for *A. pleuropneumoniae* were verified by RT-PCR
**Only for BEVs produced in aerobiosis condition
***NA: not investigated inside BEVs because they were not found in the total RNA of the vesicles.

In silico characterization of the novel sRNAs candidates

Secondary structure and genic context of the novel sRNAs candidates confirmed by RT-PCR are shown in Figure 6. Search for homologues reveals that some candidates are found in a wide variety of species, as EvsRna8, EvsRna11 and EvsRna14 (Supplementary Figure S4). Some candidates also were found in non-Pasteurellaceae species, as seen for EvsRna2, EvsRna11 and EvsRna14, found in *Neisseria* spp. *Streptococcus* spp. and some Enterobacteriaceae (Supplementary Figure S4). For promoter consensus analysis and phylogenetic analysis, we did not evaluate the candidates EvsRna9, EvsRna15, EvsRna16 because of the absence or few homologue sequences, and EvsRna16 as this one correspond to the high conserved RNA-OUT, which is widely widespread. Consensus analysis of the putative promoters reveals a conserved -35 and -10 for most of the candidates (Supplementary

Figure S5). Also, consensus analysis of putative Hfq binding sequence showed conserved sequence among the homologues for most candidates (GGGUUUUUUU) (Supplementary Figure S6).

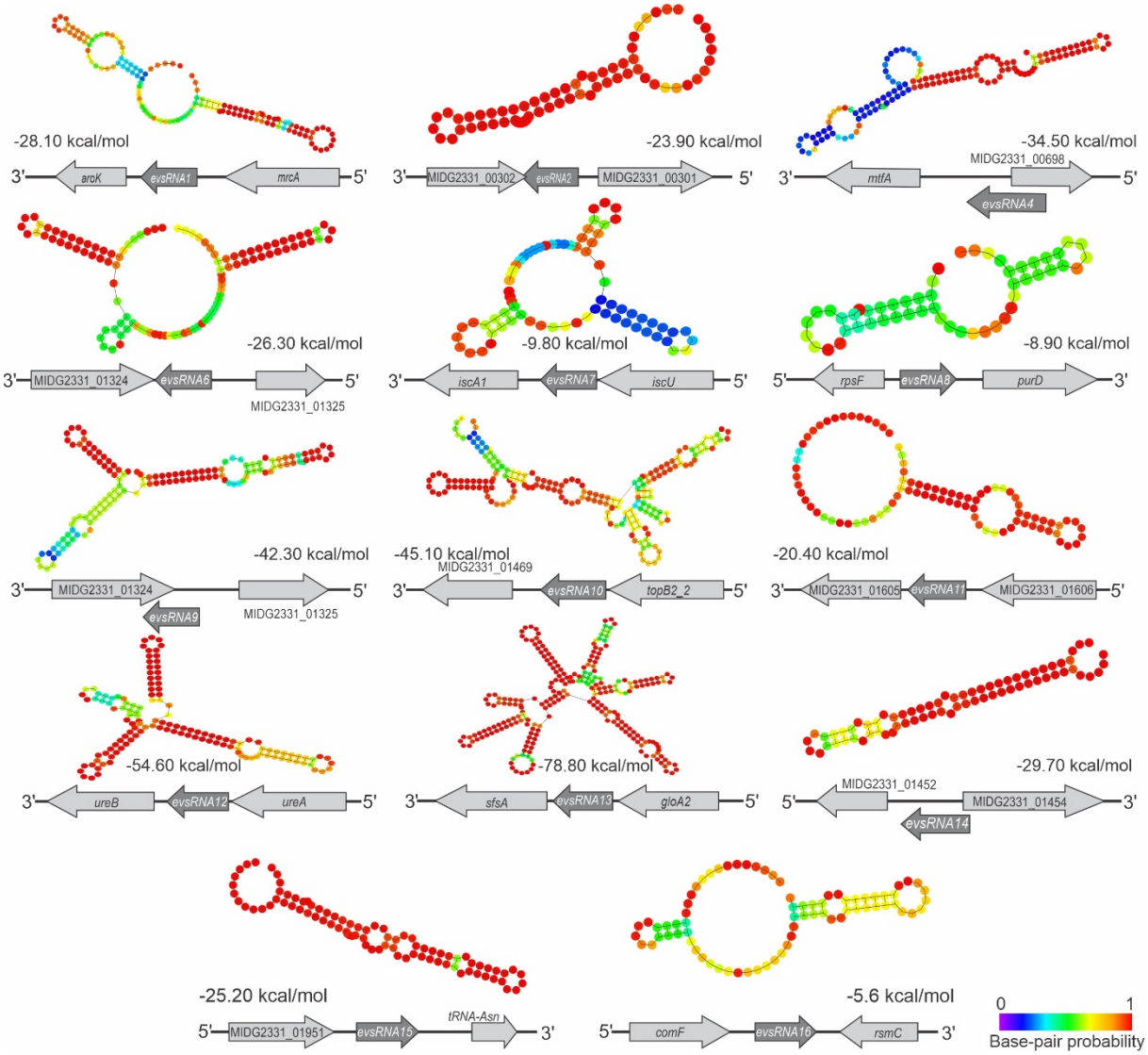

Figure 6 - Structure and context of novel sRNA candidates of *A. pleuropneumoniae*. sRNAs candidates' structure were predicted using RNAfold. Context and strand of the candidates are represented below each sRNA structure. Free energy (ΔG) of sRNA structures is showed next to each structure.

Discussion

The production of BEVs corresponds to a highly important weapon for bacteria due to its diverse capacity and versatility of transporting molecules and their interaction with the environment, that allow the BEVs to be considered a fantastic new platform to diverse application (Jan, 2017). All possible current applications justify efforts to study BEVs from bacterial pathogens, as *A. pleuropneumoniae*. The vesicles may contribute in microbial communities by transporting plasmids coding antimicrobial resistance genes to other bacteria or transporting killing molecules to overcome in an

environment. Moreover, these vesicles participate in the bacterial defense or survival and interaction with host cell during the pathogenesis process (Jan, 2017).

The growth condition of *A. pleuropneumoniae*, involving oxygen availability, affected some vesicle aspects. Here we showed that the number of vesicles produced is greater in aerobiosis than aerobiosis. However, after normalizing vesicles production by cell count, *A. pleuropneumoniae* cells growing in anaerobiosis condition produces more vesicles than cells growing in aerobiosis. Also, the size of the vesicles produced in both conditions were different. Previous studies already reported that availability of oxygen affect the BEVs production, increasing or decreasing the release of the vesicles, as described for *N. meningitidis* and *P. aeruginos*a (Gerritzen et al., 2018; Toyofuko et al., 2014; Schertzer et al., 2010). The production of BEVs is associated with biofilm formation (Schooling and Beveridge 2006), and it is already known that anaerobic stress induces biofilm formation in *A. pleuropneumoniae* (Li et al., 2014). It corroborates with our results showing the greater production of BEVs by cell in anaerobiosis.

The proteins profile analysis revealed that BEVs are similar to the outer membrane proteins of cells, but we can see some differences in protein profiles i.e. no presence of bands bigger than 98 kDa. Similar, Antenucci et al (2019) reported the identification of non-outer membrane proteins in the BEVs composition. Additionally, the lipids profile showed, despite the different abundance, a similar composition of BEVs in comparison to the cells. Altogether, these results indicate that these vesicles are possibly composed most from outer membrane. Moreover, the enriched components observed in the vesicles indicates that these vesicles are not randomly produced by the cells.

The LPS profile revealed that BEVs do not show the same profile of the cells. Fatty acid composition of the BEVs showed similarities and singularities when comparing with the respective cells. Vesicles from both conditions showed a predominancy of saturated fatty acids in the composition when compared to the respective cells. It is already known that saturated fatty acids decrease the membrane fluidity (Hac-Wydro and Wydro 2007). Previous study reported that the reduction in the membrane fluidity increases the BEVs production for *P. aeruginosa* (Mashburn-Warren et al., 2008). Altogether, this information suggests that these vesicles are most composed of saturated fatty acids, which may represent a mechanism to alleviate the tension caused by the membrane rigidity during cell growth.

The virulence of *A. pleuropneumoniae* is multifactorial and complex, commonly involving factors as LPS, capsule, siderophores and the RTX toxins ApxI, ApxII and ApxIII, that possess cytotoxic and/or hemolytic activity (Frey, 2011). But, similar to other Gram-negative bacteria, the production of extracellular vesicles also corresponds to a virulence factor, based on its composition.

In the *G. mellonella* assay, the BEVs showed to be toxic to the larvae, despite the condition, causing highly and quick melanization, however, only few larvae were killed in the assay. Previously reports identified virulence associated proteins, including Apx toxins, in the vesicles and showed that these vesicles are capable to stimulate immune response and lesions in pigs (Negrete-Abascal et al., 2000; Antenucci et al., 2017, 2018, 2019). Also, LPS is the most abundant component of the vesicles, and has the ability to stimulate immune response, which makes it a good adjuvant option for vaccines, however, this LPS may be toxic for the cells (Tan et al., 2018). As seen in the proteomic analysis described by Antenucci et al, (2019), the BEVs do not carry the full arsenal of virulence factors present in the cells. Also, Pereira et al, (2015) showed that *G. mellonella* mortality is not fully associated with the toxicity of the culture supernatant (that contains the vesicles), but probably with the virulence factors expressed by cells in the insect. Besides that, it is important to emphasize the tropism of Apx toxins for porcine cells (Kuhnert et al., 2003). Also, unlike cells, the vesicles do not have the ability of multiply and colonize the host, may being quelled, allowing the restauration of larvae integrity. Altogether, these factors may explain the ability of BEVs in stimulate the immune response in *G. mellonella*, but cause few deaths.

Here we showed that the vesicles carry nucleic acids and a particular sRNA pool. The transport of nucleic acids by extracellular vesicles to host cells or other bacteria already proved to be efficient and functional, as this mechanism provides a way protected from degradation (Collins & Brown, 2021; Dell'Annunziata et al., 2021). Despite that, it remains to be investigated if the RNA cargo of the BEVs from *A. pleuropneumoniae* participate of the infection process or microbial communication and how it works.

Small RNAs represent a surprising class of gene expression regulators and keep on the rise since its discovery. This class of regulators brought a new perspective to the central dogma of biology and has been constantly answering several questions and generating new ones. From the beginning until now, lots of information regarding behavior and physiology of bacteria were explained by sRNA activity investigation.

Although the importance of sRNAs in the virulence of diverse bacterial species had already been reported, most of the information comprises the action of these molecules on its cell regulation during the pathogenesis process. Thus, there is still very little information about the role of these RNAs outside the cell and transported by vesicles in the infection process. Here, we reported the presence of sRNAs packaged in extracellular vesicles produced by the porcine pathogen *A. pleuropneumoniae*, being one of the few reports in the Pasteurellaceae.

The RNAseq analysis revealed a diverse profile of RNAs in the vesicles content, being the tRNAs and rRNAs the most found, respectively. Also, most tRNAs showed to be enriched in the BEVs when comparing with the bacterial RNAs. The high abundance of tRNAs and rRNAs in the cell is expected because of their functions, or because many of these RNAs are expressed from genes with multiple copies in the genome, but the reason of this enrichment in the vesicles needs to be deeper explored. Koeppen et al (2016) found a fragment of a tRNA, named sRNA52320 in *P. aeruginosa*, that is associated with the modulation of immune response of human airway cells. Pérez-Cruz et al (2021) also found a high amount of tRNAs in BEVs produced by *P. aeruginosa*. Moreover, Ghosal et al (2015) identified higher amount of tRNAs in vesicles produced by *E. coli*. MiscRnas, tmRNAs and intergenic sequences also were found in the vesicles from *A. pleuropneumoniae*. So, the proportion of these classes is quite different from those described for *E. coli* and *Salmonella enterica* serovar Typhimurium (Ghosal et al, 2015; Malabirade et al, 2018), which may indicate that the RNA content of BEVs is not only a cell disposal, but it can be intrinsic to each species and its physiological and environmental condition.

We found diverse RNAs associated with the BEVs, including sRNAs previously reported for App (Rossi et al., 2016; Chapter 3), we described thirteen novel sRNAs candidates to *A. pleuropneumoniae*, increasing the amount of sRNAs described for this specie. Some of them being found in diverse species and possessing a conserved putative promoter and Hfq binding site. Also, we found some sRNAs enriched in the vesicles by comparing relative abundance with respective cells. This was already related for the human pathogen group A streptococcus (GAS), *P. aeruginosa* and *Listeria monocytogenes* (Koeppen et al., 2016; Ulrike et al., 2016; Frantz et al., 2022). Despite of these findings, the mechanism by which RNAs are sorted into the vesicles still unclear. In addition, the recent discoveries regarding the bacterial vesicles

biogenesis shows different types of vesicles, that may be intimately associated with its content (Toyofuku et al., 2019).

Based on the results regarding the BEVs described in this work, we are able to propose the type of vesicles produced by *A. pleuropneumoniae*. The comparison of proteins profile of BEVs and outer membrane from cells, supported by proteomic analysis developed by Antenucci et al, (2019), suggest that, as most proteins found in the vesicles are outer membrane associated proteins, these vesicles may be classified as outer membrane vesicles (OMVs). However, OMVs normally do not have carry inner membrane and/or cytoplasmatic content, as nucleic acids (Toyofuku et a., 2019), both of which were identified in the vesicles in this study. Some types of vesicles are able to carry this kind of content, as the outer-inner membrane vesicles (OIMVs). According to this, we believe that *A. pleuropneumoniae* produces both OMVs and OIMVs during growth. Although TEM results revealed that most of vesicles are probably OMVs, the fraction of types produced was not investigated. Moreover, it is already known that bacteria can produce different types of vesicles in different proportions (Toyofuku et a., 2019).

In this study, in addition of the characterization of novel aspects regarding BEVs produced by *A. pleuropneumoniae* and comparing them during aerobiosis and anaerobiosis growth, we reported, for the first time, the RNA cargo of extracellular vesicles produced by this pathogen. However, there is much to be investigated regarding the contribution of these findings in the host-pathogen interaction. Overall, these results bring a new perspective to the virulence of *A. pleuropneumoniae* and mean a step forward in the understanding of its pathogenesis.

Funding

This work was supported by Conselho Nacional de Desenvolvimento Científico e Tecnológico-CNPq (Process nº. 141328/2018-5), Coordenação de Aperfeiçoamento de Pessoal de Nível Superior/ Programa de Excelência Acadêmica-Finance Code 001 (CAPES ProEx grant 23038.019105/2016-86) and Fundação de Amparo à Pesquisa do Estado de Minas Gerais—FAPEMIG for the financial support. This work was also supported by the UK Biotechnology and Biological Sciences Research Council (Grants BB/S002103/1 and BB/S020543/1).

Acknowledgements

We are grateful to Katialaine Corrêa de Araújo for helping to perform anaerobiosis conditions to grow App. We also are grateful to Ciro César Rossi for the support with the sRNA analysis.

References

Antenucci, F., Fougeroux, C., Bossé, J. T., Magnowska, Z., Roesch, C., Langford, P., Holst, P. J., & Bojesen, A. M. (2017). Identification and characterization of serovar-independent immunogens in *Actinobacillus pleuropneumoniae*. *Veterinary Research*, *48*(1), 74. https://doi.org/10.1186/s13567-017-0479-5

Antenucci, F., Fougeroux, C., Deeney, A., Ørskov, C., Rycroft, A., Holst, P. J., & Bojesen, A. M. (2018). In vivo testing of novel vaccine prototypes against *Actinobacillus pleuropneumoniae*. *Veterinary Research*, *49*(1), 4. https://doi.org/10.1186/s13567-017-0502-x

Antenucci, F., Magnowska, Z., Nimtz, M., Roesch, C., Jänsch, L., & Bojesen, A. M. (2019). Immunoproteomic characterization of outer membrane vesicles from hyper-vesiculating *Actinobacillus pleuropneumoniae*. *Veterinary Microbiology*, *235*, 188–194. https://doi.org/10.1016/j.vetmic.2019.07.001

Badi, S. A., Bruno, S. P., Moshiri, A., Tarashi, S., Siadat, S. D., & Masotti, A. (2020). Small RNAs in outer membrane vesicles and their function in host-microbe interactions. *Frontiers in Microbiology*, *11*, 1209. https://doi.org/10.3389/fmicb.2020.01209

Bolger, Anthony M, Marc Lohse, and Bjoern Usadel. 2014. Trimmomatic: A flexible trimmer for Illumina sequence data. *Bioinformatics* 30(15): 2114–20. https://doi.org/10.1093/bioinformatics/btu170.

Bossé, J. T., Chaudhuri, R. R., Li, Y., Leanse, L. G., Fernandez Crespo, R., Coupland, P., Holden, M. T. G., Bazzolli, D. M., Maskell, D. J., Tucker, A. W., Wren, B. W., Rycroft, A. N., & Langford, P. R. (2016). Complete genome sequence of MIDG2331, a genetically tractable serovar 8 clinical isolate of *Actinobacillus pleuropneumoniae*. *Genome Announcements*, *4*(1). https://doi.org/10.1128/genomeA.01667-15

Carver, Tim et al. 2012. Artemis: An integrated platform for visualization and analysis of high-throughput sequence-based experimental data. *Bioinformatics* 28(4): 464–69. https://doi.org/10.1093/bioinformatics/btr703.

Choi, J.-W., Kim, S.-C., Hong, S.-H., & Lee, H.-J. (2017). Secretable small RNAs via outer membrane vesicles in periodontal pathogens. *Journal of Dental Research*, *96*(4), 458–466. https://doi.org/10.1177/0022034516685071

Collins, S. M., & Brown, A. C. (2021). Bacterial outer membrane vesicles as antibiotic delivery vehicles. *Frontiers in Immunology*, *12*, 3773. https://doi.org/10.3389/fimmu.2021.733064

Crooks, G. E., Hon, G., Chandonia, J.-M., & Brenner, S. E. (2004). WebLogo: A sequence logo generator. *Genome Research* , *14*(6), 1188–1190. https://doi.org/10.1101/gr.849004

Davis Jr, M. R. & Goldberg, J. B. (2012). Purification and visualization of lipopolysaccharide from Gram-negative bacteria by hot aqueous-phenol extraction. *JoVE*, *63*, e3916. https://doi.org/doi:10.3791/3916

Deatherage, B. L., & Cookson, B. T. (2012). Membrane vesicle release in bacteria, Eukaryotes, and Archaea: A conserved yet underappreciated aspect of microbial life. *Infection and Immunity*, *80*(6), 1948–1957. https://doi.org/10.1128/IAI.06014-11

Dell'Annunziata, F., Folliero, V., Giugliano, R., De Filippis, A., Santarcangelo, C., Izzo, V., Daglia, M., Galdiero, M., Arciola, C. R., & Franci, G. (2021). Gene transfer potential of outer membrane vesicles of Gram-negative bacteria. In *International Journal of Molecular Sciences* (Vol. 22, Issue 11). https://doi.org/10.3390/ijms22115985

Frantz, R., Teubner, L., Schultze, T., Pietra, L. La, Müller, C., Gwozdzinski, K., Pillich, H., Hain, T., Weber-Gerlach, M., Panagiotidis, G.-D., Mostafa, A., Weber, F., Rohde, M., Pleschka, S., Chakraborty, T., & Mraheil, M. A. (2022). The secRNome of *Listeria monocytogenes* harbors small noncoding rnas that are potent inducers of beta interferon. *MBio*, *10*(5), e01223-19. https://doi.org/10.1128/mBio.01223-19

Frey, J. (2011). The role of RTX toxins in host specificity of animal pathogenic Pasteurellaceae. *Veterinary Microbiology*, *153*(1), 51–58. https://doi.org/https://doi.org/10.1016/j.vetmic.2011.05.018

Gerritzen, Matthias J H et al. (2018). high dissolved oxygen tension triggers outer membrane vesicle formation by *Neisseria meningitidis*. Microbial Cell Factories 17(1): 157. https://doi.org/10.1186/s12934-018-1007-7.

Ghosal, A., Upadhyaya, B. B., Fritz, J. V, Heintz-Buschart, A., Desai, M. S., Yusuf, D., Huang, D., Baumuratov, A., Wang, K., Galas, D., & Wilmes, P. (2015). The extracellular RNA complement of *Escherichia coli*. *MicrobiologyOpen*, *4*(2), 252–266. https://doi.org/https://doi.org/10.1002/mbo3.235

Gill, S., Catchpole, R., & Forterre, P. (2019). Extracellular membrane vesicles in the three domains of life and beyond. *FEMS Microbiology Reviews*, *43*(3), 273–303. https://doi.org/10.1093/femsre/fuy042

Gottschalk, M. (2012). Actinobacillosis. In: Zimmerman, J.J. et al (Eds). Diseases of swine. *Chichester: Wiley-Blackwell*, *10*, 653–669.

Green, M. R., & Sambrook, J. (2012). Molecular cloning: a laboratory manual. *Cold Spring Harbor Laboratory Press*, *Fourth Edi*, 2028pp.

Gripenland, J., Netterling, S., Loh, E., Tiensuu, T., Toledo-Arana, A., & Johansson, J. (2010). RNAs: regulators of bacterial virulence. *Nature Reviews Microbiology*, *8*(12), 857–866. https://doi.org/10.1038/nrmicro2457

Hąc-Wydro, Katarzyna, and Paweł Wydro. (2007). The Influence of Fatty Acids on Model Cholesterol/Phospholipid Membranes. Chemistry and Physics of Lipids 150(1): 66–81. ttps://www.sciencedirect.com/science/article/pii/S0009308407003787.

Holmqvist, E., Wright, P. R., Li, L., Bischler, T., Barquist, L., Reinhardt, R., Backofen,

R., & Vogel, J. (2016). Global RNA recognition patterns of post-transcriptional regulators Hfq and CsrA revealed by UV crosslinking in vivo. *The EMBO Journal*, *35*(9), 991–1011. https://doi.org/https://doi.org/10.15252/embj.201593360

Hör, J., Matera, G., Vogel, J., Gottesman, S., & Storz, G. (2020). Trans-acting small RNAs and their effects on gene expression in *Escherichia coli* and *Salmonella enterica*. *EcoSal Plus*, *9*(1). https://doi.org/10.1128/ecosalplus.ESP-0030-2019

Jan, A. T. (2017). Outer membrane vesicles (OMVs) of Gram-negative bacteria: A Perspective update. *Frontiers in Microbiology*, *8*, 1053. https://doi.org/10.3389/fmicb.2017.01053

Jorjão, A. L., de Oliveira, F. E., Leão, M. V. P., Jorge, A. O. C., & de Oliveira, L. D. (2018). Effect of *Lactobacillus rhamnosus* on the response of *Galleria mellonella* against *Staphylococcus aureus* and *Escherichia coli* infections. *Archives of Microbiology*, *200*(3), 383–389. https://doi.org/10.1007/s00203-017-1441-7

Knox, K. W., Vesk, M., & Work, E. (1966). Relation between excreted lipopolysaccharide complexes and surface structures of a lysine-limited culture of *Escherichia coli*. *Journal of Bacteriology*, *92*(4), 1206–1217. https://doi.org/10.1128/jb.92.4.1206-1217.1966

Koeppen, K., Hampton, T. H., Jarek, M., Scharfe, M., Gerber, S. A., Mielcarz, D. W., Demers, E. G., Dolben, E. L., Hammond, J. H., Hogan, D. A., & Stanton, B. A. (2016). A novel mechanism of host-pathogen interaction through sRNA in bacterial outer membrane vesicles. *PLOS Pathogens*, *12*(6), e1005672. https://doi.org/10.1371/journal.ppat.1005672

Kuhnert, P, H Berthoud, R Straub, and J Frey. 2003. “Host cell specific activity of RTX toxins from haemolytic *Actinobacillus equuli* and *Actinobacillus suis*.” Veterinary microbiology 92(1–2): 161–67.

Langmead, B. and Salzberg, S. L. (2012) Fast gapped-read alignment with Bowtie 2. *Nature Methods*, 9(4), pp. 357–359. doi: 10.1038/nmeth.1923.

Lécrivain, A.-L., & Beckmann, B. M. (2020). Bacterial RNA in extracellular vesicles: A new regulator of host-pathogen interactions? *Biochimica et Biophysica Acta (BBA) - Gene Regulatory Mechanisms*, *1863*(7), 194519. https://doi.org/https://doi.org/10.1016/j.bbagrm.2020.194519

Li, Lu et al. (2014). Changes in gene expression of *Actinobacillus pleuropneumoniae* in response to anaerobic stress reveal induction of central metabolism and biofilm formation. Journal of microbiology (Seoul, Korea) 52(6): 473–81.

Lorenz, R., Bernhart, S. H., Höner Zu Siederdissen, C., Tafer, H., Flamm, C., Stadler, P. F., & Hofacker, I. L. (2011). ViennaRNA Package 2.0. *Algorithms for Molecular Biology : AMB*, *6*, 26. https://doi.org/10.1186/1748-7188-6-26

Malabirade, A., Habier, J., Heintz-Buschart, A., May, P., Godet, J., Halder, R., Etheridge, A., Galas, D., Wilmes, P., & Fritz, J. V. (2018). The RNA complement of outer membrane vesicles from *Salmonella enterica* serovar Typhimurium under distinct culture conditions. *Frontiers in Microbiology*, *9*, 2015. https://doi.org/10.3389/fmicb.2018.02015

Mashburn-Warren, L., Howe, J., Garidel, P., Richter, W., Steiniger, F., Roessle, M.,

Brandenburg, K., & Whiteley, M. (2008). Interaction of quorum signals with outer membrane lipids: insights into prokaryotic membrane vesicle formation. *Molecular Microbiology*, *69*(2), 491–502. https://doi.org/10.1111/j.1365-2958.2008.06302.x

Mead, G. P., Ratcliffe, N. A., & Renwrantz, L. R. (1986). The separation of insect haemocyte types on Percoll gradients; methodology and problems. *Journal of Insect Physiology*, *32*, 167–177.

Michaux, C., Verneuil, N., Hartke, A., & Giard, J.-C. (2014). Physiological roles of small RNA molecules. *Microbiology*, *160*(6), 1007–1019. https://doi.org/https://doi.org/10.1099/mic.0.076208-0

Micoli, F., & MacLennan, C. A. (2020). Outer membrane vesicle vaccines. *Seminars in Immunology*, *50*, 101433. https://doi.org/https://doi.org/10.1016/j.smim.2020.101433

Negrete-Abascal, E., García, R. M., Reyes, M. E., Godínez, D., & de la Garza, M. (2000). Membrane vesicles released by *Actinobacillus pleuropneumoniae* contain proteases and Apx toxins. *FEMS Microbiology Letters*, *191*(1), 109–113. https://doi.org/10.1111/j.1574-6968.2000.tb09326.x

Pathirana, R. D., & Kaparakis-Liaskos, M. (2016). Bacterial membrane vesicles: Biogenesis, immune regulation and pathogenesis. *Cellular Microbiology*, *18*(11), 1518–1524. https://doi.org/https://doi.org/10.1111/cmi.12658

Pattison, I. H., Howell, D. G., & Elliot, J. (1957). A haemophilus-like organism isolated from pig lung and the associated pneumonic lesions. *Journal of Comparative Pathology and Therapeutics*, *67*, 320-IN37. https://doi.org/https://doi.org/10.1016/S0368-1742(57)80031-9

Pereira, M. F., Rossi, C. C., de Queiroz, M. V., Martins, G. F., Isaac, C., Bossé, J. T., Li, Y., Wren, B. W., Terra, V. S., Cuccui, J., Langford, P. R., & Bazzolli, D. M. S. (2015). *Galleria mellonella* is an effective model to study *Actinobacillus pleuropneumoniae* infection. *Microbiology*, *161*(2), 387–400. https://doi.org/https://doi.org/10.1099/mic.0.083923-0

Pérez-Cruz, C., Briansó, F., Sonnleitner, E., Bläsi, U., & Mercadé, E. (2021). RNA release via membrane vesicles in *Pseudomonas aeruginosa* PAO1 is associated with the growth phase. *Environmental Microbiology*, *23*(9), 5030–5041. https://doi.org/10.1111/1462-2920.15436

Pors, S. E., Pedersen, I. J., Skjerning, R. B., Thøfner, I. C. N., Persson, G., & Bojesen, A. M. (2016). Outer membrane vesicles of *Gallibacterium anatis* induce protective immunity in egg-laying hens. *Veterinary Microbiology*, *195*, 123–127. https://doi.org/https://doi.org/10.1016/j.vetmic.2016.09.021

Roier, S., Blume, T., Klug, L., Wagner, G. E., Elhenawy, W., Zangger, K., Prassl, R., Reidl, J., Daum, G., Feldman, M. F., & Schild, S. (2015). A basis for vaccine development: Comparative characterization of *Haemophilus influenzae* outer membrane vesicles. *International Journal of Medical Microbiology*, *305*(3), 298–309. https://doi.org/https://doi.org/10.1016/j.ijmm.2014.12.005

Robinson, J. T., Thorvaldsdóttir, H., Turner, D., & Mesirov, J. P. (2020). igv.js: an embeddable JavaScript implementation of the Integrative Genomics Viewer (IGV). BioRxiv, 2020.05.03.075499. https://doi.org/10.1101/2020.05.03.075499

Roier, S., Fenninger, J. C., Leitner, D. R., Rechberger, G. N., Reidl, J., & Schild, S. (2013). Immunogenicity of *Pasteurella multocida* and *Mannheimia haemolytica* outer membrane vesicles. *International Journal of Medical Microbiology*, *303*(5), 247–256. https://doi.org/https://doi.org/10.1016/j.ijmm.2013.05.001

Rossi, C.C., Bossé, J.T., Li, Y., Witney, A.A., Gould, K.A., Langford, P.R., Bazzolli, D. M. S. (2016). A computational strategy for the search of regulatory small RNAs in *Actinobacillus pleuropneumoniae*. *RNA*, *Sep*; *22(9)*, 1373–1385.

Schertzer, Jeffrey W, Stacie A Brown, and Marvin Whiteley. (2010). oxygen levels rapidly modulate *Pseudomonas aeruginosa* social behaviours via substrate limitation of PqsH. Molecular microbiology 77(6): 1527–38. http://europepmc.org/abstract/MED/20662781.

Schooling, Sarah R, and Terry J Beveridge. (2006). "Membrane vesicles: An overlooked component of the matrices of biofilms." Journal of bacteriology 188(16): 5945–57. https://pubmed.ncbi.nlm.nih.gov/16885463.

Schwechheimer, C., & Kuehn, M. J. (2015). Outer-membrane vesicles from Gram-negative bacteria: biogenesis and functions. *Nature Reviews Microbiology*, *13*(10), 605–619. https://doi.org/10.1038/nrmicro3525

Shannon, P., Markiel, A., Ozier, O., Baliga, N. S., Wang, J. T., Ramage, D., Amin, N., Schwikowski, B., & Ideker, T. (2003). Cytoscape: A software environment for integrated models of biomolecular interaction networks. *Genome Research* , *13*(11), 2498–2504. https://doi.org/10.1101/gr.1239303

Sierra, G. V, Campa, H. C., Varcacel, N. M., Garcia, I. L., Izquierdo, P. L., Sotolongo, P. F., Casanueva, G. V, Rico, C. O., Rodriguez, C. R., & Terry, M. H. (1991). Vaccine against group B *Neisseria meningitidis*: protection trial and mass vaccination results in Cuba. *NIPH Annals*, *14*(2), 110–195. http://europepmc.org/abstract/MED/1812432

Soler, N., & Forterre, P. (2020). Vesiduction: the fourth way of HGT. *Environmental Microbiology*, *22*(7), 2457–2460. https://doi.org/https://doi.org/10.1111/1462-2920.15056

Su, Z., Zhu, J., Xu, Z., Xiao, R., Zhou, R., Li, L., & Chen, H. (2016). A transcriptome map of *Actinobacillus pleuropneumoniae* at Single-Nucleotide Resolution Using Deep RNA-Seq. *PLOS ONE*, *11*(3), e0152363. https://doi.org/10.1371/journal.pone.0152363

Tan, K., Li, R., Huang, X., & Liu, Q. (2018). Outer membrane vesicles: Current status and future direction of these novel vaccine adjuvants. *Frontiers in Microbiology*, *9*. https://doi.org/10.3389/fmicb.2018.00783

Thein, M., Sauer, G., Paramasivam, N., Grin, I., & Linke, D. (2010). Efficient subfractionation of Gram-negative bacteria for proteomics studies. *Journal of Proteome Research*, *9*(12), 6135–6147. https://doi.org/10.1021/pr1002438

Toyofuku, M., et al. (2014). Membrane vesicle formation is associated with pyocin production under denitrifying conditions in *Pseudomonas aeruginosa* PAO1. environmental microbiology 16(9): 2927–38.

Toyofuku, M., Nomura, N., & Eberl, L. (2019). Types and origins of bacterial membrane

vesicles. *Nature Reviews Microbiology*, *17*(1), 13–24. https://doi.org/10.1038/s41579-018-0112-2

Uchino, Y., & Ken-Ichiro, S. (2011). A simple preparation of liquid media for the cultivation of strict anaerobes. *Journal of Petroleum & Environmental Biotechnology*, *S3*(001).

Ulrike, R., Anthony, T. J., Anaïs, L. R., Gerald, S., Manfred, R., Sergo, K., Susanne, H., Philip, T., Nyunt, W. S., Emmanuelle, C., & Peter, G. E. (2016). A two-component regulatory system impacts extracellular membrane-derived vesicle production in Group A Streptococcus. *MBio*, *7*(6), e00207-16. https://doi.org/10.1128/mBio.00207-16

Westermann, A. J., Förstner, K. U., Amman, F., Barquist, L., Chao, Y., Schulte, L. N., Müller, L., Reinhardt, R., Stadler, P. F., & Vogel, J. (2016). Dual RNA-seq unveils noncoding RNA functions in host–pathogen interactions. *Nature*, *529*(7587), 496–501. https://doi.org/10.1038/nature16547

Supplementary material

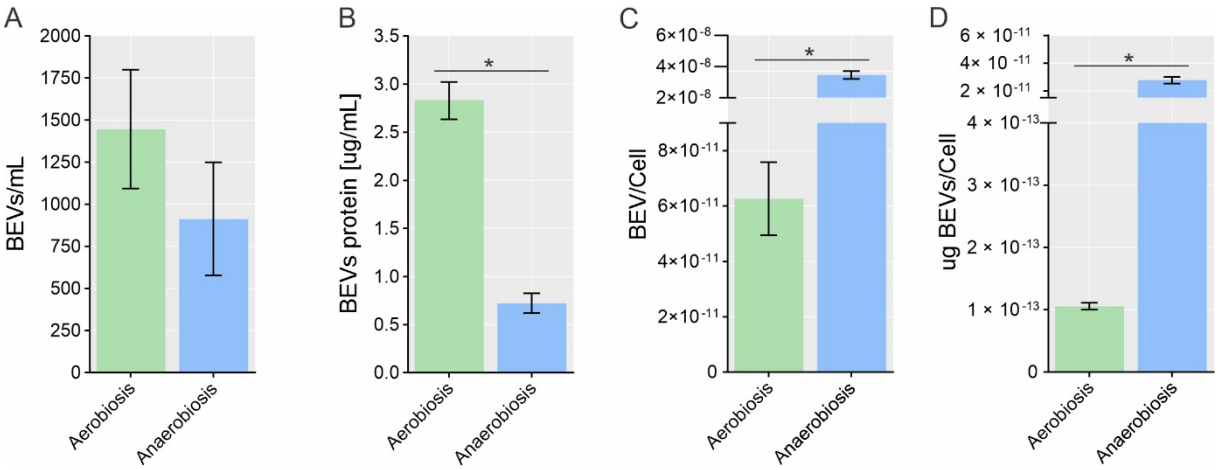

Supplementary Figure 1 - Production of BEVs by *A. pleuropneumoniae* in aerobiosis and anaerobiosis condition. (A) Quantification of BEVs produced in aerobiosis and anaerobiosis growth by flow cytometry. (B) Quantification of vesicle's proteins produced in aerobiosis and anaerobiosis growth. Standardization of BEVs production quantified by flow cytometry (C) or by protein (D) per cell for both aerobiosis and anaerobiosis growth. Significative difference between BEVs production in aerobiosis and anaerobiosis is represented by "*" by t-test ($p<0.05$).

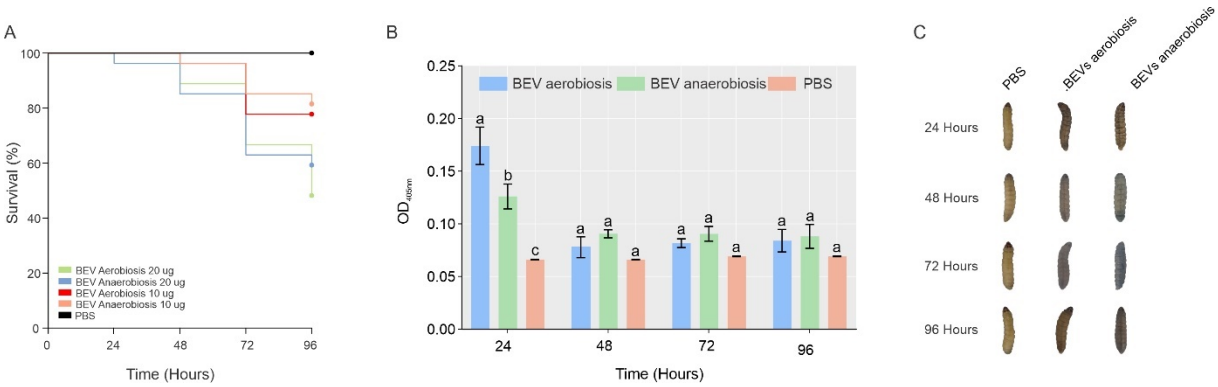

Supplementary Figure 2 – Toxicity effect of BEVs on the wax moth *G. mellonella*. (A) Killing assay of *G. mellonella*. (B) Optical density and melanization of larval haemolymph post-infection. (C) visual observation of larval melanization through the course of the experiment. Means with different letters are significantly different by Tuckey's test ($p<0.05$).

Supplementary Table 1 – Small RNAs previously confirmed to *A. pleuropneumoniae*

Name	Type	Position	Reference
Arrc01/Rna05	*trans* – acting	149354..149556	Rossi et al., 2016
Arrc05	*trans* – acting	760650..760819	
Arrc06	*housekeeping*	896755..896868	
Arrc07	*trans* – acting	1279204..1279310	
Arrc08	*trans* – acting	1997375..1997557	
Arrc10/6S	*housekeeping*	131770..131947	
Arrc11	*trans* – acting	211986..212067	
Arrc13	*cis*-acting	440496..440646	
Arrc14/Rna08	*trans* – acting	451950..452112	
Arrc15	*housekeeping*	563241..563629	
Arrc17	*trans* – acting	2064961..2065080	
Arrc19	*cis*-acting	2308407..2308602	
Arrc20	*trans* – acting	2118118..2118483	
Arrc21	*trans* – acting	2100216..2100291	
Arrc23/tmRNA	*housekeeping*	2118118..2118483	
Rna01	*trans* – acting	738604..738689	Chapter 3
Rna02	*trans* – acting	662472..662552	
Rna06	*trans* – acting	195041..195191	
Rna09	*trans* – acting	1869469..1869534	
Rna10	*trans* – acting	1996019..1996142	
Rna12	*trans* – acting	2292548..2292720	

Supplementary Table 2 – Oligonucleotides used in this work

sRNA	Primer name	Sequence (5'->3')	Amplicon lenght (bp)	Reference
Arrc01	ARRC01_F ARRC01_R	TGTTGTGTTTGCATATTGGTCTAGG TGGACGGTTATAAACCAAAAAGGT	122	Rossi et al., 2016
Arrc05	ARRC05_F ARRC05_R	CGGTGTGTAAGCGGTCTGAT GGATACCGAGCTTGTATGCCT	103	
Arrc07	ARRC07_F ARRC07_R	AGGTAGCTGGAGAAGAGCGA TTCTCCCCTGTCCTTTTGCC	182	
Arrc08	ARRC08_F ARRC08_R	AGAGCAAGCTGATGGTGCTT CGCTTGCATCGCAAGTAGC	160	
Arrc11	ARRC11_F ARRC11_R	TGTCCAATAAATAGGCTTCCCA AACTATCCAAATAAAAAGTACGGCT	126	
Arrc14	ARRC14_F ARRC14_R	ACGACTATCTCTTCGACTGCT GCATCAATGTGCGGGCAAAG	103	
Arrc17	ARRC17F ARRC17R	TTCTTTCTTGCAAAGAACCCGC ATGCTGATCTTGAAAAGCCCG	100	
Arrc20	ARRC20_F ARRC20_R	GCATTTGACGCTAAAACGGT AATTAGTGGCTCCTCCTGCG	128	
Arrc21	ARRC21_F ARRC21_R	GACCCTTTAGAAGGCGTTGC CGCAACGTTAAGGGTCGTTAG	115	
Rna01	RNA01_F RNA01_R	CTAACTGACAGAATTTATGTAAG ACCAAGAAAGCGATGCCG	72	Chapter 3
Rna02	RNA02_F RNA02_R	ACTTAATAAAAAGTGTTGTG AAGCCCCTCAACTTAGG	76	
Rna06	RNA06_F RNA06_R	TCATTGGGGTGCTTTACG TCAGATCAGGTTCTACGG	55	
Rna09	RNA09F RNA09R	GCTGAACCGACAGCGGAA TCCTTAGGTAAGGCGAGCTTC	103	
Rna10	RNA10_F RNA10_R	CGATTTAATATTCGGGCACTT CAACTCGTATAGGGCGGT	95	
Rna12	RNA12_F RNA12_R	GAGTGTCAGGTTGTTTT GTCAGAAGCTCCTTTTCA	45	
EvsRna1	EvsRna1_F EvsRna1_R	TTGGGCAATTTGTGGTATTTCTT TGCTTCGTGTTTTTAGCAACG	101	This study
EvsRna2	EvsRna2_F EvsRna2_R	AACTCCCCCTGCTTTGC GAAAGCCCCCAACCTTGT	55	
EvsRna3	EvsRna3_F EvsRna3_R	ACAGTGATTCATACCTCCAG GAAACCCCGTAGAAAACCTAC	66	
EvsRna4	EvsRna4_F EvsRna4_R	GCAATTTACCTTCGTTACAGG GGGAACAGGGATTTTGTGT	97	
EvsRna5	EvsRna5_F EvsRna5_R	AAGCGGTCGGATTTTTAGC AGCGGTCAAGATTCATAGC	64	
EvsRna6	EvsRna6_F EvsRna6_R	ATGTTTAGCCTTTTGATAAGC GGTAGTTTAGTCAGTCGTAG	64	
EvsRna7	EvsRna7_F EvsRna7_R	TTCGGACGACACGGAAAG GCGAAAAAACAACCGCTTG	45	
EvsRna8	EvsRna8_F EvsRna8_R	GGTTAGCAGCCTCCAACT ATCCTTGCTTCCACAAGTTG	50	
EvsRna9	EvsRna9_F EvsRna9_R	AGGGTTTAGCTATTTCGCCA GGCTTAACCTTTCCAGTTTCAG	59	
EvsRna10	EvsRna10_F EvsRna10_R	GACCGTTCGTGAATTGTCG CGAGAGTAAATTGGGGCGT	152	
EvsRna11	EvsRna11_F EvsRna11_R	CAGAAAAAGCCCGCAAATTG TCTGCACCTTAATCCGTTAGAG	69	
EvsRna12	EvsRna12_F EvsRna12_R	CTTGTGGGAGAGGGACAG GCAGAGAGAGGGGAATTTGC	101	
EvsRna13	EvsRna13_F EvsRna13_R	ATACCTGCCGTGTAGTTGG ATTAACGGTTGGTCAGGTTG	194	
EvsRna14	EvsRna14_F EvsRna14_R	GCACATCTTGTTGTCTGA ATTAAGTTAAGGTGGATAC	80	
EvsRna15	EvsRna15_F EvsRna15_R	TTTGATCTGTTACTGG TGTTACGCCCTCTCTC	68	
EvsRna16	EvsRna16_F EvsRna16_R	TGCTTCTTGTAATATTAACGT ACTGACGGTTGCATATCAA	53	
5S	APP5SF APP5SR	GCGATGCCCTACTCTCACAT GAGTGCTGTGGCTCTACCTG	100	Rossi et al., 2016

Supplementary Figure 3 – *A. pleuropneumoniae* carries packages DNA extraction in BEVs. DNA extracted from BEVs produced by *A. pleuropneumoniae* in aerobiois condition. The DNA untreated (left) and DNA treated (right) were observed in a 0.8% agarose gel.

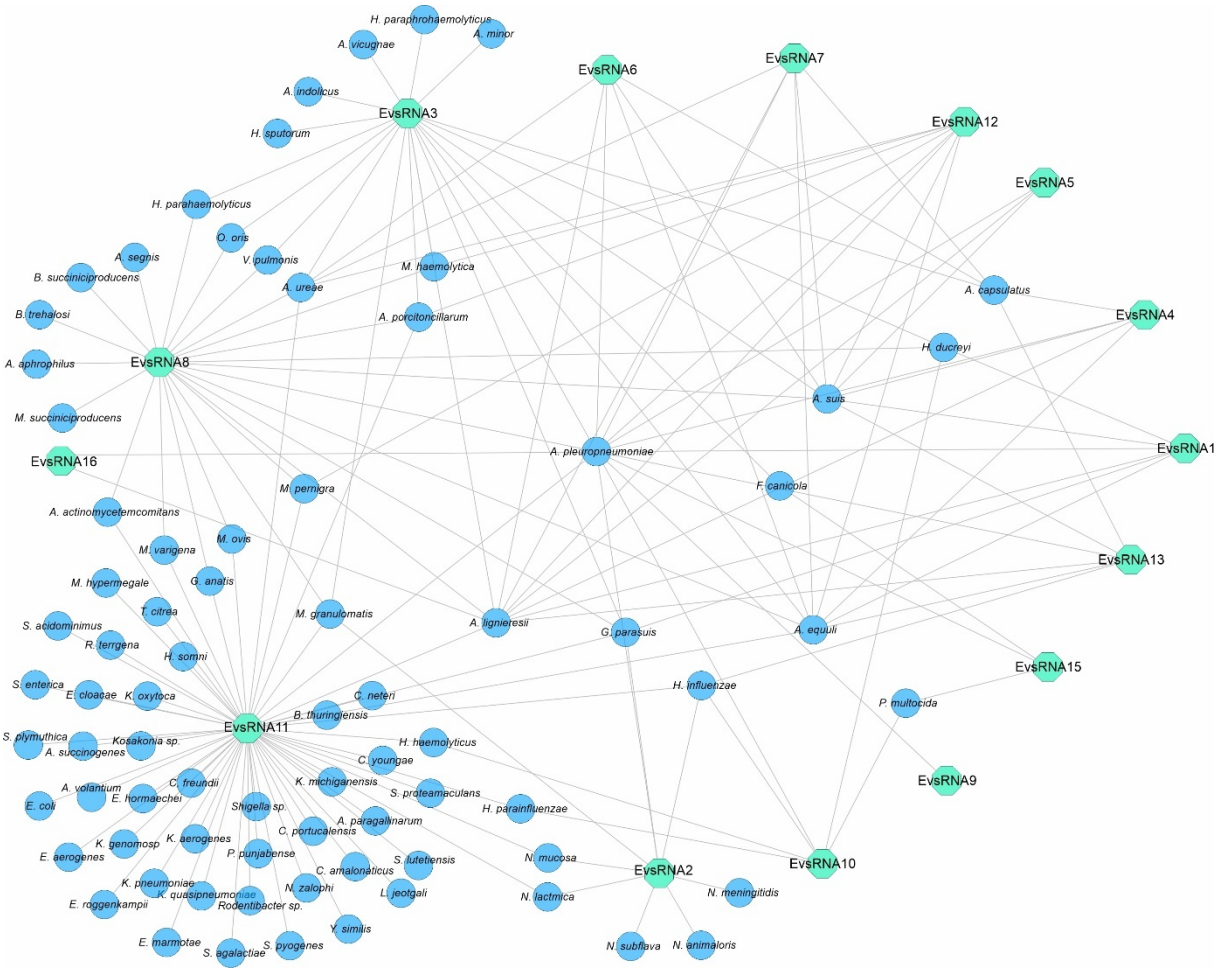

Supplementary Figure 4 – Dissemination of the novels sRNAs from *A. pleuropneumoniae* among species. The novel *A. pleuropneumoniae* sRNA candidates are represented by the green nodes and the species are represented by the blue nodes in the network.

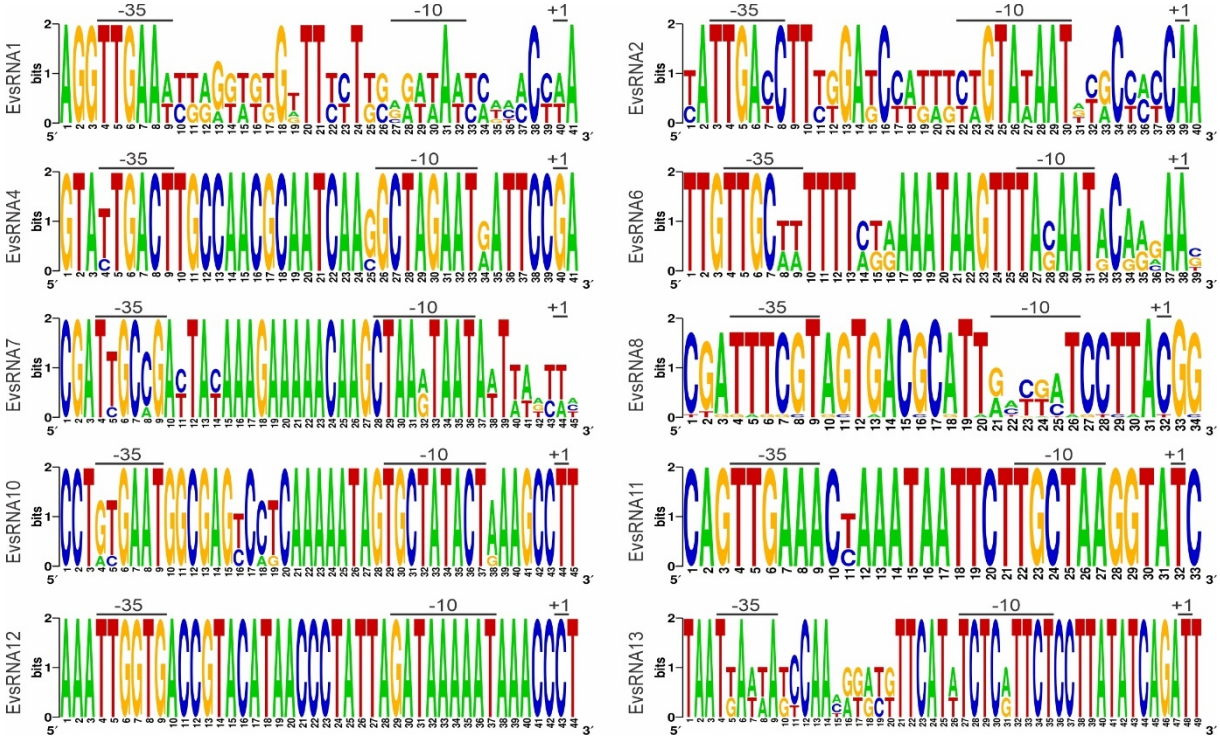

Supplementary Figure 5 -Putative promoters of novel sRNAs. Consensus sequence of putative -35 and -10 of the novel sRNAs candidates. Putative transcriptional starting site is represented by "+1"

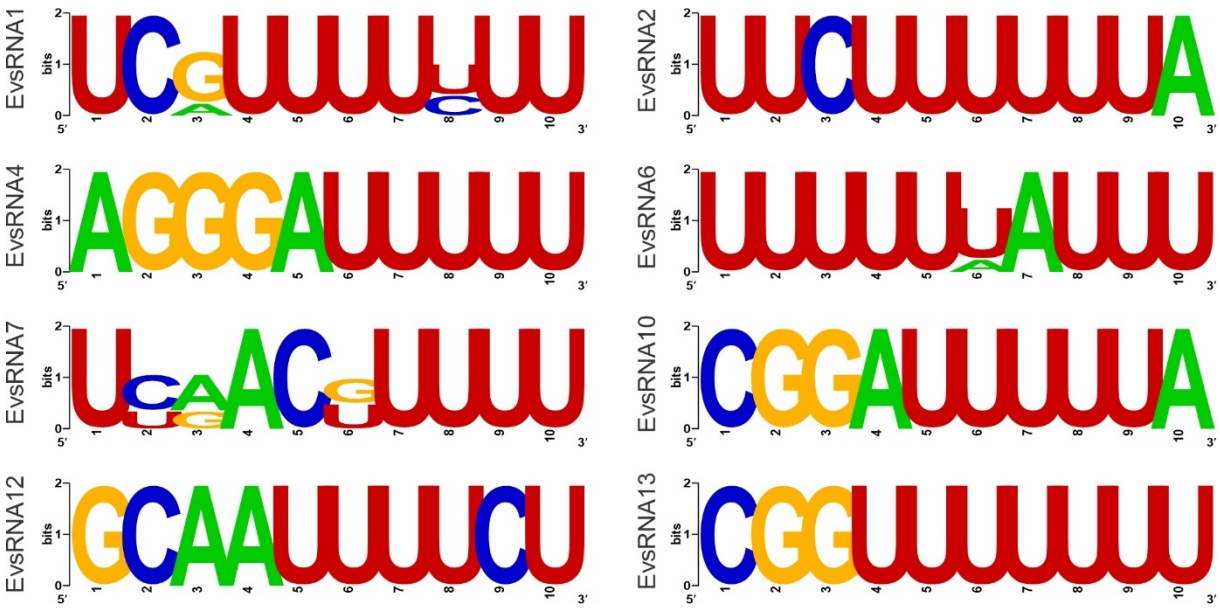

Supplementary Figure 6 - Putative Hfq binding site of novel sRNAs. Consensus sequence of putative Hfq binding site of the novel sRNAs candidates.

Chapter 3

Identification of novel small RNAs associated with RNA chaperone Hfq reveals a new extracytoplasmic stress response regulator in *Actinobacillus pleuropneumoniae*

(Manuscript written according to the guidelines of the Nucleic Acids Research journal)

Giarlã Cunha da Silva[1†], Ciro César Rossi[1,2†], Jéssica Nogueira Rosa[1†], Newton Moreno Sanches[1], Daniela Lopes Cardoso[3], Yanwen Li[4], Adam A. Witney[5], Kate A. Gould[5], Patrícia Pereira Fontes[6], Everton de Almeida Alves Barbosa[2], Anastasia J. Callaghan[3], Janine Thérèse Bossé[4], Paul Richard Langford[4*], and Denise Mara Soares Bazzolli[1*]

[1]Laboratório de Genética Molecular de Bactérias, Departamento de Microbiologia, Instituto de Biotecnologia Aplicada à Agropecuária - Bioagro, Universidade Federal de Viçosa, Viçosa, Brazil.

[2]Departamento de Bioquímica e Biologia Molecular, Universidade Federal de Viçosa, Viçosa, Brazil.

[3]School of Biological Sciences and Institute of Biological and Biomedical Sciences, University of Portsmouth, Portsmouth, United Kingdom

[4]Section of Paediatrics, Department of Medicine, Imperial College London, London, United Kingdom.

[5]Institute for Infection and Immunity, St. George's, University of London, London SW17 0RE, United Kingdom

[6]Departamento de Microbiologia, Universidade Federal de Viçosa, Viçosa, Brazil.

† Equal contribution

Abstract

The RNA chaperone Hfq promotes the association of small RNAs (sRNAs) with cognate mRNAs, controlling the expression of several phenotypes in bacteria. *Actinobacillus pleuropneumoniae hfq* mutants are attenuated for virulence in pigs, impaired in the ability to form biofilms, more susceptible to stress, but the sRNAs involved remained to be described. Here, 14 sRNAs were identified by co-immunoprecipitation with Hfq and the expression of eight, identified as *trans*-acting sRNAs, were confirmed by Northern blotting. We focused on one of these sRNAs, named Rna01, which was found in extracellular vesicles produced by *A. pleuropneumoniae*, and presented a putative promoter for RpoE (stress regulon) recognition. A knockout mutant for *rna01* and a double knockout mutant for *rna01* and *hfq,* were constructed. Both presented decreased biofilm formation and hemolytic activity, attenuation for virulence in *Galleria mellonella,* altered stress susceptibility and a different outer membrane protein composition. Rna01 also affected bacterial extracellular vesicles (BEVs) production, size and toxicity. qRT-PCR for *rna01* and potential mRNA targets indicated that Rna01 is associated with extracytoplasmic stress response. This work sheds light on our understanding of the influence of sRNAs in the physiology and virulence of *A. pleuropneumoniae*; which is demonstrated to be multilayered and complex, and greatly influenced by Hfq and associated RNAs.

Keywords: Pasteurellaceae; Porcine pleuropneumonia; *trans*-acting small RNA; *Galleria mellonella*; Stress response; Extracellular vesicles

Introduction

Actinobacillus pleuropneumoniae is the etiological agent of porcine pleuropneumonia, a contagious and severe respiratory disease with high lethality, economic impact and worldwide distribution (Pattison et al., 1957; Sassu et al., 2018). Currently, 19 serovars of *A. pleuropneumoniae* are known (Stringer et al., 2021). Although virulence of *A. pleuropneumoniae* is multifactorial and complex (Pereira et al., 2018), it is strongly related to the production of different combinations of the pore-forming and/or cytolytic repeat-in-toxin (RTX) proteins ApxI, ApxII, ApxIII (Frey, 2011). We and other researchers have shown that the RNA chaperone Hfq influences, in a serovar-dependent manner, different phenotypes of *A. pleuropneumoniae*, including adherence, susceptibility to stress conditions and virulence (Crispim et al., 2020; Pereira et al., 2015; Subashchandrabose et al., 2013).

The Hfq protein forms a homo-hexameric ring and it is involved in several essential processes, such as rRNA processing, ribosome biogenesis, tRNA maturation, control of mRNA translation, DNA compaction, and activity of c-di-GMP metabolic enzymes (dos Santos et al., 2019; Fu et al., 2021; Kavita et al., 2018). However, its most prominent activity involves dynamically binding to small non-coding RNA molecules (sRNAs) (Quendera et al., 2020). Hfq typically interacts with sRNAs with its proximal pore, via their Rho-independent terminators ending with 4–6 uridines, while the distal face of Hfq recognizes A-rich motifs that are often present in mRNA targets (Otaka et al., 2011; Sauer & Weichenrieder, 2011). This initial interaction then prompts Hfq to sweep the sRNA from the core to establish the sRNA-mRNA interaction (Santiago-Frangos & Woodson, 2018). Hfq acts thus as an RNA “matchmaker” that binds to several sRNAs and ensures their binding to equally diverse mRNA targets, leading to pleiotropic effects that make it a global regulator of post-transcriptional gene expression in bacteria (Updegrove et al., 2016).

Bacterial sRNAs are a diverse class of molecules, ranging from 50 to 500 nucleotides in length, that may act in *cis* (anti-sense RNAs) or in *trans*. *Trans*-acting sRNAs are not in the same locus of the target, and present partial complementarity to their mRNA cognates. They act through either blocking the ribosome binding site (RBS) and preventing translation initiation, or by destabilizing RBS sequestering RNA structures, favoring translation. Hfq interaction with RNAs can lead to to degradation by RNAse E or by polyadenylation of the 3' UTR region (Carrier et al., 2018; Vogel &

Luisi, 2011). The partial complementarity between the sRNA-mRNA pair and the small span of the pairing sites (about 7-12 nucleotides) allows a single sRNA to bind a variety of targets, forming a complex and intricate network of gene regulation (Carrier et al., 2018; Nitzan et al., 2017).

Previously, our group has combined computational prediction and experimental methods to show that the genome of *A. pleuropneumoniae* L20 encodes several sRNAs potentially involved in stress resistance and virulence (Rossi et al., 2016). However, not all sRNAs depend on the activity of Hfq, and although the data available for *hfq* mutants do indicate that stress response and virulence in *A. pleuropneumoniae* may be controlled by Hfq-dependent sRNAs (Crispim et al., 2020; Pereira et al., 2015; Subashchandrabose et al., 2013), the sRNAs involved remain to be characterized. Thus, the goals of this study were to identify sRNAs that act through binding Hfq and investigate their involvement with the fitness and pathogenicity in *A. pleuropneumoniae*.

Material and methods

A. pleuropneumoniae strains, growth and maintenance conditions

All experiments for the identification of Hfq-dependent sRNAs were conducted with strains described in Table 1. The two *A. pleuropneumoniae* wild type (WT) strains used were serovar 5 L20 (Foote et al., 2008) and serovar 8 MIDG2331 (Bossé et al., 2016) hereafter referred to as Ap8WT which was used to derive mutants in genes of interest. Strains were cultivated aerobically in brain heart infusion (BHI, BD - 237500) broth supplemented with nicotinamide adenine dinucleotide (NAD, 10 µg. mL^{-1}, Sigma-Aldrich - N0632-5G) at 37°C in an orbital incubator (180 rpm). For anaerobic growth, BHI broth was prepared with removal of oxygen and addition of N_2, according to Uchino & Ken-Ichiro, (2011), with strains being cultivated in hermetically sealed bottles without shaking at 37°C until they reached early stationary phase, DO_{600}: ~2,5 and 2,36 $x10^{13}$ $CFU.mL^{-1}$ for aerobiosis and DO_{600} = ~1 and 2,64 x 10^{10} $CFU.mL^{-1}$ for anaerobiosis.

Table 1 | *A. pleuropneumoniae* strains and mutants used in this study.

Strain	Description	Reference
Serotype 5		
L20	Reference strain of serotype 5b/ used as positive control for biofilm assay	Foote et al., 2008
Serotype 8		
Ap8WT	Clinical isolate from UK/used in all analyses	Bossé et al., 2016
Ap8hfq::3XFLAG	WT containing a 3XFLAG tag replacing the last codon of the *hfq* gene/used	Crispim et al., 2020
Ap8Δ*hfq*	Δ*hfq* mutant of MIDG2331/used in all analyses	Crispim et al., 2020
Ap8Δ*rna*01	Δ*rna*01 mutant of MIDG2331/used in all analyses	This study
Ap8Δ*hfq*Δ*rna*01	Δ*hfq*Δ*rna*01 mutant of MIDG2331/used in all analyses	This study

Hfq co-immunoprecipitation (co-IP) and RNA sequencing

Cells from Ap8*hfq*::3xFLAG strain were cultured in 100 mL BHI broth until early stationary phase, split into aliquots of 50 mL (Test, samples from Ap8WT, Ap8*hfq*::3xFLAG and Ap8Δ*hfq* subjected to co-IP; and Control, samples from same strains not subjected to co-IP), and centrifuged for 20 min at 5000 g at 4°C. The supernatant was discarded, and pellets were washed twice in 1.0 mL nuclease/protease free PBS (50TAB, Sigma-Aldrich, USA) and transferred into 2.0 mL microtubes. The microtubes were centrifuged again and pellets were frozen in liquid nitrogen and kept at -80ºC until use, when they were thawed on ice and re-resuspended in 1.0 mL ice cold lysis buffer (20 mM Tris pH 8, 150 mM KCl, 1 mM $MgCl_2$, 1 mM DTT) before being transferred to tubes containing Lysing Matrix B beads (MP Biomedicals, CA, USA). Lysis was conducted in the FastPrep-24™apparatus (MP Biomedicals, CA, USA), setting program 5. This procedure was performed twice, with a 1 min interval of cooling of samples on ice between homogenization. The lysate was cleared by centrifugation (40 min, 16000 x g at 4 ºC), supernatants (800 µL) transferred to new tubes, to which 400 $U.mL^{-1}$ of RNAsin inhibitor (Promega, WI, USA) had been added. co-IP was performed as previously described (Sittka et al., 2008) with modifications. Briefly, Hfq-3xFLAG expressed by Ap8 *hfq*::3xFLAG was co-immunoprecipitated with associated RNAs by the addition of 35 µL anti-FLAG M2 monoclonal antibody (F1804 - Sigma-Aldrich, MO, USA), following the manufacturer's instructions. The tubes were gently agitated for 60 min at 4°C, and 75 µL of prewashed Protein A Sepharose (P6649 - Sigma-Aldrich) added, and gently agitated for an additional 60 min. After the agitation period, the tubes were centrifuged (1000 *g* 1 min at 4°C), the supernatant was discarded, and the beads washed with lysis buffer as described above. TRIzol (1 mL, Invitrogen, CA, USA) was added to the beads, and RNA isolation was performed as suggested by the manufacturers. The co-IP procedure

was also performed with Ap8WT and Ap8Δ*hfq* strains as controls to assess the effectiveness of the technique to enrich for Hfq-associated RNAs. Total RNA obtained and analyzed using a Bioanalyzer (Agilent Technologies, CA, USA). RNA sequencing was done using Ion Total RNA-seq kit v2 (Life Technologies), according to the manufacturers' protocols. Samples were loaded onto a 318 chip and sequenced on Ion torrent-PGM (Life Technologies) using default manufacturer's parameters (single-end, forward sequencing).

Mapping, assembly and analysis of RNA sequencing results

RNA sequence reads were mapped onto the genome of *A. pleuropneumoniae* MIDG2331 (Ap8WT strain) (Genbank access LN908249) using Burrows-Wheeler Aligner (BWA-MEM algorithm, default parameters) version 0.7.10 (Li & Durbin, 2010). The resulting bam files were uploaded to NCBI's Short Read Archive (SRA, experiment SRX810211). Transcriptome assembly was made with Cufflinks version 2.2.1 (Ghosh & Chan, 2016). Results were analyzed using the sequence viewers JBrowse and Tablet (Buels et al., 2016; Milne et al., 2010). Putative *trans* sRNA candidates were identified by increased reads within intergenic regions in the annotated genome. After delimiting the sRNA candidates, the effectiveness of co-IP was evaluated by normalizing read counts as reads per kilobase million (RPKM). Normalized reads of the sRNA candidates from the three strains in aerobic and anaerobic conditions were used to plot a heatmap using the ggplot R package. Read coverage of the candidates were visualized using the integrative genome viewer (Robinson et al., 2020). The sRNA candidates were evaluated regarding their novelty by searching in the Rfam database.

Northern blotting

The Ap8WT, Ap8Δ*hfq* and Ap8*hfq*::3XFLAG strains were cultivated until early stationary phase under aerobic and anaerobic conditions as described above. Bacterial pellets from 1 mL of culture were disrupted with Lysing Matrix B tubes (MP Biomedicals), and RNA extraction was then performed with the miRNeasy Mini Kit (Qiagen) following the manufacturer's instructions. The resulting total RNA was quantified and treated with one unit of RQ1 DNAse (Promega) per µg of nucleic acid and incubated for 60 min at 37°C. DNA removal from the sample was confirmed by PCR with the oligonucleotide pair APP5SF and APP5SR for the 5S rRNA (Table 2) as

previously described (Rossi et al., 2016). Total treated RNA (10 µg) was loaded and run on a 10% TBE-urea polyacrylamide gel abnd transferred by electrophoresis to a Brightstar Plus nylon membrane (Applied Biosystems, CA, USA). Hybridization was conducted with the DIG High Prime DNA Labeling and Detection Starter kit II (Roche, Switzerland), according to the manufacturer's instructions. Primers designed for each sRNA (Table 2) were used to construct 109±18 bp digoxigenin-marked probes with the PCR DIG probe synthesis kit (Roche). As hybridization controls, all membranes were re-hybridized with probes for the rRNA 5S.

Table 2 | Primers used in this work

Primer	Sequence 5'-3'	Amplicon size	Target/purpose
Rna01F	CCGGCACCAAGAAAGCGAT	100	
Rna01R	AAACGGCTCAGTCTTAAATAACGC		
Rna02F	GTTCACATTGTAAGAAGAAGAAGCA	159	
Rna02R	CCTCAACTTAGGGGCTACTCG		
Rna03F	CTTACCAGTCAGAGTATCATTGG	96	
Rna03R	TGCGGCACTACTTTTAAGAAGCC		
Rna04F	TTACAATGTGGTCGTTCTATGACAA	101	
Rna04R	TCCTAGCCAATATATTAGGAATGAAT		
Rna05F	TGTTGTGTTTGCATATTGGTCTAGG	104	
Rna05R	TGGACGGTTATAAACCAAAAAGGT		
Rna06F	GAGCCAAGCACCATAGCGA	103	
Rna06R	GTCCTAGTGCCAGAAAGGAACT		
Rna08F	ACGACTATCTCTTCGACTGCT	103	
Rna08R	GCATCAATGTGCGGGCAAAG		
Rna09F	GCTGAACCGACAGCGGAA	103	
Rna09R	TCCTTAGGTAAGGCGAGCTTC		
Rna10F	ATCGGCGATTTAATATTCGGGC	106	
Rna10R	GCAAGCCAACTCGTATAGGG		
Rna12F	AGCGATTGTTATCCGGTCGT	147	Synthesis of probes for Northern blotting
Rna12R	AGACGGTCAGAAGCTCCTTT		
Rna13F	CACTAAGGTTGGGGCAAAGG	102	
Rna13R	GCAATAAAATAATACGACCG		
Rna14F	ACATTAAGCACATCTAAGAG	100	
Rna14R	AGCAAGTAGAAGGAGTTCTA		
APP5SF	GCGATGCCCTACTCTCACAT	100	Positive control for Northern blotting and RT-PCR
APP5SR	GAGTGCTGTGGCTCTACCTG		
Rna01_up	TGCCGTTAGCTTAGTGAGATTC	683	Confirmation of replacement of the *rna01* gene by natural transformation
dfrA_5'out	CACGGTTCTCATCCTAATTCCTCC		
sbcB_for	ACGATGAAATGACCCGTTATACC	453	
sbcB_rev	CTTGATTTTGATTAGTTGGGTGCC		
eriC_for	AAGTGCAAACGAGCTTATGGC	265	Analysis of the flanking genes to confirm no polar effect in Δ*rna01* expression
eriC_rev	GCACACCACACCGCATAATG		
ompp2B_F	CGTAACCACCCTCAGCAT	73	qPCR of the ompP2B target
ompp2B_R	GCATATGGTTTAGGTGCGGT		
ata2_F	GGTTTCCAATCCATCGCTCG	118	qPCR of the ata_2 target
ata2_R	CAGAACCGACACCCATAGC		
Rna01_F1	CTAACTGACAGAATTTATGTAAG	72	qPCR of the sRNA Rna01
Rna01_F2	ACCAAGAAAGCGATGCCG		
tolR_F	AATACACTCTTCCTTGTCGCTGC	100	qPCR of the tolR target
tolR_R	ACCCTGCGTTCTTAATACCCG		
gyrA_F	GTCGTGGCGGTAAAGGTAAA	111	Endogenous control for qPCR analysis
gyrA_R	GACCACGGCTTGAGAAACAT		

In silico analysis of Rna01

From the RNAseq / Northern blotting and initial *in silico* results, we decided to focus on one of the sRNA candidates discovered, named Rna01. The promoter sequence of Rna01 was predicted with Softberry BProm (available at http://www.softberry.com), and the putative Hfq-binding sequence (Holmqvist et al., 2016) was inspected visually. The Rna01 sequence was listed in the Rfam database as a possible sRNA. Additionally, we searched for homologues by alignment of the Ap8WT Rna01 sequence against NCBI's Genbank and PATRIC databases, using BLASTn with a 70% cut-off for both coverage and sequence identity. The alignments of the putative promoter and Hfq binding sequences were observed using WebLogo (Crooks et al., 2004).

Analysis of mRNA targets

Potential mRNA targets of Rna01 were searched in the genome of Ap8WT by combining TargetRNA2 and CopraRNA prediction tools (Kery et al., 2014; P. R. Wright et al., 2014), considering a p-value below 0.05 for predictions in both tools and a false discovery rate (fdr) below 0.5 (Benjamini & Hochberg, 1995) for CopraRNA. The MIDG2331 genome was used as a reference for target prediction in TargetRNA2, while CopraRNA required three Rna01 homologs, which were extracted from GenBank using NCBI accession numbers NZ_LN908249 for *A. pleuropneumoniae* serovar 8 MIDG2331, NC_009053 for *A. pleuropneumoniae* serovar 5 str. L20 and NC_010942 for *A. pleuropneumoniae* serovar 7 str. AP76. We also did manual inspections searching for potential targets by aligning the predicted seed regions with the genome of MIDG2331. Target's functions were investigated using the UniProT database as reference (The UniProT Consortium, 2019). Conservation of putative seed regions of Rna01 among the homologues was verified using Jalview (Waterhouse et al., 2009) using the homologues alignment. We also analyzed the expression of these mRNA's reads in our RNAseq data to verify their possible association with Hfq.

To investigate protein-protein interaction among the targets, the predicted mRNA targets were analyzed in STRING (Szklarczyk et al., 2019) using a moderate confidence 0.400 and Markov clustering method (MCL) with inflation parameter 1.1.

Comparative analysis of Rna01 and extracytoplasmic stress associated sRNAs

To investigate Rna01 as a possibly novel sRNA associated with extracytoplasmic stress responses, its homology with stress-associated sRNAs from other bacteria, such as MicA, MicF, MicC, MicL, OmrA, OmrB, RseX (all from *E. coli*), VrrA (*Vibrio cholerae*),and RybB (*Salmonella enterica*), was analysed for sequence alignment with Clustal Omega (Sievers & Higgins, 2014). The identity matrix generated was plotted in a heatmap using the ggplot R package. Additionally, sRNAs structures and putative seed regions of OM targets were predicted using RNAfold and TargetRNA2, respectively.

Construction of Rna01 knockout mutants

Two different Rna01 knockout strains were constructed in this work: a single *rna01* mutant (Δ*rna01*) from the parental *A. pleuropneumoniae* Ap8WT strain and a double *rna01* and *hfq* mutant (Ap8Δ*hfq*Δ*rna01*) from the previous Ap8Δ*hfq* strain (Table 1). A DNA cassette was designed to allow the replacement of the *rna01* gene by natural transformation, using the method previously described (Bossé et al., 2014) with modifications. This construct contained 500 bp of the upstream and downstream regions of *rna01* (flanking sequences), with the *rna01* gene being interrupted by the trimethoprim resistance gene *dfrA14* from the plasmid pM3389T (Bossé et al., 2015), which was put under the control of the *sodC* promoter and was immediately followed downstream by the 9 bp 5' ACAAGCGGT3' DNA Uptake Sequence (DUS), which enables efficient natural transformation by *A. pleuropneumoniae* (Redfield et al., 2006), and a Rho-independent terminator sequence (5´ AGC CGC CTA ATG AGC GGG CTT TTT TTT 3´), as described in Supplementary Figure S1. The entire 1625 bp cassette was synthesized and cloned into the pEX4K vector by Eurofins Genomics (Germany). The plasmid was cloned into ultracompetent *Escherichia coli* DH5α (Sambrook & Russell, 2006), purified with the Qiaprep Spin Miniprep kit (Qiagen), and linearized by digestion with NotI (Promega) at 37°C for 3 h, followed by heat inactivation at 65°C for 20 min. The linearized plasmid (1 µg DNA) was then used to naturally transform *A. pleuropneumoniae* strains as previously described (Bossé et al., 2014). Transformants were selected on BHI agar supplemented with 10 µg/mL NAD and 10 µg/mL trimethoprim. Correct replacement of the *rna01* gene with the *dfrA14* cassette was confirmed by PCR amplification of a 683 bp fragment using the primers RNA01_up (which binds further upstream than the sequence contained in the replacement

construct, so that no residual donor DNA could be detected) and dfrA_5'out (Table 2), and sequencing.

Absence of polar effects on the expression of the *rna01* flanking genes, *sbcB* and *eriC*, was confirmed by RT-PCR. Briefly, DNAse-treated RNA, prepared as described above, was used to synthesize cDNA with the ImProm-II Reverse Transcription System kit (Promega), following the manufacturer's suggestions. Subsequently, a PCR was performed with the primers sbcB_for and sbcB_rev to detect the expression of the *scbB* gene, and eriC_for eriC_rev for the *eriC* gene (Table 2).

Phenotypic analysis of *rna01* mutants

Growth parameters

Aliquots from overnight cultures of Ap8WT, Ap8Δ*hfq*, Ap8Δ*rna*01 and Ap8Δ*hfq*Δ*rna*01 strains were transferred to a fresh 50 mL BHI-NAD broth with an initial starting OD_{600} = 0.1. Strains were cultivated under constant agitation (180 rpm) at 37 ºC in aerobic conditions, and ODs measured every 20 min for the first five hours and, subsequently, every hour, for the next 12 h. The experiment was performed in biological triplicate.

Biofilm formation assay

Cell adherence was evaluated in microtiter plates as previously described (Stepanović et al., 2007), with modifications. Briefly, the Ap8WT, Ap8Δ*hfq*, Ap8Δ*rna*01 and Ap8Δ*hfq*Δ*rna*01 strains were grown overnight in BHI-NAD at 37°C and 5% CO_2, the cultures adjusted to OD_{600} = 0.1, and 150 µL were transferred to the microtiter plate wells, followed by incubation at 37°C and 5% CO_2 for 24 h. After this period, the wells were gently washed 3x with distilled water, stained with 150 µL of 0.1% crystal violet solution for 10 min, washed again with distilled water, then stained cells were re-suspended in 95% ethanol and kept at room temperature for 45 min. The OD_{595} was measured in a Multiskan Go spectrophotometer (Thermo Scientific). The experiment was performed in triplicate and negative controls consisted of wells to which sterile BHI-NAD was added at the beginning of the experiment. The *A. pleuropneumoniae* strain L20 was used as a positive control for biofilm formation (Foote et al., 2008).

Stress tolerance assay

The following agents and their concentrations were used in BHI-NAD agar to investigate the sensitivity of the Ap8WT, Ap8Δ*hfq*, Ap8Δ*rna*01 and Ap8Δ*hfq*Δ*rna*01 strains to osmotic stress (0.1 M KCl), oxidative stress (0.2 mM H_2O_2), temperature stress (42°C) and exposure to the antibiotics tylosin and ampicillin by minimum inhibitory concentration (MIC) test. Bacterial cultures with an initial OD_{600} of 1.0 were serially diluted in PBS to 10^{-7} and 10 µL of each 10-fold dilution was spotted onto each selective stress agar. As a control, cultures were plated on BHI-NAD agar containing no stressing agent. All plates were incubated at 37°C for 24 h. Antimicrobial sensitivity was evaluated by the microdilution method, according to the Clinical and Laboratory Standards Institute recommendations – Document M31-A3 (CLSI, 2008). After incubating the microplates at 37°C for 24 h, 50 µL of resazurin 0.01% (Sigma-Aldrich - R2127) were added to each well and the microplate was incubated again for 1 h at 37 ºC, in the dark. The minimum inhibitory concentration of each antibiotic was considered as the highest concentration at which resazurin was not reduced, i.e., no change in color from blue to pink. BHI-NAD broth was used without the addition of antibiotics as a positive control for bacterial growth.

Virulence assay in *G. mellonella*

Virulence effects of the deletion of the *rna01* gene, alone or with *hfq*, were evaluated using *G. mellonella* as an infection model. Propagation and rearing of *G. mellonella* larvae and experiments with last-instar larvae were conducted as previously described (Pereira et al., 2015). Survival was monitored every 24 h, for 96 h post-infection. Negative controls consisted of larvae inoculated with PBS. Tests were performed in biological and experimental triplicate, with 10 larvae per replicate.

Melanin production was quantified as previously described (Jorjão et al., 2018), with modifications. Briefly, incisions were made in the larvae's prolegs with a micro scissor to allow the haemolymph to leak. The haemolymph was collected with a micropipette and transferred to refrigerated microtubes, which were centrifuged at 9500 *g* for 10 min at 4ºC. The supernatant was diluted in anticoagulant solution (Mead et al., 1986), and the OD_{405} measured.

Hemolytic activity

The hemolytic activity of the Ap8WT, Ap8Δ*hfq*, Ap8Δ*rna*01 and Ap8Δ*hfq*Δ*rna*01 strains in defibrinated sheep blood (Ebefarma, RJ, Brazil) was evaluated as previously described (Shin et al., 1999), with modifications. Cultures were initially adjusted to OD_{600} = 0.1 and cultivated in 50 mL BHI-NAD under agitation (180 rpm) at 37 ºC in aerobic conditions until late exponential phase (OD_{600} ~ 2.5). Subsequently, 5 mL of cultures were centrifuged (5000 *g* for 5 min), and re-suspended in PBS to OD_{600} = 2.0. An aliquot of this suspension (0.75 mL) was added to an equal volume of 1% sheep blood and incubated for 1 h at room temperature (25°C) under gentle agitation. Then, samples were centrifuged (1000 x *g* / 5 min), and the OD_{405} measured. Negative and positive controls consisted of blood suspensions in PBS alone or with 1% Tween 20, respectively. Percentage of hemolysis was calculated using the following formula: hemolysis (%) = [(sample OD_{405} – PBS OD_{405}) / (Tween20 OD_{405} - PBS OD_{405}) x 100]. The experiment was performed in triplicate.

Outer membrane protein (OMP) extraction

The fractions of OMPs from the Ap8WT, Ap8Δ*hfq*, Ap8Δ*rna*01 and Ap8Δ*hfq*Δ*rna*01 strains were obtained following the “method 1” previously described (Thein et al., 2010), with 25 mL of cells culture being cultivated in BHI-NAD broth at 37° C and 180 rpm until late exponential and stationary phases. The proteins were separated by 12% SDS-PAGE followed by Coomassie blue staining.

***rna01* and targets expression by quantitative PCR**

A total of 2 µg of RQ1 DNAse-treated RNA was used to synthesize cDNA with the High-Capacity cDNA Reverse Transcription kit (Applied Biosystems). The expressions of the targets *ompP2B*, *tolR*, *ata_2* and the *rna01 gene* were evaluated by qRT-PCR in the Ap8WT, Ap8Δ*hfq*, Ap8Δ*hfq*Δ*rna01* and Ap8Δ*rna01* strains (except for the Δ*rna01* strains to evaluate *rna01* expression). Reactions were performed in the CFX96 Touch Real-Time PCR Detection System (Bio-Rad) with primers depicted in Table 2. The R2 was calculated for each primer set, and the reaction efficiency was calculated. Amplifications were performed under the following conditions: 2 min at 95ºC, followed by 40 cycles of 15 s at 95ºC and 1 min at 60ºC. After the amplification step, a melting curve was performed for each primer set. The relative quantification was done by a standard curve obtained for each gene, by the equation of the line

relating average Ct and log10 of control cDNA concentration. The results were normalized with *gyrA* as reference gene.

Extracellular vesicle (EV) extraction and analysis

Hydrostatic filtration to obtain BEVs

BEVs were obtained from the Ap8WT, Ap8Δ*hfq*, Ap8Δ*rna*01 and Ap8Δ*hfq*Δ*rna*01 strains using the hydrostatic filtration method for purification (Antenucci et al., 2017). Aliquots from overnight cultures of the strains were inoculated into 600 ml of fresh BHI such that the initial starting OD_{600} = 0.01, and cultivated until late exponential phase (OD_{600} ~2.5). After EV purification, the volume of BEVs recovered from each strain was equally adjusted to enable comparison BEVs production among the strains by relative protein abundance. Relative quantification was done by use of a standard curve obtained using bovine serum albumin (BSA - Sigma-Aldrich - A-4503) and the Bradford reagent (Sigma-Aldrich B6916).

EV size measurement

The size of the BEVs obtained was measured in an electrophoretic light scattering apparatus (Zetasizer Nano ZS, Malvern Instruments, United Kingdom). The data were analyzed with malvern zetasizer software version 7.11 to obtain the average hydrodynamic diameter of the particles in solution. The measurements were conducted at 25ºC with three replica runs of 5 min each, and the average intensity weighted diameter was calculated. To measure these parameters, 300 µg of BEVs diluted with PBS pH 7, with a refractive index of 1.332 and a viscosity of 0.9043, were used.

Transmission electron microscopy (TEM) of BEVs

For TEM, 10 µL containing ~0.3 µg of EV samples from each strain above were placed on a formvar coated grids, stained with 3% uranyl acetate and analyzed under a Zeiss EM 109 transmission electron microscope at 80 kV at the Center of Microscopy and Microanalysis (NMM-UFV) at the Universidade Federal de Viçosa.

Protein's profile of BEVs

To analyze the protein profile, the BEVs were dissolved in lysis buffer (50 mM Tris-Cl pH 6.8; 100 mM dithiothreitol; 2% SDS; 0.1% bromophenol blue; 10% glycerol),

and heated for 10 min at 100°C. The samples were separated in a 12% SDS-PAGE gel, and stained with Coomassie blue (Green & Sambrook, 2012).

Toxicity of BEVs produced by *A. pleuropneumoniae* in *G. mellonella*

The toxicity of BEVs produced by the strains was evaluated as described above by inoculating larvae of *G. mellonella* with 20 µg of BEVs from each strain. Negative controls consisted of larvae inoculated with PBS. Tests were performed in biological and experimental triplicate, with 10 larvae per replicate. Survival was monitored every 24 h, for 96 h post-infection. Survival curves were plotted as described above. The melanization levels of the larvae infected with BEVs were evaluated by infecting larvae with 3 µg of BEVs from each strain, as described above.

Statistical analysis

For toxicity in *G. mellonella* assay, survival curves were plotted using the Kaplan-Meier method (Kleinbaum & Klein, 2012), and differences in survival were estimated by using the log rank test using the software *R*, version 2.13.0, with *p* values <0.05 considered as statistically significant. For melanization and phenotypic analysis, the differences were analyzed using analysis of variance (ANOVA) followed by Tuckey test for multiple comparisons with *p* values <0.05 considered as statistically significant. For the quantitative expression of genes, the t-test was used considering *p* values <0.1 as statistically significant.

Results

sRNA candidates were enriched in the Hfq FLAG-tagged strain

Co-IP assays resulted in 31.5 ng, 135.5 ng and 18.1 ng of RNA total / µL being isolated from Ap8WT, Ap8*hfq*::3XFLAG and Ap8Δ*hfq*, respectively, showing the highest enrichment for the *hfq*::3XFLAG strain (4.3x Ap8WT and 7.5x to Ap8Δ*hfq* strain). Sequencing of co-immunoprecipitated RNAs produced an average of 924834 ± 66055 reads for each strain. To improve sRNA discovery, we merged the data from aero/anaerobiosis, which were then mapped to the genome of MIDG2331, available at the NCBI's Sequence Read Archive (SRA, access SRX810211). The search for abundant intergenic transcripts led to the discovery of 14 sRNA candidates, named Rna01-14 (Table 3 and Figure 1A). Normalized reads showed higher values for the co-immunoprecipitated sRNA candidates in the RNAseq data of Ap8*hfq*::3XFLAG in

comparison to WT and Ap8Δ*hfq* strains, showing the efficacy of the technique (Figure 1B). From their Rfam database identities, the candidates Rna07 and Rna11 were removed from the analysis, as they were identified as cis-acting sRNAs: they are the ribosomal S15 leader sequence and the FMN riboswitch, respectively.

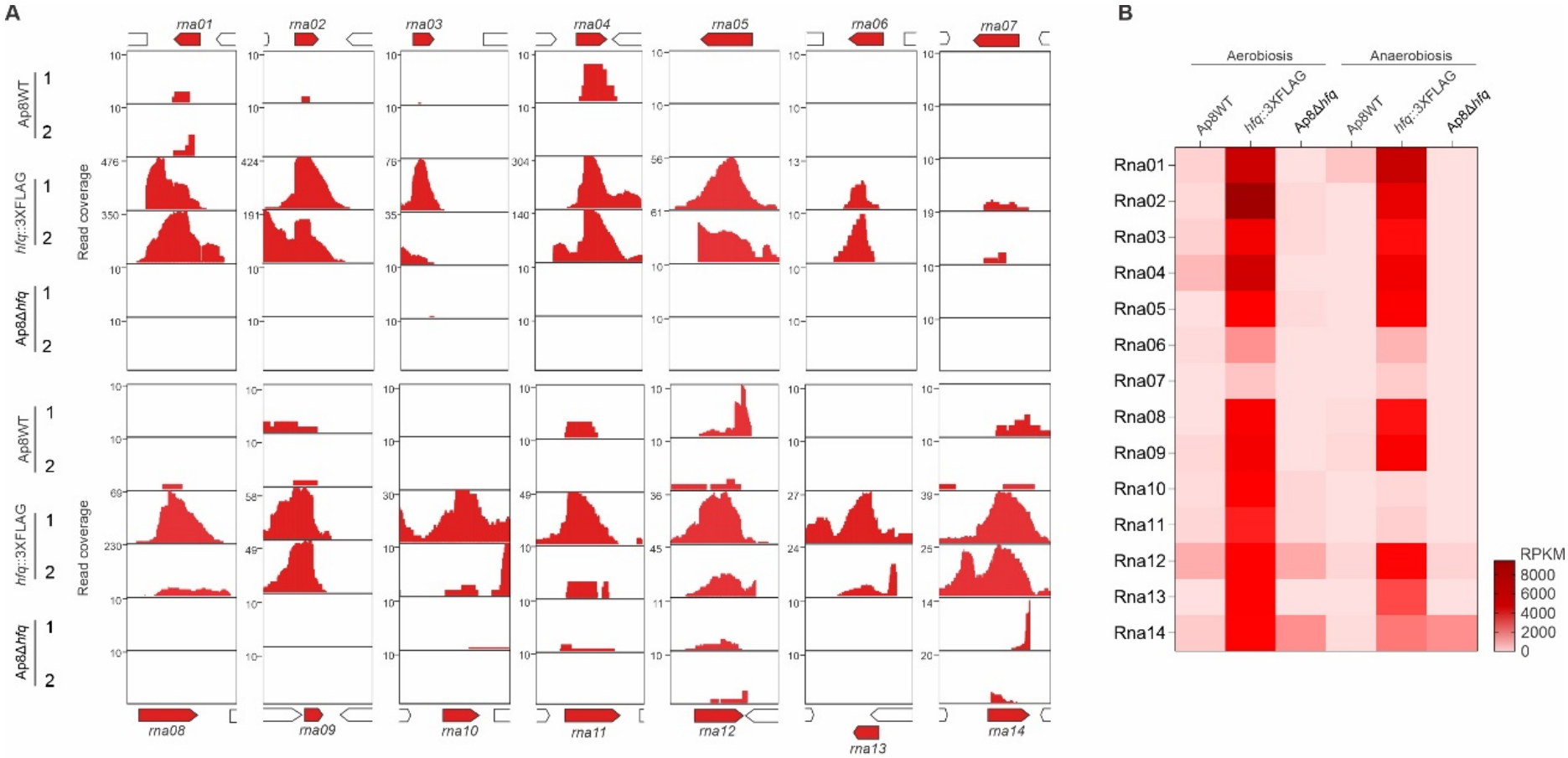

FIGURE 1 | Identification of novel sRNA candidates associated with the chaperone Hfq. (A) Mapping regions of the RNA sequences from the WT, Ap8*hfq*::3XFLAG and Ap8Δ*hfq* strains showing increased intergenic reads in aerobiosis (1) and anaerobiosis (2), corresponding to the 14 sRNA candidates selected in this study. (B) Heatmap showing the coverage, in RPKM, of the 14 putative novel sRNAs identified by co-IP.

Table 3 | Small regulatory RNAs identified in this work by Hfq Co-immunoprecipitation in *A. pleuropneumoniae*

sRNA	Genome position[a]	Strand	Size (nt)	*Upstream* gene	*Downstream* gene	Rfam classification (Access)
Rna01	738604-738689	-	86	*eriC*	*sbcB*	no match
Rna02	662472-662552	+	81	MIDG2331_00602	MIDG2331_00603	AaHKsRNA020 (RF02898)
Rna03	2035731-2035807	+	77	tRNA-Asn(gtt)	*ffh*	no match
Rna04	358279-358387	+	109	*rlu_A2*	*ampD*	no match
Rna05/ Arrc01[b]	149354-149556	-	203	*gcvA*	MIDG2331_00135	GcvB RNA (RF00022)
Rna06	195041-195191	-	150	MIDG2331_00179	MIDG2331_00180	TPP RNA (RF00059)
Rna07	1144541-1144667	+	127	*nhaP*	*rpsO*	Ribosomal S15 leader (RF00114)
Rna08/ Arrc14[b]	451950-452112	+	163	MIDG2331_00410	*leuA*	*Actinobacillus* sRNA 14 (RF02860)
Rna09	1869469-1869534	+	191	*mscL*	*lipA*	no match
Rna10	1996019-1996142	+	124	*nusG*	*rplK*	no match
Rna11/ Arcc13[b]	440504-440700	+	197	*glpC*	*ribD*	FMN riboswitch (RF00050)
Rna12	2292548-2292720	+	173	*comF*	*rsmC*	no match
Rna13	1561789-1561875	-	87	MIDG2331_01471	MIDG2331_01472	no match
Rna14	1518462-1518604	+	143	MIDG2331_01413	MIDG2331_01414	no match

[a]Position in the genome of *A. pleuropneumoniae* MIDG2331 strain (Genbank Access LN908249); [b]Original names of RNAs previously described by our group (Rossi et al., 2016)

Eight candidates, Rna01, Rna03, Rna04, Rna09, Rna10, Rna12, Rna13 and Rna14 corresponded to novel sRNA candidates with no previous identification/classification in the Rfam database version 14.7, available at http://rfam.xfam.org/ (Kalvari et al., 2021). These were considered as possible *trans*-acting sRNAs for the next analysis. Two candidates, Rna13 and Rna14, were located in an integrative and conjugative element, ICE*Apl1*, so far only found in some serovar 8 isolates of *A. pleuropneumoniae* (Bossé et al., 2016). Other *trans-acting s*RNAs have been described before. Rna02 is classified in the yet poorly characterized AaHKsRNA020 family (Rfam access RF02898). Rna05 is the well-studied sRNA GcvB, known to bind several sRNAs, mainly involved in amino acid biosynthesis and transport (Gulliver et al., 2018; Lalaouna et al., 2019). This sRNA corresponds to the sRNA Arrc01, previously identified by our group by computational approaches (Rossi et al., 2016). The same applies to Rna08, which corresponds to sRNA Arrc14 (Rossi et al., 2016). And Rna06 is described in the Rfam as a TPP sRNA (Rfam family RF00059).

Small RNA expression analysis

The expression of 8 of the 12 candidates obtained from co-IP was confirmed by Northern blotting in aerobic and anaerobic conditions from the total RNA of the Ap8WT,

Ap8*hfq*::3XFLAG and Ap8Δ*hfq* strains (Figure 2A). The predicted secondary structures of the confirmed sRNAs are shown in Figure 2B. Most of the sRNAs show stable secondary structures, based on the base-pair probability. Northern blot results for four of the sRNAs analyzed, Rna01, Rna02, Rna08 and Rna12, indicate their protection by Hfq from RNAse degradation, as they were either undetected in the Ap8Δ*hfq* mutant or were detected in lower concentrations than in the WT or Ap8*hfq*::3XFLAG strains. Rna02 and Rna06 were mostly (or exclusively) expressed during aerobic growth.

Although most RNA bands match their approximate expected size, RNAs 06 and 12 were detected with additional shorter bands, which could be by products of RNA processing or degradation products under the conditions analyzed, however further analyses need to be performed to confirm this. From the confirmed sRNAs, we chose to focus on Rna01, given its novelty, stability and Hfq dependency.

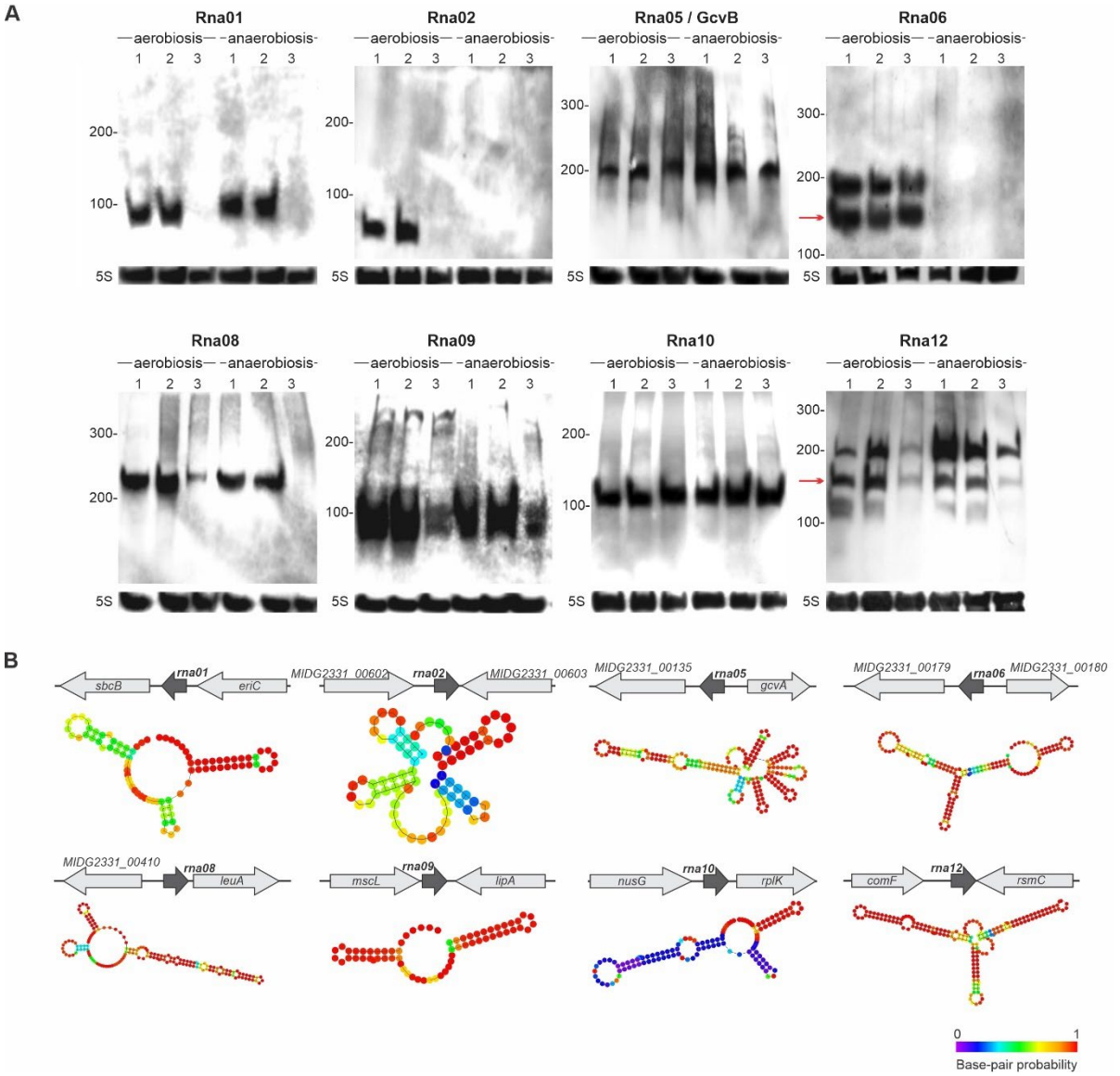

FIGURE 2 | Expression of Hfq-associated sRNAs identified in this work (A) Northern blotting validation of the expression of Hfq-associated sRNAs. Expression was assessed in *A. pleuropneumoniae* Ap8WT (1), Ap8*hfq*::3XFLAG (2) and Ap8Δ*hfq* (3) strains growing under aerobic and anaerobic conditions. All membranes were previously tested with probes to detect the rRNA 5S, expressed constitutively. The red arrow represents the band that corresponds to the predicted size for the respective sRNA. (B) Secondary structure of confirmed sRNA candidates, predicted by RNAfold (Lorenz et al., 2011).

In silico analysis of Rna01

Based on the expression of the Rna01 in aerobiosis and anaerobiosis conditions and the indicative of dependence of the chaperone Hfq, both revealed in the Northern blot results, we selected this sRNA for further characterization.

The Rna01 (86 bp) encoding gene *rna01* is located in in the intergenic region between *sbcB* and *eriC* on the opposite strand. The *rna01* gene σ^{70} promoter sequence (5' TTGGAA-21bp-TTAAAT 3') is shown in Supplementary Figure S2A. Also, typical sequences of genes controlled by stress sigma factor σ^{E} were found (5' GAACTT-16 bp-TCTTA 3'), in addition to the putative Hfq-binding sequence (GGGUUUUUUU)

(Supplementary Figure S2A). The secondary structure of Rna01 showed 3 stem loops, a putative Rho - independent terminator and a free energy (ΔG) of -23.9 kcal/mol (Supplementary Figure S2A).

Rna01 homologues were observed in a wide variety of Pasteurellaceae family species as other *Actinobacillus* spp., *Frederiksenia canicola*, *Glaesserella parasuis*, *Haemophilus ducreyi*, *Bibersteinia trehalose*, *Mannheimia haemolytica* and *Mannheimia varigena*. These sequences have conserved -35 and -10 for both σ^{70} and σ^{E} promoters and Hfq-binding sites, with minor differences among homologues (Supplementary Figure S2B).

Potential targets of Rna01

Combination of the results from TargetRna2 and CopraRna target predictors, revealed several cognate mRNA targets involved with various aspects of cell physiology and metabolism (Figure 3A and Supplementary Table S1). Among the predicted targets, mRNAs encoding the protease Lon (lon mRNA), and the ABC transporter complex MalEFGK through identification of MalK and MalE mRNAs were identified. We also identified genes encoding the proteins AccC, involved in fatty acid biosynthesis, AroQ, involved in chorismite metabolism, Asd, involved in aspartate metabolism, ZnuA, involved in zinc uptake, Ata, involved in cell adhesion, MetQ, involved in amino acid transport, and BioB, involved in biotin biosynthesis.

The genes encoding the SufE protein, associated with oxidative stress, and TolR protein, component of Tol-Pal system, were also identified as potential targets of Rna01. Target prediction showed a common region of interaction of the targets in the Rna01 sequence, which allowed us to identify two putative seed regions in the Rna01 structure (seed regions 1 and 2, Figure 3A and Supplementary Figure S3). Rna01 may interact with different regions of the different targets, mostly with the 5' UTR, but also 3' UTR, or inside the coding sequences (Supplementary Figure S4).

The alignment of Rna01 homologues showed conserved sequences on the putative seed regions, mostly for seed region 1 (Figure 3B). By manual prediction of targets based on the conserved sequence of the seed region 1, we found a substantial number of potential targets for the Rna01, including diverse genes involved with membrane processes (Figure 3C; Supplementary table S2). Interestingly, all the additional targets revealed a putative region of interaction around the ribosomal

binding site (RBS) and translation starting site (+1 translation), which were highly conserved among these targets (Figure 3C).

Both Rna01 targets predicted manually or by software were compared against STRING databases using *A. pleuropneumoniae* serovar 5 L20 genome for reference, to enquire whether their products shared metabolic pathways and functions, based on gene ontology (GO) terms. STRING analysis of the software-predicted targets showed few protein associations and no functional enrichment (Supplementary Figure 5A). However, the results for the manually predicted targets showed an association of targets mostly with OMPs, such as OmpP2, OmpP2A2, momP2 and ompP2, among others, with mostly high free energy (-4,92 to -12,55 kcal/mol, Supplementary Figure S5B; Supplementary table 2). The expression of some of these targets was detected in the RNA seq/ co-IP sequences, being most of the above mentioned targets enriched in the *hfq*::3xFLAG strain in at least one of the conditions tested, indicating their interaction with Hfq (Supplementary Figure S6).

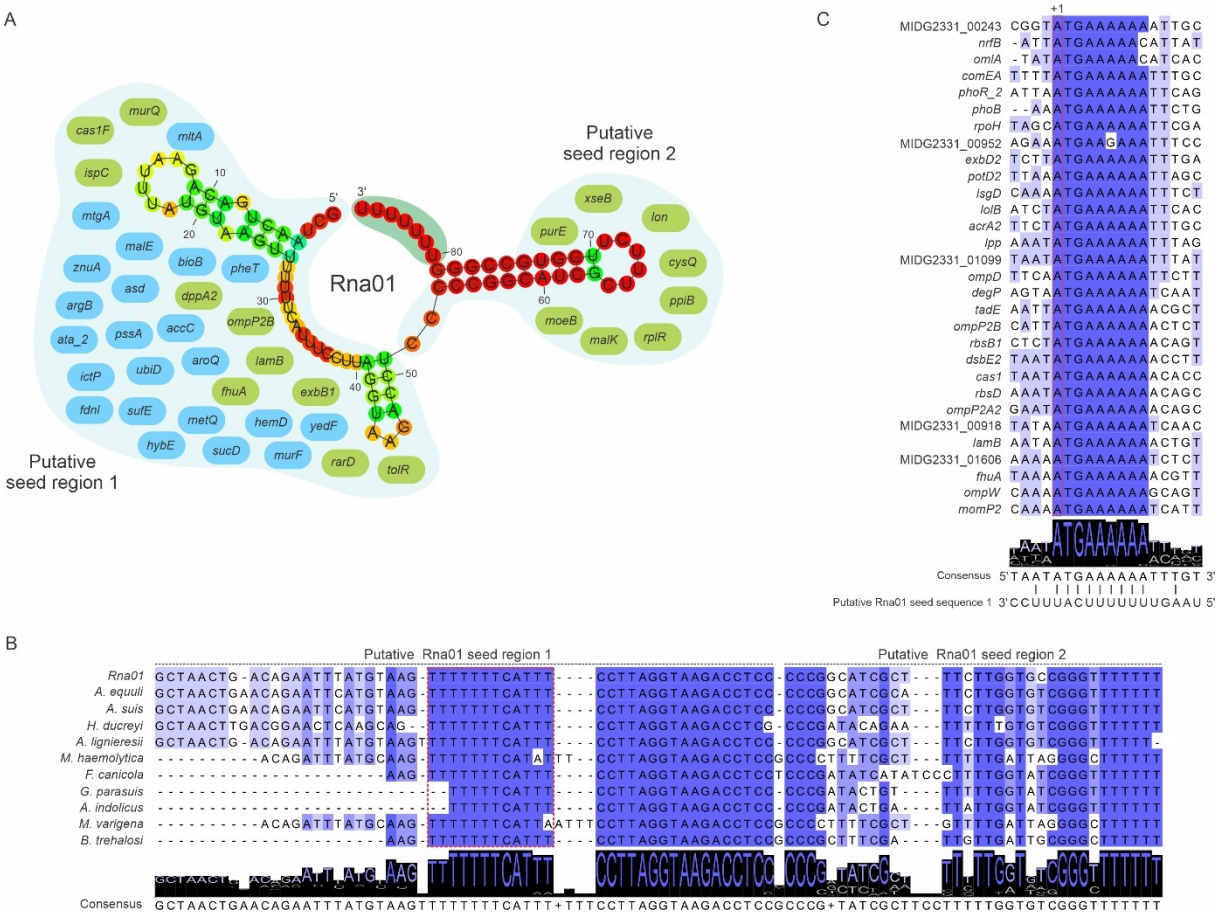

FIGURE 3 | mRNA Targets predicted to Rna01 in *Actinobacillus pleuropneumoniae*. (A) mRNA targets associated with their putative seed regions in the Rna01 structure. Nucleotides circled in dark green represent the Hfq binding site. Targets predicted by TargetRNA2 are shown in green and targets predicted by CopraRna, in blue. (B) Alignment of Rna01 and its homologues in Pasteurellaceae shows the conservation of the putative seed regions. (C) targets of Rna01 manually predicted in the MIDG2331 genome and the interaction with the seed region 1 of the Rna01 Translational starting site of the targets is represented by the "+1" in the figure.

Phenotypic analysis of Rna01 knockout strains

Gene replacements were confirmed by selecting the strains on trimethoprim (whose resistance is conferred by the newly added gene *dfrA14*), and by PCR for the presence of the sequence between *dfrA14* and *eriC* genes in the resulting Δ*rna*01 and Ap8Δ*hfq*Δ*rna*01 strains (Supplementary Figure S1). Our strategy to replace the *rna01* gene by *dfrA14* did not affect the expression of the flanking genes *sbcB* and *eriC*, as detected by RT-PCR (Supplementary Figure S1E).

Effects of *rna01* deletion on bacterial growth

Growth curves for the WT and mutant strains are presented in Figure 4A. No statistically significant difference ($p>0.05$) in maximum growth rate (μ_{max}) of the Ap8WT, Ap8Δ*hfq* and Ap8Δ*hfq*Δ*rna*01 strains was found, although the μ_{max} for the Δ*rna*01 was lower than the others ($p<0.05$) (Figure 4A).

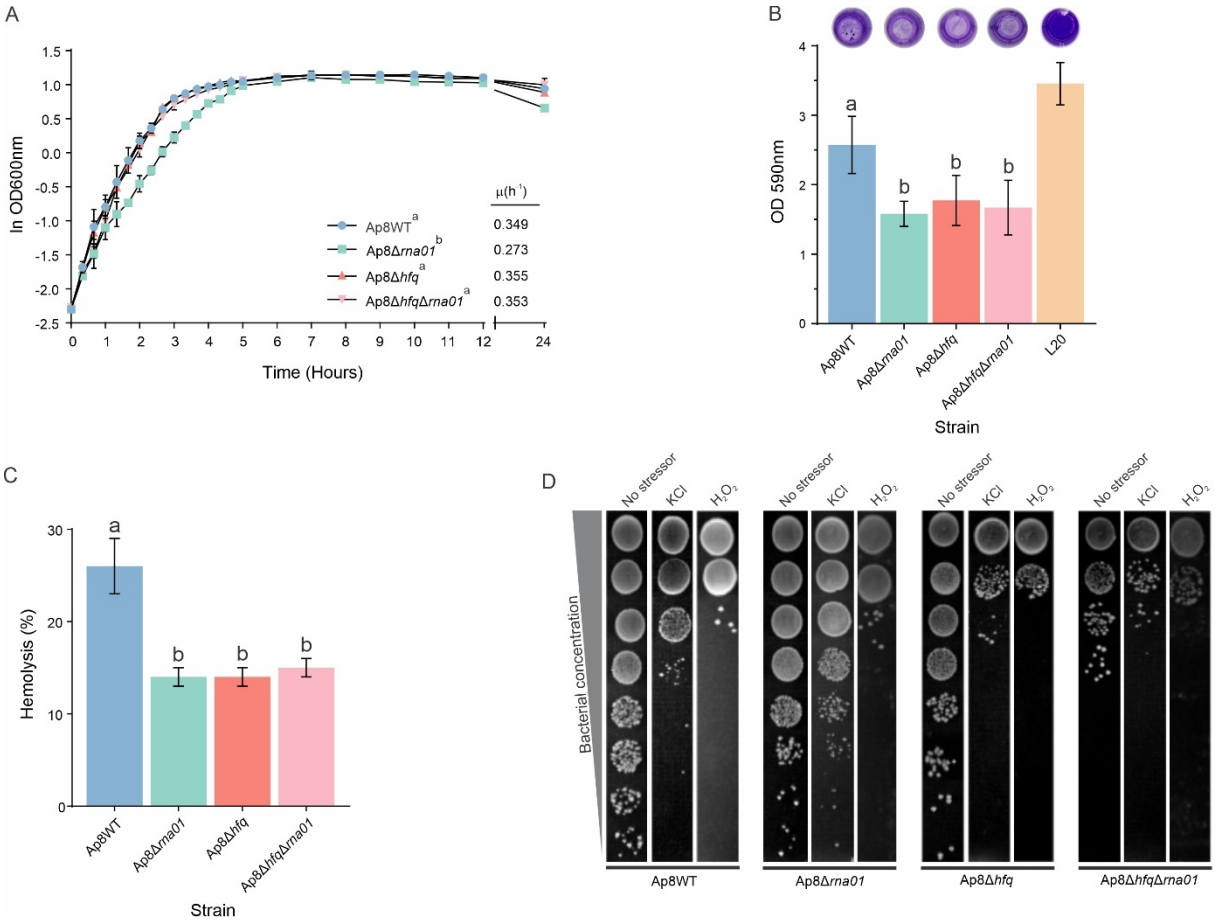

FIGURE 4 | Phenotypic characterization of *Actinobacillus pleuropneumoniae rna01* mutant strains (A) Bacterial growth in BHI-NAD at 37°C. Maximum growth rates (μ) are shown in the bottom-right corner. (B) Biofilm formation in polystyrene microtiter plates. (C) Hemolytic activity on sheep blood. (D) Stress tolerance in KCl 0,1M and H_2O_2 0,2 mM. Means with different letters are significantly different by Tuckey's test ($p<0.05$).

Effects of *rna01* deletion on bacterial adhesion and hemolysis

All mutant strains, Δ*rna01*, Ap8Δ*hfq*Δ*rna*01 and Ap8Δ*hfq* had reduced biofilm-forming ability when compared to the Ap8WT and positive control ($p<0.05$) (Figure 4B). Unlike its derivatives, the Ap8WT strain also formed depositions of bacterial lumps, while all mutant strains displayed uniform adherence in polystyrene wells (Figure 4B). All mutants displayed significant impaired hemolytic activity ($p<0.05$) (Figure 4C). No additive effects on hemolysis were observed for the double mutant, Ap8Δ*hfq*Δ*rna*01.

Effects of *rna01* deletion on susceptibility to stress

Upon osmotic stress with KCl 0.1 M, all strains were more susceptible than the WT. Oxidative stress (H_2O_2) caused a significant growth reduction for mutants (Figure 4D). No strains were able to grow at 42°C, and no difference was observed in their susceptibility to ampicillin and tylosin (the MIC remained 4 μg/mL for all).

Virulence in *G. mellonella*

Only ~34% of the *G. mellonella* larvae infected with the Ap8WT strain survived within 96 h post-infection (Figure 5A). Survival rates increased significantly, all above 70%, for the Ap8Δ*hfq*, Ap8Δ*rna*01 and Ap8Δ*hfq*Δ*rna*01 strains, as 72%, 89% and 95% of the larvae infected, respectively, survived during the 96 h experiment. The results obtained for the single mutants were statistically equivalent to those obtained for the double mutant strains ($p<0.05$) (Figure 5B) (Supplementary table 3).

Visually, larvae infected with the negative control (PBS), the Ap8Δ*hfq* and Ap8Δ*hfq*Δ*rna*01 strains showed no clear points of melanization (Figure 5C). However, quantitatively, the Ap8Δ*hfq* and Ap8Δ*hfq*Δ*rna*01 strains induced a minor production of melanin, as their hemolymph was slightly more turbid than the negative controls (Figure 5D). The Ap8WT and Ap8Δ*rna*01 strains, on the other hand, induced more melanization than the other strains ($p<0.05$). The results in Figure 5C show that the Ap8Δ*rna*01 strain, despite being attenuated in virulence, is capable of inducing an immune response in *G. mellonella* based on the melanization results. Dead larvae were completely melanized and dehydrated, thus no hemolymph was available for analysis.

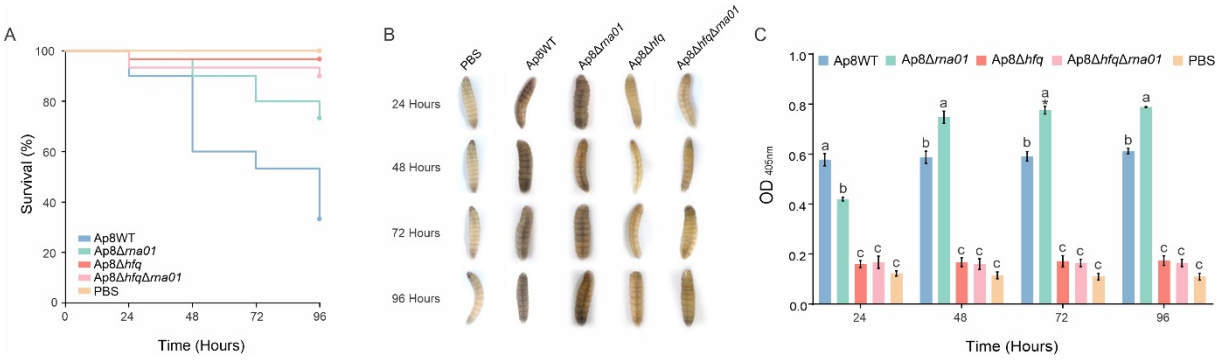

FIGURE 5 | Effects of the deletion of the *rna01* gene on *Actinobacillus pleuropneumoniae* virulence. (A) killing assay of *Galleria mellonella*; (B) visual observation of larval melanization through the course of the experiment (only living larvae are shown, since dead larvae get completely darkened and dehydrated). (C) optical density of larval hemolymph post-infection. Means with different letters are significantly different by Tuckey's test ($p<0.05$).

Expression of *rna01* and target genes

Quantitative PCR of *rna01* showed that this sRNA was up-regulated during the stationary phase in Ap8WT and Ap8Δ*hfq* strains (Figure 6A). However, *rna01* was down-regulated in the Ap8Δ*hfq* strain during exponential growth (Figure 6A), indicating that the stability of Rna01 is Hfq-dependent under this growth condition. The putative target gene *ompP2B* is more expressed during stationary growth in Rna01-absent

strains (p<0.10) (Figure 6B). The *ata_2* gene was down-regulated in the mutant strains during the exponential phase (Supplementary figure 7A), which corroborates the reduced bacterial adhesion of the mutants in stationary phase. The gene *tolR* (Tol-Pal system) was up-regulated in the double mutant strain during exponential growth and in the mutant strains during stationary phase (Supplementary Figure S7B). In contrast with *ompP2B*, the *ata_2* and *tolR* targets showed similar profiles of expression in the *rna01* and *hfq* mutants.

OMP extraction revealed clear differences between the WT and Ap8Δ*hfq*, Ap8Δ*rna01* and Ap8Δ*hfq*Δ*rna01* strains, when adjudged by the presence and absence of protein bands. Minor differences were observed between exponential and stationary phases for the Ap8Δ*hfq* strain (Figure 6C).

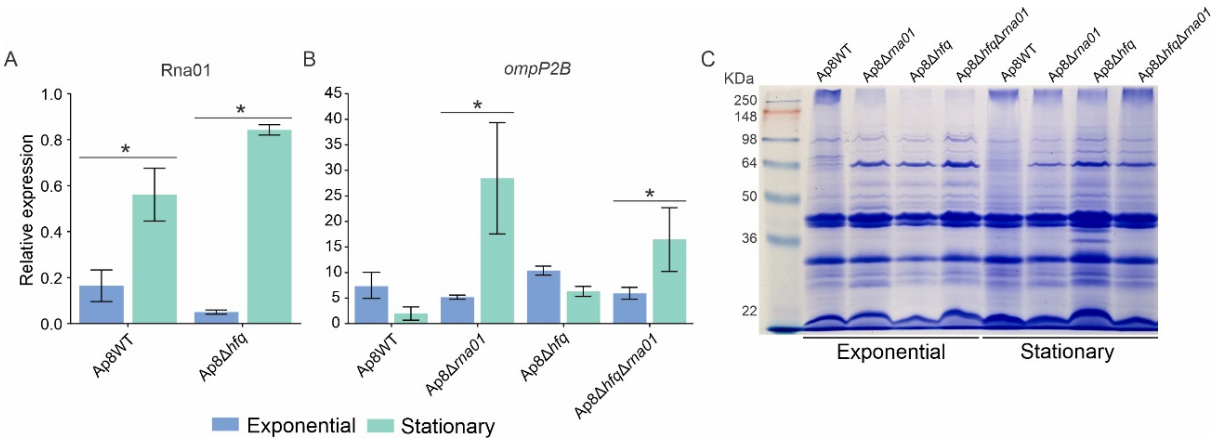

FIGURE 6 | *rna01* and *ompP2B* expression and their effect in the outer membrane protein contents. qPCR of *rna01* (A) *ompP2B* (B) during exponential and stationary phases in the WT and mutant strains. (C) OMPs profile of the strains in exponential and stationary phases. Significative difference between Cells and BEVs is represented by "*" by t-test (p<0.1).

Effect of Rna01 on EV production

Transmission electron microscopy showed the integrity of the vesicles (Figure 7A). BEVs produced by the Ap8Δ*hfq* strain were the biggest, while the BEVs from *rna01*-mutant strains were the smallest, in comparison to WT (Figure 7B). All mutants produced less BEVs than the WT (Figure 7C). The protein profile did not differ significantly among the BEVs (Figure 7D). However, BEVs produced by the Δ*rna01* strain were more toxic to the *G. mellonella* than the others (p<0.05) (Supplementary table 4) (Figure 7E), although, no significant differences were observed in the melanization of the larvae (p>0.05) (Supplementary Figures S8A and S8B).

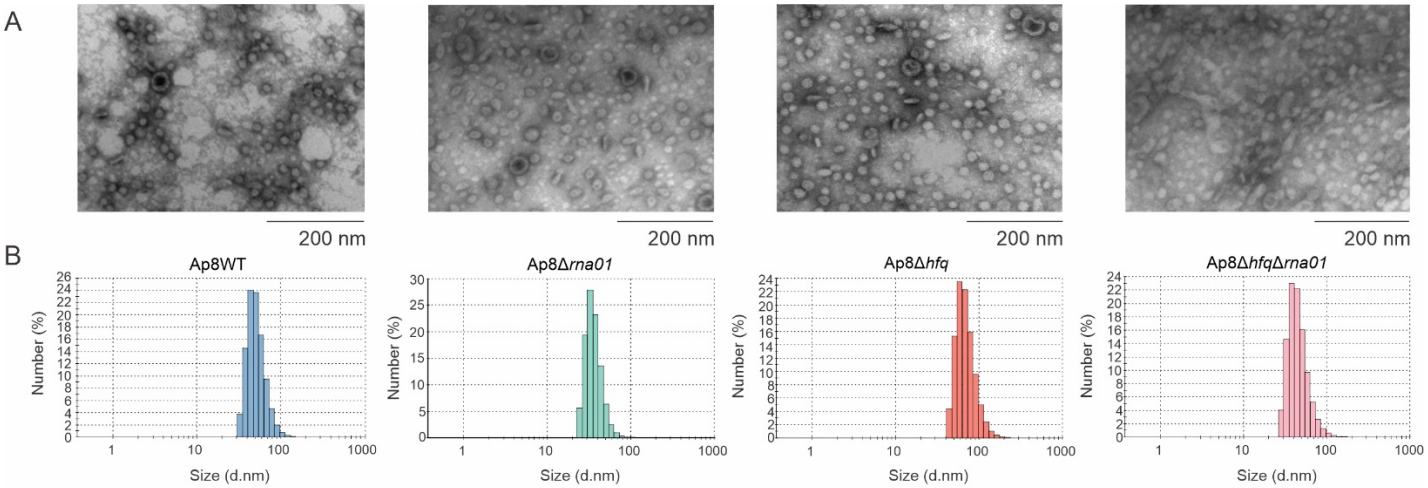

Strain	Particles size (diameter)		
	Minimum (nm)	Most frequently (nm)	Maximum (nm)
Ap8WT	32.67	43.82	190
Ap8Δ*rna01*	24.3	37.6	255
Ap8Δ*hfq*	43.82	58.77	295.3
Ap8Δ*hfq* Δ*rna01*	28.21	37.8	255

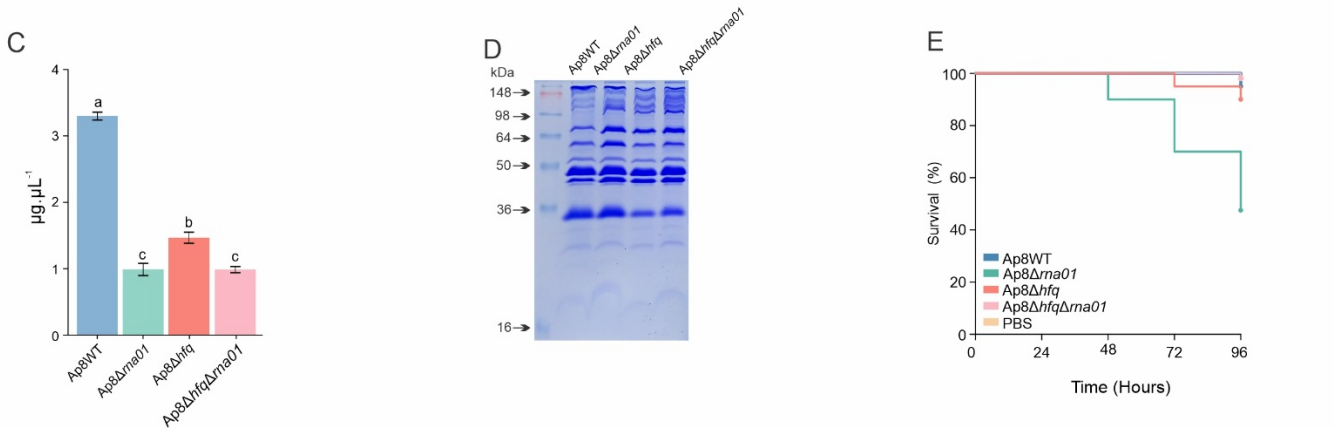

FIGURE 7 | Effect of Rna01 in the extracellular vesicles production. (A) Transmission electron microscopy of BEVs produced by *A. pleuropneumoniae* strains. (B) Size measuring by dynamic scattering light (DLS) of the vesicles produced by the strains. (C) Relative abundance of vesicles production among strains. (D) Protein profile of the vesicles produced by the strains. (E) Killing assay of *Galleria mellonella* infected with the vesicles.

Rna01 is an sRNA unique to *A. pleuropneumoniae* and is involved in regulating stress responses

Rna01 is not closely related to any other sRNAs associated with extracytoplasmic stress, and is not phylogenetically grouped with any of the sRNAs studied (Figures 8A and 8B). However, Rna01 has a secondary structure similar to MicAs (Figure 8C). All stress response-associated sRNAs analyzed were absent in the *A. pleuropneumoniae* MIDG2331 genome.

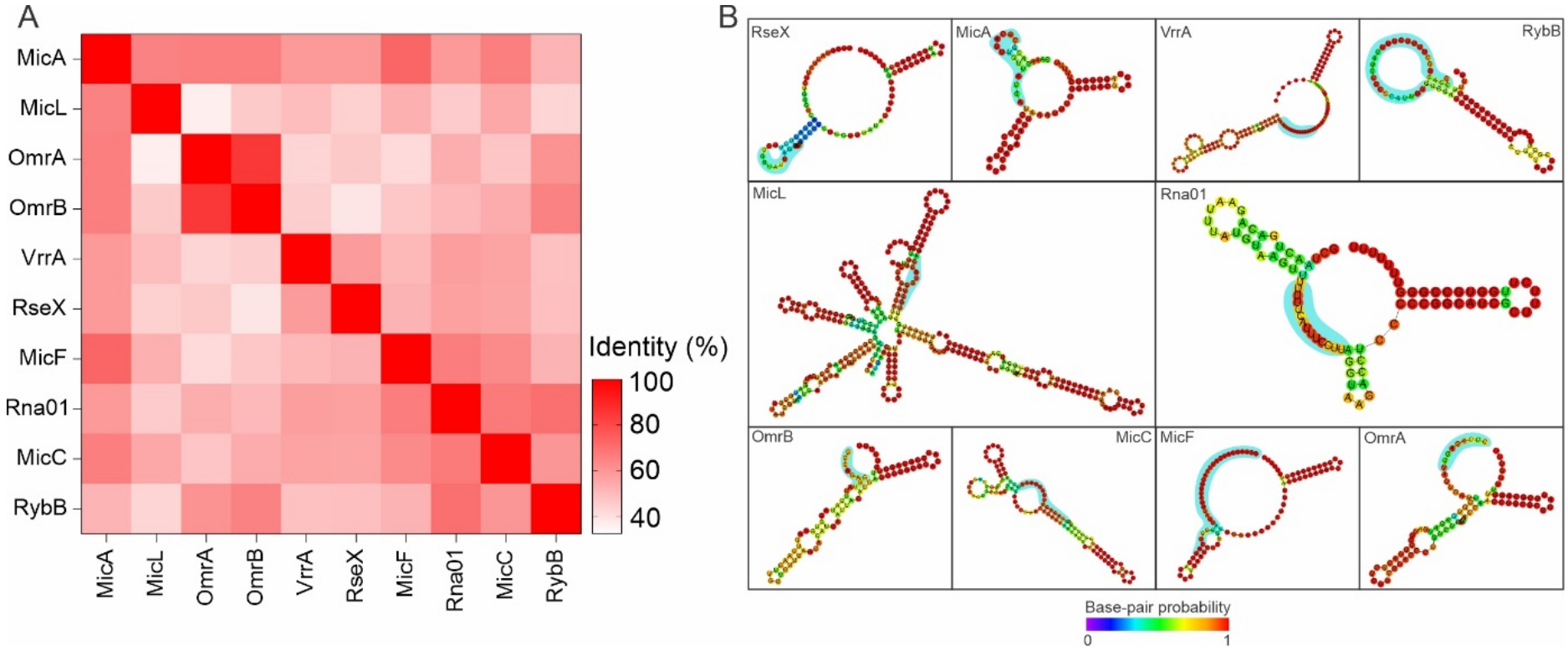

FIGURE 8 | Comparative analysis among Rna01 and other extracytoplasmic stress associated sRNAs. (A) Heatmap based on matrix identity of the sRNAs. (B) Secondary structure of the sRNAs. The blue shades represent the seed region of interaction with outer membrane proteins mRNA targets.

Discussion

In this work we described, for the first time, the existence of sRNAs interacting with the RNA chaperone Hfq in *A. pleuropneumoniae*, the causative agent of porcine pleuropneumonia. Of the 14 sRNAs candidates identified here by co-IP/RNA-seq, eight have never been described before, according to our knowledge. Three were amongst the 17 of 23 computationally predicted sRNAs that were confirmed experimentally by our group in a previous study (Rossi et al., 2016). This work then expands the set of sRNAs identified in *A. pleuropneumoniae* from 23 to 37. Although only approximately 50% of bacteria harbor the *hfq* gene (Orans et al., 2020), in those that do it can be an important RNA chaperone as demonstrated by *hfq* mutants of *A. pleuropneumoniae* being attenuated for virulence (Crispim et al., 2020; Pereira et al., 2015; Subashchandrabose et al., 2013). In some other bacteria, less widespread RNA chaperones, such as CsrA and ProQ, may play the same role of Hfq (Müller et al., 2019; Smirnov et al., 2016). These three chaperones are not mutually exclusive, for example, *E. coli*, *Salmonella enterica, Bacillus subtilis,* and *Clostridium botulinum* have been described to encode combinations of two RNA chaperones (Quendera et al., 2020). Although the *proQ* and *csrA* genes are present in *A. pleuropneumoniae* genomes, there are no reports of the respective proteins acting as RNA chaperones for this species.

Additionally, not all sRNAs bind RNA chaperones to exert their activities, nor do all the Hfq-associated sRNAs depend on the chaperone to be protected from RNAse degradation in the cell. In fact, growing evidence indicates that Hfq can not only bind sRNAs to (i) facilitate their interaction with mRNA cognates; (ii) protect them from; or (iii) lead them to degradation (Vogel & Luisi, 2011), but can also play additional regulatory roles. These include binding mRNAs alone to control their translation or modification, binding rRNAs and tRNAs to help with their maturation/processing, and affecting DNA conformation and compaction (dos Santos et al., 2019; Jiang et al., 2015). This likely explains why our co-IP was not only enriched with *trans-acting* RNAs, but also with two *cis*-acting RNAs, the FMN riboswitch and the S15 leader sequence.

The sRNA we chose to focus on, Rna01, is involved with the stress response and virulence in *A. pleuropneumoniae*. Some of the targets predicted are related with the phenotypes observed for *A. pleuropneumoniae hfq* and *rna01* mutants. These include those obtained in this study, as well as previous data for *hfq* mutants showing reduced fitness and virulence in pigs and *G. mellonella* and impaired capacity to

respond to different types of stress (Crispim et al., 2020; Pereira et al., 2015; Subashchandrabose et al., 2013). Because the lack of Hfq can lead to different phenotypes in different serovars of *A. pleuropneumoniae* (Crispim et al., 2020), and targets are included in a complex and integrated network, it is complex to define which Hfq-sRNA-mRNA interactions will lead to a certain phenotype. Additionally, approximately 10% of the protein-coding genes from *A. pleuropneumoniae* serovar 8 strains still have unknown functions (Prado et al., 2020).

Although *A. pleuropneumoniae* virulence is highly attributed to the serovar-associated pattern of production of RTX toxins (Frey, 2011), different strains of the same serovar can exhibit varying degrees of virulence, since other features may contribute to the outcome of infection (Pereira et al., 2015; 2018). Thus, the activities conferred by Hfq, Hfq-dependent and -independent sRNAs, add extra layers of complexity to this bacterium's virulence.

In silico analysis of Rna01 also showed putative σ^{70} and σ^{E} promoters and typical Hfq binding sites, with minor differences among homologues. The search for homologues for this sRNA showed a wide distribution among Pasteurellaceae species, being mostly present in related veterinary pathogens, but also the human pathogen *H. ducreyi*, which may reflect the importance of this sRNA among Pasteurellaceae members in different environments.

Although it was not possible to identify the abundance of Rna01 by Northern blotting analysis in the *hfq* mutant strain, Rna01 was up-regulated in stress but down-regulated in non-stressful conditions as observed in the qPCR analysis. This suggests that Rna01 is dependent on Hfq in some, but not all, conditions for action and stability.

Some of the phenotypes presented by the *rna01* mutant matched those of the *hfq* mutant, and were not additive in the double mutant strain. This means that, in the absence of Hfq, Rna01 may be automatically also absent, probably due to RNAse degradation. Biofilm formation contributes to pathogenicity (Hathroubi et al., 2018), and the hemolysis observed is related to the expression of the RTX proteins. As the mutant strains showed reduced biofilm formation and hemolytic activity, we evaluated the virulence of these strains in *G. mellonella*, that has been shown to be an excellent predictor of virulence found in pigs. We found significant differences between the Ap8Δ*hfq* and Δ*rna*01 strains observed here related to the stimulation of *G. mellonella*'s immune response. Melanization is an essential and readily observed characteristic of the larva's humoral response against microorganisms, resulting in synthesis and

deposition of melanin around the invading pathogen (Pereira et al., 2020). Here we observed that, even though all mutations reduced larval killing, melanization was still observed for the *rna01*, but not the *hfq* or double mutant. Interestingly, for the osmotic stress, the ∆*rna*01 showed to be less sensitive than the WT strain, while the opposite was observed for the Ap8∆*hfq* and double mutant. This indicates that some phenotypes of *A. pleuropneumoniae* are independent of Rna01 (as seen for osmotic stress) but influenced by the global regulator Hfq.

Although the interactions of Rna01 with its predicted targets remain to be confirmed experimentally, some of the targets predicted may be responsible for the phenotypes observed in this work and are corroborated by previous studies. A previous study (Xie et al., 2016), for example, showed that a *lonA* mutant (annotated as *lon*) in MIDG2331, displayed reduced biofilm formation, stress tolerance and pathogenicity. However, the ∆*rna*01 strain showed higher tolerance to osmotic stress in relation to the other strains, although the same was not observed in the other phenotypic analyses. *sufE*, another Rna01 predicted target, showed reduced tolerance to oxidative and acid stress in *E. coli* (Lee et al., 2010). Likewise, Rna01's targets *malK* and *malE* are known to regulate *malT* in *E. coli* (Böhm et al., 2002). A study with *A. pleuropneumoniae* showed that knocking out the *malT* gene led to reduction in growth rate (Lone et al., 2009). These results suggest that the interaction of Rna01 with these predicted targets are worthy of investigation, with a potential to affect the fitness of *A. pleuropneumoniae*.

Studies with an *aroQ* mutant showed an attenuated phenotype for *A. pleuropneumoniae* (Ingham et al., 2002). Analysis of a *znuA* mutant showed attenuation in experiments with animals for *Brucella abortus* and the members of the Pasteurellaceae family *Haemophilus ducreyi*, *Pasteurella multocida* and *A. pleuropneumoniae* (Yang et al., 2006; Yuan et al., 2014).

Despite the absence of studies involving *tolR* and *metQ* targets in *A. pleuropneumoniae,* attenuated phenotypes for the Rna01 putative target mRNAs were reported for *Edwardsiella ictalurid* (Abdelhamed et al., 2016) and *Streptococcus pneumoniae* (Basavanna et al., 2013), respectively. Studies with *Acinetobacter baumanii* reported that the absence of the adhesin Ata strongly affects the virulence and adhesion of this specie (Weidensdorfer et al., 2019). Also, studies with *Salmonella enterica* serovar Typhimurium showed attenuation phenotypes in mutants for the *bioB* and *asd* genes (Denkel et al., 2013; Piao et al., 2010).

Investigation of the putative seed regions of the Rna01 showed a conserved fragment of the seed region 1. Interestingly, this fragment is in a single-strand region of the secondary structure of Rna01 predicted to interact with the outer membrane associated genes. Previous studies reported that seed regions need to be unstructured and base pairing regions are commonly single strands, as previously reviewed (Updegrove et al., 2015).

The stress sigma fator σ^E promoter and the targets predicted indicate that Rna01 might be associated with post-transcriptional regulation of diverse genes in a stress response condition, mostly extracytoplasmic stress. These findings are consistent with some previously reports, as showed to *S. enterica* serovar Typhimurium, in which σ^E sRNAs, such as MicA and RybB, respond to membrane stress (Papenfort et al., 2006). The well-studied MicA and RybB sRNAs are responsible of alleviating stress and mediating interconnection with envelope stress network. Also, these sRNAs target all *omp* mRNAs and some non-*omp* targets (Klein & Raina, 2017).

Like other well studied sRNAs associated with stress response, such as MicA, RybB and VrrA, Rna01 may interact, by base-pairing next to the ribosomal binding site (RBS), with diverse genes that code for outer membrane proteins, which is commonly associated with down-regulation of these targets in an extracytoplasmic stress condition (Pfeiffer et al., 2009).

Analysis focused on investigating Rna01 as an extracytoplasmic stress associated sRNA showed strong evidence of this function, as seen in the qPCR analysis, as this sRNA is up-regulated during stationary growth (a stressful condition). Also, the same experiment showed that Rna01 is expressed in the absence of Hfq during the stationary phase, but seems to be unstable in *hfq* mutants in a non-stressful condition. By investigating *ompP2B* expression, a putative Rna01 target, we found that, in the absence of Rna01 in the stationary phase, this target had increased expression, which corroborates the hypothesis that Rna01 acts by inhibiting the translation of OMPs by blocking RBS sequences. The effect of Rna01 on OMP expression was also observed by SDS_PAGE and Coomassie Blue staining of OMP preparations. Curiously, for the *ata_2* and *tolR* targets, the strains lacking Rna01 or Hfq showed similar expression, which may result from Hfq-dependence. This may be explained considering that the seed region of Rna01 that interact with OMPs targets are in a single strand (considering the native secondary structure predicted here).

However, the seed region of Rna01 that interact with other targets is located in a double strand portion of Rna01, where the free energy is higher and may depend on Hfq, which structures the sRNA sequence to form the complex sRNA-Hfq-mRNA (Updegrove et al., 2016).

As Rna01 showed clear evidence of being associated with OMP regulation, we also investigated its effect on BEVs (as also called outer membrane vesicles – OMVs). There was less production of the BEVs by mutants lacking Rna01, and these were smaller and of higher toxicity for *G. mellonella*. A similar study with *Vibrio cholerae* revealed that VrrA, a stress response associated sRNA, which also regulates OMPs expression, affects the EV production (Song et al., 2008).

Based on the results showed in this study regarding Rna01 and targets expression, the phenotypes affected and dependence of Hfq, we propose a mechanism of activity for this sRNA which is summarized in Figure 9.

Considering that other sRNAs (MicA, MicF, MicC, MicL, OmrA, OmrB, VrrA, RseX and RybB), associated with the stress response in other species, were not found in the *A. pleuropneumoniae* genome, and that comparative analysis with these sRNAs showed Rna01 as a different sRNA, altogether these results suggest that Rna01 as the sRNA associated with the extracytoplasmic stress in *A. pleuropneumoniae*.

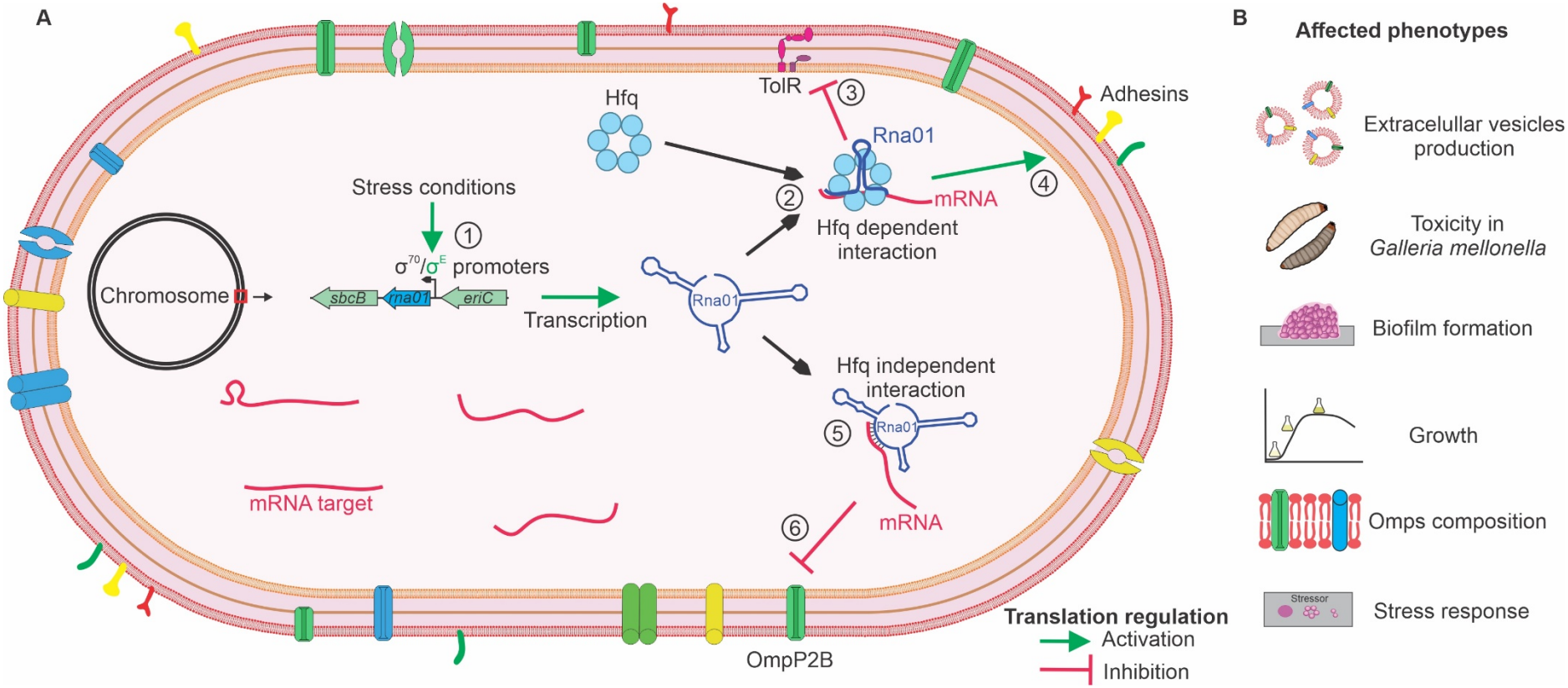

FIGURE 9 | Mechanism of activity proposed for the novel sRNA Rna01. (A) The figure summarizes the expression of *rna01* in normal and stress conditions (by σ^{70} and σ^{E}, respectively) (1), followed by regulation of the targets in a Hfq dependent manner (2), inhibiting (3) or inducing (4) translation of the targets. Also, Rna01 regulates translation of the OMP targets in a Hfq-independent manner (5) inhibiting the translation (6). (B) The activity of Rna01, mediated or not by chaperone Hfq, affects diverse phenotypes of *A. pleuropneumoniae*.

In conclusion, this work is a step forward in the understanding of the influence of sRNAs in the physiology and virulence of *A. pleuropneumoniae*, which our studies indicate are multilayered and complex, and are greatly influenced by the molecular chaperone Hfq and associated RNAs. Also, this study reports for the first time an *A. pleuropneumoniae* sRNA (Rna01) that is associated with extracytoplasmic stress, virulence and EV production. Further analyses of sRNAs, such as those we have identified as being Hfq-dependent in our co-IP experiments, are worthy of study to elucidate the molecular basis of gene regulation and virulence of *A. pleuropneumoniae*.

Data availability

RNAseq data were deposited in NCBI's Short Read Archive (SRA, experiment SRX810211). The remaining data were previously publicly available, as cited throughout the text.

Funding

The authors thank CNPq (201840/2011-1, 407849/2012-2, 142495/2014-0 and 141328/2018); FAPEMIG (APQ-01586-18; APQ-00772-19); CAPES/PROEX (23038.019105/2016-86 and 23038.002486/2018-26), FINEP (Núcleo de Microscopia e Microanálise – UFV), BBSRC (BB/K021109/1, BB/G019177/1, BB/M023052/1, BB/M020576/1, BB/S020543/1, BB/P001262/1, and BB/G018553), and CONFAP - the UK Academies (CBB- APQ-00689-16).

Author contributions

All authors helped conceiving the study. GCS, CCR, JNR, NMS, JTB, YL, AAW, KAG, PPF, EAAB, MRT and DMSB produced the data. GCS, CCR, JNR, JTB and DLC analyzed the data. JTB, AJC, DMSB and PRL coordinated the study. GCS and CCR wrote the paper.

References

Abdelhamed, H., Lu, J., Lawrence, M. L., & Karsi, A. (2016). Involvement of *tolQ* and *tolR* genes in *Edwardsiella ictaluri* virulence. *Microbial Pathogenesis*, *100*, 90–94. https://doi.org/10.1016/j.micpath.2016.09.011

Antenucci, F., Fougeroux, C., Bossé, J. T., Magnowska, Z., Roesch, C., Langford, P., Holst, P. J., & Bojesen, A. M. (2017). Identification and characterization of serovar-independent immunogens in *Actinobacillus pleuropneumoniae*. *Veterinary Research*, *48*(1), 74. https://doi.org/10.1186/s13567-017-0479-5

Basavanna, S., Chimalapati, S., Maqbool, A., Rubbo, B., Yuste, J., Wilson, R. J., Hosie, A., Ogunniyi, A. D., Paton, J. C., Thomas, G., & Brown, J. S. (2013). The effects of methionine acquisition and synthesis on *Streptococcus pneumoniae* growth and virulence. *PloS One*, *8*(1), e49638. https://doi.org/10.1371/journal.pone.0049638

Benjamini, Y., & Hochberg, Y. (1995). Controlling the false discovery rate: A practical and powerful approach to multiple testing. *Journal of the Royal Statistical Society: Series B (Methodological)*, *57*(1), 289–300. https://doi.org/https://doi.org/10.1111/j.2517-6161.1995.tb02031.x

Böhm, A., Diez, J., Diederichs, K., Welte, W., & Boos, W. (2002). Structural model of MalK, the ABC subunit of the maltose transporter of *Escherichia coli*: implications for *mal* gene regulation, inducer exclusion, and subunit assembly. *The Journal of Biological Chemistry*, *277*(5), 3708–3717. https://doi.org/10.1074/jbc.M107905200

Bossé, J. T., Bazzolli, D. M. S., Li, Y., Wren, B. W., Tucker, A. W., Maskell, D. J., Rycroft, A. N., & Langford, P. R. (2014). The generation of successive unmarked mutations and chromosomal insertion of heterologous genes in *Actinobacillus pleuropneumoniae* using natural transformation. *PLoS ONE*, *9*(11), 7–12. https://doi.org/10.1371/journal.pone.0111252

Bossé, J. T., Chaudhuri, R. R., Li, Y., Leanse, L. G., Fernandez Crespo, R., Coupland, P., Holden, M. T. G., Bazzolli, D. M., Maskell, D. J., Tucker, A. W., Wren, B. W., Rycroft, A. N., & Langford, P. R. (2016). Complete genome sequence of midg2331, a genetically tractable serovar 8 clinical isolate of *Actinobacillus pleuropneumoniae*. *Genome Announcements*, *4*(1). https://doi.org/10.1128/genomeA.01667-15

Bossé, J. T., Li, Y., Walker, S., Atherton, T., Fernandez Crespo, R., Williamson, S. M., Rogers, J., Chaudhuri, R. R., Weinert, L. A., Oshota, O., Holden, M. T. G., Maskell, D. J., Tucker, A. W., Wren, B. W., Rycroft, A. N., & Langford, P. R. (2015). Identification of *dfrA14* in two distinct plasmids conferring trimethoprim resistance in *Actinobacillus pleuropneumoniae*. *Journal of Antimicrobial Chemotherapy*, *70*(8), 2217–2222. https://doi.org/10.1093/jac/dkv121

Buels, R., Yao, E., Diesh, C. M., Hayes, R. D., Munoz-Torres, M., Helt, G., Goodstein, D. M., Elsik, C. G., Lewis, S. E., Stein, L., & Holmes, I. H. (2016). JBrowse: a dynamic web platform for genome visualization and analysis. *Genome Biology*, *17*, 66. https://doi.org/10.1186/s13059-016-0924-1

Carrier, M.-C., Lalaouna, D., & Massé, E. (2018). Broadening the Definition of Bacterial Small RNAs: Characteristics and Mechanisms of Action. *Annual Review of*

Microbiology, *72*, 141–161. https://doi.org/10.1146/annurev-micro-090817-062607

Consortium, T. U. (2019). UniProt: a worldwide hub of protein knowledge. *Nucleic Acids Research*, *47*(D1), D506–D515. https://doi.org/10.1093/nar/gky1049

Crispim, J. S., da Silva, T. F., Sanches, N. M., da Silva, G. C., Pereira, M. F., Rossi, C. C., Li, Y., Terra, V. S., Vohra, P., Wren, B. W., Langford, P. R., Bossé, J. T., & Bazzolli, D. M. S. (2020). Serovar-dependent differences in Hfq-regulated phenotypes in *Actinobacillus pleuropneumoniae*. *Pathogens and Disease*, *78*(9). https://doi.org/10.1093/femspd/ftaa066

Crooks, G. E., Hon, G., Chandonia, J.-M., & Brenner, S. E. (2004). WebLogo: A sequence logo generator. *Genome Research* , *14*(6), 1188–1190. https://doi.org/10.1101/gr.849004

Denkel, L. A., Rhen, M., & Bange, F.-C. (2013). Biotin sulfoxide reductase contributes to oxidative stress tolerance and virulence in *Salmonella enterica* serovar Typhimurium. *Microbiology (Reading, England)*, *159*(Pt 7), 1447–1458. https://doi.org/10.1099/mic.0.067256-0

dos Santos, R. F., Arraiano, C. M., & Andrade, J. M. (2019). New molecular interactions broaden the functions of the RNA chaperone Hfq. *Current Genetics*, *65*(6), 1313–1319. https://doi.org/10.1007/s00294-019-00990-y

Foote, S. J., Bossé, J. T., Bouevitch, A. B., Langford, P. R., Young, N. M., & John H E Nash. (2008). The complete genome sequence of *Actinobacillus pleuropneumoniae* L20 (Serotype 5b). *Journal of Bacteriology*, *190*(4), 1495–1496. https://doi.org/10.1128/JB.01845-07

Frey, J. (2011). The role of RTX toxins in host specificity of animal pathogenic Pasteurellaceae. *Veterinary Microbiology*, *153*(1), 51–58. https://doi.org/https://doi.org/10.1016/j.vetmic.2011.05.018

Fu, Y., Yu, Z., Zhu, L., Li, Z., Yin, W., Shang, X., Chou, S.-H., Tan, Q., & He, J. (2021). The multiple regulatory relationship between RNA-chaperone Hfq and the second messenger c-di-GMP. *Frontiers in Microbiology*, *12*, 1923. https://doi.org/10.3389/fmicb.2021.689619

Ghosh, S., & Chan, C.-K. K. (2016). Analysis of RNA-Seq data using TopHat and Cufflinks. *Methods in Molecular Biology (Clifton, N.J.)*, *1374*, 339–361. https://doi.org/10.1007/978-1-4939-3167-5_18

Green, M. R., & Sambrook, J. (2012). Molecular cloning: a laboratory manual. *Cold Spring Harbor Laboratory Press*, *Fourth Edi*, 2028pp.

Gulliver, E. L., Wright, A., Lucas, D. D., Mégroz, M., Kleifeld, O., Schittenhelm, R. B., Powell, D. R., Seemann, T., Bulitta, J. B., Harper, M., & Boyce, J. D. (2018). Determination of the small RNA GcvB regulon in the Gram-negative bacterial pathogen *Pasteurella multocida* and identification of the GcvB seed binding region. *RNA (New York, N.Y.)*, *24*(5), 704–720. https://doi.org/10.1261/rna.063248.117

Hathroubi, S., Loera-Muro, A., Guerrero-Barrera, A. L., Tremblay, Y. D. N., & Jacques, M. (2018). *Actinobacillus pleuropneumoniae* biofilms: Role in pathogenicity and

potential impact for vaccination development. *Animal Health Research Reviews*, *19*(1), 17–30. https://doi.org/10.1017/S146625231700010X

Holmqvist, E., Wright, P. R., Li, L., Bischler, T., Barquist, L., Reinhardt, R., Backofen, R., & Vogel, J. (2016). Global RNA recognition patterns of post-transcriptional regulators Hfq and CsrA revealed by UV crosslinking in vivo. *The EMBO Journal*, *35*(9), 991–1011. https://doi.org/https://doi.org/10.15252/embj.201593360

Ingham, A., Zhang, Y., & Prideaux, C. (2002). Attenuation of *Actinobacillus pleuropneumoniae* by inactivation of *aroQ*. *Veterinary Microbiology*, *84*(3), 263–273. https://doi.org/10.1016/s0378-1135(01)00465-5

Jiang, K., Zhang, C., Guttula, D., Liu, F., van Kan, J. A., Lavelle, C., Kubiak, K., Malabirade, A., Lapp, A., Arluison, V., & van der Maarel, J. R. C. (2015). Effects of Hfq on the conformation and compaction of DNA. *Nucleic Acids Research*, *43*(8), 4332–4341. https://doi.org/10.1093/nar/gkv268

Jorjão, A. L., de Oliveira, F. E., Leão, M. V. P., Jorge, A. O. C., & de Oliveira, L. D. (2018). Effect of *Lactobacillus rhamnosus* on the response of *Galleria mellonella* against *Staphylococcus aureus* and *Escherichia coli* infections. *Archives of Microbiology*, *200*(3), 383–389. https://doi.org/10.1007/s00203-017-1441-7

Kalvari, I., Nawrocki, E. P., Ontiveros-Palacios, N., Argasinska, J., Lamkiewicz, K., Marz, M., Griffiths-Jones, S., Toffano-Nioche, C., Gautheret, D., Weinberg, Z., Rivas, E., Eddy, S. R., Finn, R. D., Bateman, A., & Petrov, A. I. (2021). Rfam 14: expanded coverage of metagenomic, viral and microRNA families. *Nucleic Acids Research*, *49*(D1), D192–D200. https://doi.org/10.1093/nar/gkaa1047

Kavita, K., de Mets, F., & Gottesman, S. (2018). New aspects of RNA-based regulation by Hfq and its partner sRNAs. *Current Opinion in Microbiology*, *42*, 53–61. https://doi.org/10.1016/j.mib.2017.10.014

Kery, M. B., Feldman, M., Livny, J., & Tjaden, B. (2014). TargetRNA2: identifying targets of small regulatory RNAs in bacteria. *Nucleic Acids Research*, *42*(W1), W124–W129. https://doi.org/10.1093/nar/gku317

Klein, G., & Raina, S. (2017). Small regulatory bacterial RNAs regulating the envelope stress response. *Biochemical Society Transactions*, *45*(2), 417–425. https://doi.org/10.1042/BST20160367

Kleinbaum, D. G., and Klein, M. (2012). Kaplan-Meier survival curves and the Log-Rank test in survival analysis*:* A Self-Learning Text (Third Edit). Springer Science.

Lalaouna, D., Eyraud, A., Devinck, A., Prévost, K., & Massé, E. (2019). GcvB small RNA uses two distinct seed regions to regulate an extensive targetome. *Molecular Microbiology*, *111*(2), 473–486. https://doi.org/10.1111/mmi.14168

Lee, J., Hiibel, S. R., Reardon, K. F., & Wood, T. K. (2010). Identification of stress-related proteins in *Escherichia coli* using the pollutant cis-dichloroethylene. *Journal of Applied Microbiology*, *108*(6), 2088–2102. https://doi.org/10.1111/j.1365-2672.2009.04611.x

Li, H., & Durbin, R. (2010). Fast and accurate long-read alignment with Burrows-Wheeler transform. *Bioinformatics (Oxford, England)*, *26*(5), 589–595. https://doi.org/10.1093/bioinformatics/btp698

Lone, A. G., Deslandes, V., Nash, J. H. E., Jacques, M., & MacInnes, J. I. (2009). *malT* knockout mutation invokes a stringent type gene-expression profile in *Actinobacillus pleuropneumoniae* in bronchoalveolar fluid. *BMC Microbiology*, *9*(1), 195. https://doi.org/10.1186/1471-2180-9-195

Mead, G. P., Ratcliffe, N. A., & Renwrantz, L. R. (1986). The separation of insect haemocyte types on Percoll gradients; methodology and problems. *Journal of Insect Physiology*, *32*, 167–177.

Milne, I., Bayer, M., Cardle, L., Shaw, P., Stephen, G., Wright, F., & Marshall, D. (2010). Tablet--next generation sequence assembly visualization. *Bioinformatics (Oxford, England)*, *26*(3), 401–402. https://doi.org/10.1093/bioinformatics/btp666

Müller, P., Gimpel, M., Wildenhain, T., & Brantl, S. (2019). A new role for CsrA: promotion of complex formation between an sRNA and its mRNA target in *Bacillus subtilis*. *RNA Biology*, *16*(7), 972–987. https://doi.org/10.1080/15476286.2019.1605811

Nitzan, M., Rehani, R., & Margalit, H. (2017). Integration of bacterial small RNAs in regulatory networks. *Annual Review of Biophysics*, *46*, 131–148. https://doi.org/10.1146/annurev-biophys-070816-034058

Orans, J., Kovach, A. R., Hoff, K. E., Horstmann, N. M., & Brennan, R. G. (2020). Crystal structure of an *Escherichia coli* Hfq Core (residues 2–69)–DNA complex reveals multifunctional nucleic acid binding sites. *Nucleic Acids Research*, *48*(7), 3987–3997. https://doi.org/10.1093/nar/gkaa149

Otaka, H., Ishikawa, H., Morita, T., & Aiba, H. (2011). PolyU tail of rho-independent terminator of bacterial small RNAs is essential for Hfq action. *Proceedings of the National Academy of Sciences*, *108*(32), 13059 LP – 13064. https://doi.org/10.1073/pnas.1107050108

Papenfort, K., Pfeiffer, V., Mika, F., Lucchini, S., Hinton, J. C. D., & Vogel, J. (2006). σE-dependent small RNAs of Salmonella respond to membrane stress by accelerating global omp mRNA decay. *Molecular Microbiology*, *62*(6), 1674–1688. https://doi.org/https://doi.org/10.1111/j.1365-2958.2006.05524.x

Pattison, I. H., Howell, D. G., & Elliot, J. (1957). A haemophilus-like organism isolated from pig lung and the associated pneumonic lesions. *Journal of Comparative Pathology and Therapeutics*, *67*, 320-IN37. https://doi.org/https://doi.org/10.1016/S0368-1742(57)80031-9

Pereira, M. F., Rossi, C. C., da Silva, G. C., Rosa, J. N., & Bazzolli, D. M. S. (2020). *Galleria mellonella* as an infection model: an in-depth look at why it works and practical considerations for successful application. *Pathogens and Disease*, *78*(8), ftaa056. https://doi.org/10.1093/femspd/ftaa056

Pereira, M. F., Rossi, C. C., de Queiroz, M. V., Martins, G. F., Isaac, C., Bossé, J. T., Li, Y., Wren, B. W., Terra, V. S., Cuccui, J., Langford, P. R., & Bazzolli, D. M. S. (2015). *Galleria mellonella* is an effective model to study *Actinobacillus pleuropneumoniae* infection. *Microbiology*, *161*(2), 387–400. https://doi.org/https://doi.org/10.1099/mic.0.083923-0

Pereira, M. F., Rossi, C. C., Seide, L. E., Martins Filho, S., Dolinski, C. de M., & Bazzolli, D. M. S. (2018). Antimicrobial resistance, biofilm formation and virulence

reveal *Actinobacillus pleuropneumoniae* strains' pathogenicity complexity. *Research in Veterinary Science*, *118*, 498–501. https://doi.org/10.1016/j.rvsc.2018.05.003

Pfeiffer, V., Papenfort, K., Lucchini, S., Hinton, J. C. D., & Vogel, J. (2009). Coding sequence targeting by MicC RNA reveals bacterial mRNA silencing downstream of translational initiation. *Nature Structural & Molecular Biology*, *16*(8), 840–846. https://doi.org/10.1038/nsmb.1631

Piao, H. H., Tam, V. T. M., Na, H. S., Kim, H. J., Ryu, P. Y., Kim, S. Y., Rhee, J. H., Choy, H. E., Kim, S. W., & Hong, Y. (2010). Immunological responses induced by asd and wzy/asd mutant strains of *Salmonella enterica* serovar Typhimurium in BALB/c mice. *Journal of Microbiology (Seoul, Korea)*, *48*(4), 486–495. https://doi.org/10.1007/s12275-010-0023-z

Prado, I. G. de O., da Silva, G. C., Crispim, J. S., Vidigal, P. M. P., Nascimento, M., Santana, M. F., & Bazzolli, D. M. S. (2020). Comparative genomics of *Actinobacillus pleuropneumoniae* serotype 8 reveals the importance of prophages in the genetic variability of the species. *International Journal of Genomics*, *2020*, 9354204. https://doi.org/10.1155/2020/9354204

Quendera, A. P., Seixas, A. F., dos Santos, R. F., Santos, I., Silva, J. P. N., Arraiano, C. M., & Andrade, J. M. (2020). RNA-binding proteins driving the regulatory activity of small Non-coding RNAs in bacteria. *Frontiers in Molecular Biosciences*, *7*, 78. https://doi.org/10.3389/fmolb.2020.00078

Redfield, R. J., Findlay, W. A., Bossé, J., Kroll, J. S., Cameron, A. D. S., & Nash, J. H. E. (2006). Evolution of competence and DNA uptake specificity in the Pasteurellaceae. *BMC Evolutionary Biology*, *6*(1), 82. https://doi.org/10.1186/1471-2148-6-82

Robinson, J. T., Thorvaldsdóttir, H., Turner, D., & Mesirov, J. P. (2020). igv.js: an embeddable JavaScript implementation of the Integrative Genomics Viewer (IGV). *BioRxiv*, 2020.05.03.075499. https://doi.org/10.1101/2020.05.03.075499

Rossi, C.C., Bossé, J.T., Li, Y., Witney, A.A., Gould, K.A., Langford, P.R., Bazzolli, D. M. S. (2016). A computational strategy for the search of regulatory small RNAs in *Actinobacillus pleuropneumoniae*. *RNA*, *Sep*; *22(9)*, 1373–1385.

Sambrook, J., & Russell, D. W. (2006). The inoue method for preparation and transformation of competent E. coli: "ultra-competent" cells. *CSH Protocols*, *2006*(1). https://doi.org/10.1101/pdb.prot3944

Santiago-Frangos, A., & Woodson, S. A. (2018). Hfq chaperone brings speed dating to bacterial sRNA. *Wiley Interdisciplinary Reviews. RNA*, *9*(4), e1475. https://doi.org/10.1002/wrna.1475

Sassu, E. L., Bossé, J. T., Tobias, T. J., Gottschalk, M., Langford, P. R., & Hennig-Pauka, I. (2018). Update on *Actinobacillus pleuropneumoniae*—knowledge, gaps and challenges. *Transboundary and Emerging Diseases*, *65*(S1), 72–90. https://doi.org/https://doi.org/10.1111/tbed.12739

Sauer, E., & Weichenrieder, O. (2011). Structural basis for RNA 3′-end recognition by Hfq. *Proceedings of the National Academy of Sciences*, *108*(32), 13065 LP – 13070. https://doi.org/10.1073/pnas.1103420108

Shin, S. Y., Kang, J. H., & Hahm, K. S. (1999). Structure-antibacterial, antitumor and hemolytic activity relationships of cecropin A-magainin 2 and cecropin A-melittin hybrid peptides. *The Journal of Peptide Research : Official Journal of the American Peptide Society*, *53*(1), 82–90. https://doi.org/10.1111/j.1399-3011.1999.tb01620.x

Sievers, F., & Higgins, D. G. (2014). Clustal Omega, accurate alignment of very large numbers of sequences bt - multiple sequence alignment methods (D. J. Russell (ed.); pp. 105–116). *Humana Press*. https://doi.org/10.1007/978-1-62703-646-7_6

Sittka, A., Lucchini, S., Papenfort, K., Sharma, C. M., Rolle, K., Binnewies, T. T., Hinton, J. C. D., & Vogel, J. (2008). Deep sequencing analysis of small noncoding RNA and mRNA targets of the global post-transcriptional regulator, Hfq. *PLOS Genetics*, *4*(8), e1000163. https://doi.org/10.1371/journal.pgen.1000163

Smirnov, A., Förstner, K. U., Holmqvist, E., Otto, A., Günster, R., Becher, D., Reinhardt, R., & Vogel, J. (2016). Grad-seq guides the discovery of ProQ as a major small RNA-binding protein. *Proceedings of the National Academy of Sciences of the United States of America*, *113*(41), 11591–11596. https://doi.org/10.1073/pnas.1609981113

Song, T., Mika, F., Lindmark, B., Liu, Z., Schild, S., Bishop, A., Zhu, J., Camilli, A., Johansson, J., Vogel, J., & Wai, S. N. (2008). A new *Vibrio cholerae* sRNA modulates colonization and affects release of outer membrane vesicles. *Molecular Microbiology*, *70*(1), 100–111. https://doi.org/https://doi.org/10.1111/j.1365-2958.2008.06392.x

Stepanović, S., Vuković, D., Hola, V., Bonaventura, G. Di, Djukić, S., Cirković, I., & Ruzicka, F. (2007). Quantification of biofilm in microtiter plates: overview of testing conditions and practical recommendations for assessment of biofilm production by staphylococci. *APMIS*, *115*(8), 891–899. https://doi.org/https://doi.org/10.1111/j.1600-0463.2007.apm_630.x

Stringer, O. W., Bossé, J. T., Lacouture, S., Gottschalk, M., Fodor, L., Angen, Ø., Velazquez, E., Penny, P., Lei, L., Langford, P. R., & Li, Y. (2021). Proposal of *Actinobacillus pleuropneumoniae* serovar 19, and reformulation of previous multiplex PCRs for capsule-specific typing of all known serovars. *Veterinary Microbiology*, *255*, 109021. https://doi.org/https://doi.org/10.1016/j.vetmic.2021.109021

Subashchandrabose, S., Leveque, R. M., Kirkwood, R. N., Kiupel, M., & Mulks, M. H. (2013). The RNA chaperone Hfq promotes fitness of *Actinobacillus pleuropneumoniae* during porcine pleuropneumonia. Infection and Immunity, 81(8), 2952–2961. https://doi.org/10.1128/IAI.00392-13

Szklarczyk, D., Gable, A. L., Lyon, D., Junge, A., Wyder, S., Huerta-Cepas, J., Simonovic, M., Doncheva, N. T., Morris, J. H., Bork, P., Jensen, L. J., & Mering, C. von. (2019). STRING v11: protein–protein association networks with increased coverage, supporting functional discovery in genome-wide experimental datasets. *Nucleic Acids Research*, *47*(D1), D607–D613. https://doi.org/10.1093/nar/gky1131

Thein, M., Sauer, G., Paramasivam, N., Grin, I., & Linke, D. (2010). Efficient subfractionation of Gram-negative bacteria for proteomics studies. *Journal of*

Proteome Research, *9*(12), 6135–6147. https://doi.org/10.1021/pr1002438

Uchino, Y., & Ken-Ichiro, S. (2011). A simple preparation of liquid media for the cultivation of strict anaerobes. *Journal of Petroleum & Environmental Biotechnology*, *S3*(001).

Updegrove, T. B., Shabalina, S. A., & Storz, G. (2015). How do base-pairing small RNAs evolve? *FEMS Microbiology Reviews*, *39*(3), 379–391. https://doi.org/10.1093/femsre/fuv014

Updegrove, T. B., Zhang, A., & Storz, G. (2016). ScienceDirect Hfq : the flexible RNA matchmaker. *Current Opinion in Microbiology*, *30*, 133–138. https://doi.org/10.1016/j.mib.2016.02.003

Vogel, J., & Luisi, B. F. (2011). Hfq and its constellation of RNA. *Nature Reviews Microbiology*, *9*(8), 578–589. https://doi.org/10.1038/nrmicro2615

Waterhouse, A. M., Procter, J. B., Martin, D. M. A., Clamp, M., & Barton, G. J. (2009). Jalview Version 2—a multiple sequence alignment editor and analysis workbench. *Bioinformatics*, *25*(9), 1189–1191. https://doi.org/10.1093/bioinformatics/btp033

Weidensdorfer, M., Ishikawa, M., Hori, K., Linke, D., Djahanschiri, B., Iruegas, R., Ebersberger, I., Riedel-Christ, S., Enders, G., Leukert, L., Kraiczy, P., Rothweiler, F., Cinatl, J., Berger, J., Hipp, K., Kempf, V. A. J., & Göttig, S. (2019). The Acinetobacter trimeric autotransporter adhesin Ata controls key virulence traits of *Acinetobacter baumannii*. *Virulence*, *10*(1), 68–81. https://doi.org/10.1080/21505594.2018.1558693

Wright, P. R., Georg, J., Mann, M., Sorescu, D. A., Richter, A. S., Lott, S., Kleinkauf, R., Hess, W. R., & Backofen, R. (2014). CopraRNA and IntaRNA: predicting small RNA targets, networks and interaction domains. *Nucleic Acids Research*, *42*(W1), W119–W123. https://doi.org/10.1093/nar/gku359

Xie, F., Li, G., Zhang, Y., Zhou, L., Liu, S., Liu, S., & Wang, C. (2016). The Lon protease homologue LonA, not LonC, contributes to the stress tolerance and biofilm formation of *Actinobacillus pleuropneumoniae*. *Microbial Pathogenesis*, *93*, 38–43. https://doi.org/10.1016/j.micpath.2016.01.009

Yang, X., Becker, T., Walters, N., & Pascual, D. W. (2006). Deletion of znuA virulence factor attenuates *Brucella abortus* and confers protection against wild-type challenge. *Infection and Immunity*, *74*(7), 3874–3879. https://doi.org/10.1128/IAI.01957-05

Yuan, F., Liao, Y., You, W., Liu, Z., Tan, Y., Zheng, C., BinWang, Zhou, D., Tian, Y., & Bei, W. (2014). Deletion of the *znuA* virulence factor attenuates *Actinobacillus pleuropneumoniae* and confers protection against homologous or heterologous strain challenge. *Veterinary Microbiology*, *174*(3), 531–539. https://doi.org/https://doi.org/10.1016/j.vetmic.2014.10.016

Supplementary material

Supplementary Table 1 | Potential mRNA targets of the Rna01 predicted by TargetRna2 and CopraRna in *Actinobacillus pleuropneumoniae*.

TargetRNA2

Target	Locus on MIDG2331	Energy	P-value	Description
lon	MIDG2331_RS01940	-19.62	0.000	Lon protease
rarD	MIDG2331_RS05305	-13.5	0.003	Thiosulfate sulfurtransferase
ppiB	MIDG2331_00946	-10,77	0,016	Peptidyl-prolyl cis-trans isomerase
murQ	MIDG2331_RS08355	-10.41	0.019	N-acetylmuramic acid 6-phosphate etherase
dppA2	MIDG2331_00067	-10,15	0,022	ABC transporter substrate-binding protein
xseB	MIDG2331_RS04060	-9.74	0.027	Exodeoxyribonuclease 7 small subunit
fhuA	MIDG2331_02245	-9,66	0,028	TonB-dependent siderophore receptor
malK	MIDG2331_RS06255	-9.58	0.029	Maltose/maltodextrin import ATP-binding protein MalK
cysQ	MIDG2331_RS06740	-9.57	0.029	3'(2'),5'-bisphosphate nucleotidase CysQ
cas1f	MIDG2331_RS01085	-9.27	0.033	CRISPR-associated endonuclease Cas1
exbB1	MIDG2331_01754	-9,13	0,035	MotA/TolQ/ExbB proton channel family protein
ompP2B	MIDG2331_00658	-9,09	0,036	porin
tolR	MIDG2331_RS01555	-9.05	0.036	Tol-Pal system protein TolR
lamB	MIDG2331_01276	-8,96	0,038	maltoporin
rplR	MIDG2331_RS09745	-8.89	0.039	50S ribosomal protein L18
ispC	MIDG2331_RS02090	-8.79	0.041	1-deoxy-D-xylulose 5-phosphate reductoisomerase
purE	MIDG2331_RS03280	-8.77	0.041	N5-carboxyaminoimidazole ribonucleotide mutase
moeB	MIDG2331_RS01610	-8.69	0.042	Molybdopterin-synthase adenylyltransferase

CopraRna

Target	Locus on MIDG2331	Fdr	P-value	Description
malE	MIDG2331_RS06260	0,090615546	0,000183598	maltose/maltodextrin ABC transporter substrate-binding protein MalE
bioB	MIDG2331_RS00605	0,090615546	0,000186356	biotin synthase
accC	MIDG2331_RS10255	0,180388642	0,000463724	acetyl-CoA carboxylase biotin carboxylase subunit
aroQ	MIDG2331_RS10240	0,186751572	0,000714664	3-dehydroquinate dehydratase
pssA	MIDG2331_RS00215	0,186751572	0,000779764	phosphatidylserine synthase
hemD	MIDG2331_RS05130	0,186751572	0,000942524	uroporphyrinogen-III synthase
yedF	MIDG2331_RS10805	0,186751572	0,001027049	SirA-like protein
ubiD	MIDG2331_RS07875	0,186751572	0,001056179	4-hydroxy-3-polyprenylbenzoate decarboxylase
mtgA	MIDG2331_RS02450	0,273161438	0,001966201	monofunctional biosynthetic peptidoglycan transglycosylase
asd	MIDG2331_RS00025	0,323193418	0,002658661	aspartate-semialdehyde dehydrogenase
lctP	MIDG2331_RS02310	0,337316752	0,00295043	L-lactate permease
plpB	MIDG2331_RS04595	0,337316752	0,003282774	methionine ABC transporter substrate-binding protein MetQ
znuA	MIDG2331_RS07880	0,337316752	0,003295125	zinc ABC transporter substrate-binding protein
sufE	MIDG2331_RS06570	0,368974332	0,004190709	Derived by automated computational analysis using gene prediction method: Protein Homology.
argB	MIDG2331_RS01235	0,368974332	0,004363193	acetylglutamate kinase
fdnI	MIDG2331_RS04515	0,409768106	0,005056264	formate dehydrogenase subunit gamma
murF	MIDG2331_RS00070	0,455255302	0,006085674	UDP-N-acetylmuramoyl-tripeptide--D-alanyl-D- alanine ligase
mltA	MIDG2331_RS04100	0,457230577	0,006379401	murein transglycosylase A
hybE	MIDG2331_RS06855	0,457230577	0,006731636	hydrogenase
sucD	MIDG2331_RS02330	0,457230577	0,006817319	succinate--CoA ligase subunit alpha
pheT	MIDG2331_RS02930	0,492356498	0,008100466	phenylalanine--tRNA ligase subunit beta

Supplementary Table 2 | Potential mRNA targets of the Rna01 manually predicted in *Actinobacillus pleuropneumoniae*.

Target	Locus on MIDG2331	Energy (kcal/mol)	Description
MIDG2331_00243	MIDG2331_00243	-10.78	putative lipoprotein
nrfB	MIDG2331_00104	-5.14	nitrate reductase, cytochrome-C type protein
omlA	MIDG2331_01204	-4.92	outer membrane lipoprotein A precursor
comEA	MIDG2331_01571	-6.16	DNA uptake protein-binding protein
phoR_2	MIDG2331_01297	-6.24	phosphate regulon sensor protein
phoB	MIDG2331_01298	-7.63	phosphate regulon transcriptional regulatory protein
rpoH	MIDG2331_02050	-5.92	RNA polymerase sigma-32 factor
MIDG2331_00952	MIDG2331_00952	-9.15	TPR repeat-containing protein
exbD2	MIDG2331_00080	-5.99	biopolymer transport protein
potD2	MIDG2331_00385	-7.97	spermidine/putrescine-binding periplasmic protein
lsgD	MIDG2331_01068	-7.79	glycosyltransferase involved in LPS biosynthesis
lolB	MIDG2331_00799	-5.47	outer membrane lipoprotein LolB
acrA2	MIDG2331_00863	-6.2	membrane-fusion protein
lpp	MIDG2331_00037	-6.56	outer membrane lipoprotein
MIDG2331_01099	MIDG2331_01099	-6.3	NirD/YgiW/YdeI family stress tolerance protein
ompD	MIDG2331_00430	-6.99	outer membrane protein D-15
degP	MIDG2331_01359	-6.91	periplasmic serine protease
tadE	MIDG2331_00535	-10.46	tight adherence protein E
ompP2B	MIDG2331_00658	-9,09	outer membrane protein P2-like protein
MIDG2331_00918	MIDG2331_00918	-6.92	YdgA family protein
lamB	MIDG2331_01276	-8,96	maltoporin
MIDG2331_01616	MIDG2331_01616	-9.41	thioredoxin-like protein
fhuA	MIDG2331_02245	-9,66	outer membrane ferric hydroxamate receptor
ompW	MIDG2331_01124	-12.55	outer membrane protein ompW precursor
momP2	MIDG2331_02079	-6.98	major outer membrane protein
rbsB1	MIDG2331_01591	-10.54	periplasmic sugar-binding protein
dsbE2	MIDG2331_01091	-10.06	putative thiol:disulfide interchange protein
cas1f	MIDG2331_00220	-9.27	CRISPR-associated protein
rbsD	MIDG2331_01859	-10.57	high affinity ribose transport protein
ompP2A2	MIDG2331_00006	-11.76	outer membrane protein P2

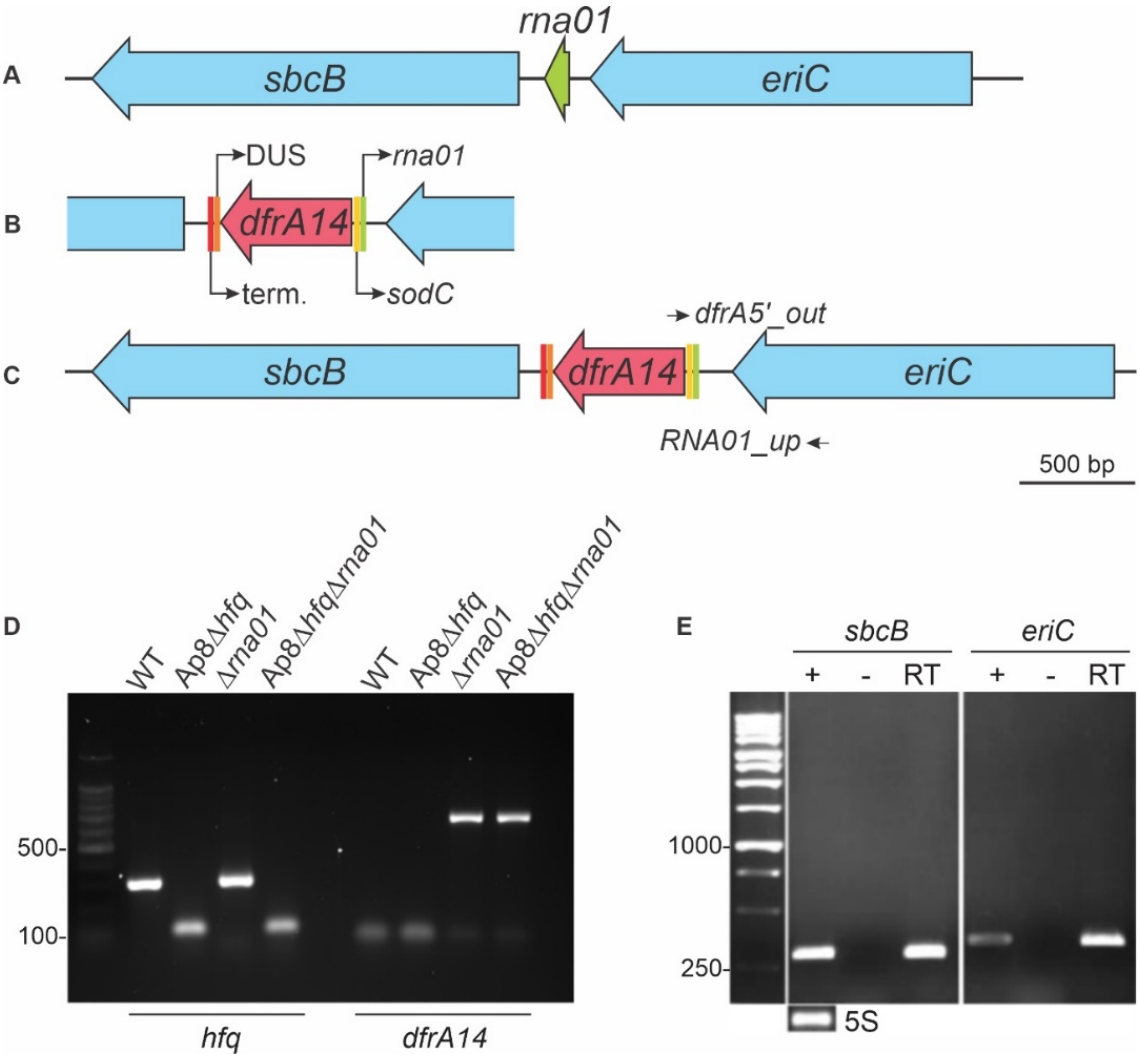

Supplementary Figure 1 | Construction and confirmation of *A. pleuropneumoniae* Rna01 mutant strains. The original sequences of the *rna01* gene in MIDG2331 (WT) and Ap8Δ*hfq* strains (A) were replaced by a cassette containing the trimethoprim resistance gene *dfrA14*, controlled by the *sodC* promoter sequence, followed by a DNA uptake sequence (DUS) and a terminator (term.) (B), flanked by 500 bp of the genes *scbB* and *eriC* (C). The Rna01 and *hfq* single and double mutants were confirmed by PCR to detect the absence of *hfq* and presence of *dfrA14*, in the corresponding strains (D). The maintenance of expression of *rna01*'s flanking genes *sbcB* and *eriC* in the Δ*rna01* strains (RT) was verified by RT-PCR (E) Total DNA free-RNA isolated from the WT strain subjected to cDNA synthesis of untreated were used as positive (+) and negative (-) controls.

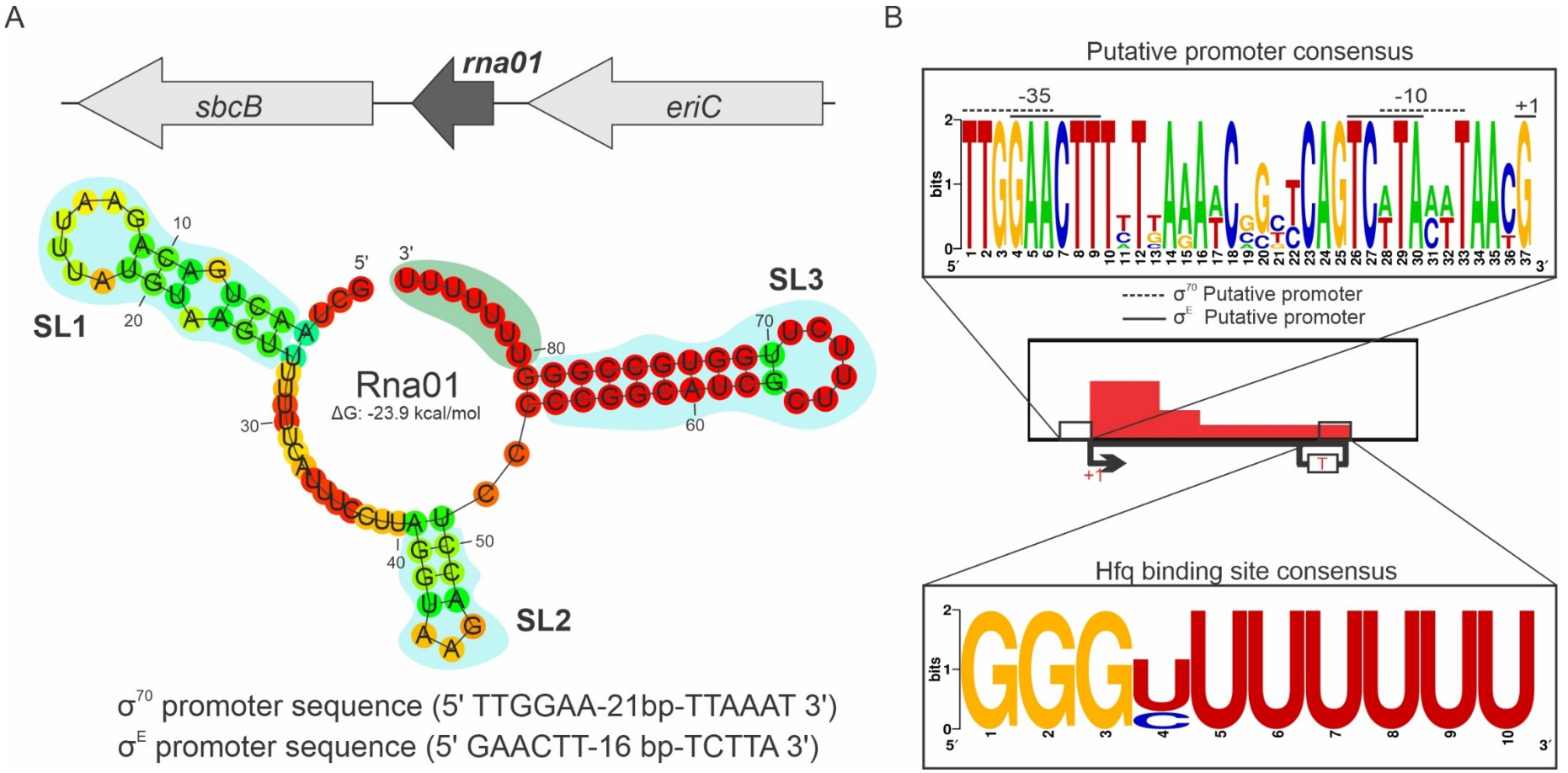

Supplementary Figure 2 | Characterization of the Rna01. (A) analysis of secondary structure and promoter of Rna01. The blue and green shades represent the stem loops (SLs) and Hfq binding site, respectively. (B) Conservation of Rna01's putative Hfq-binding site and promoters' regions.

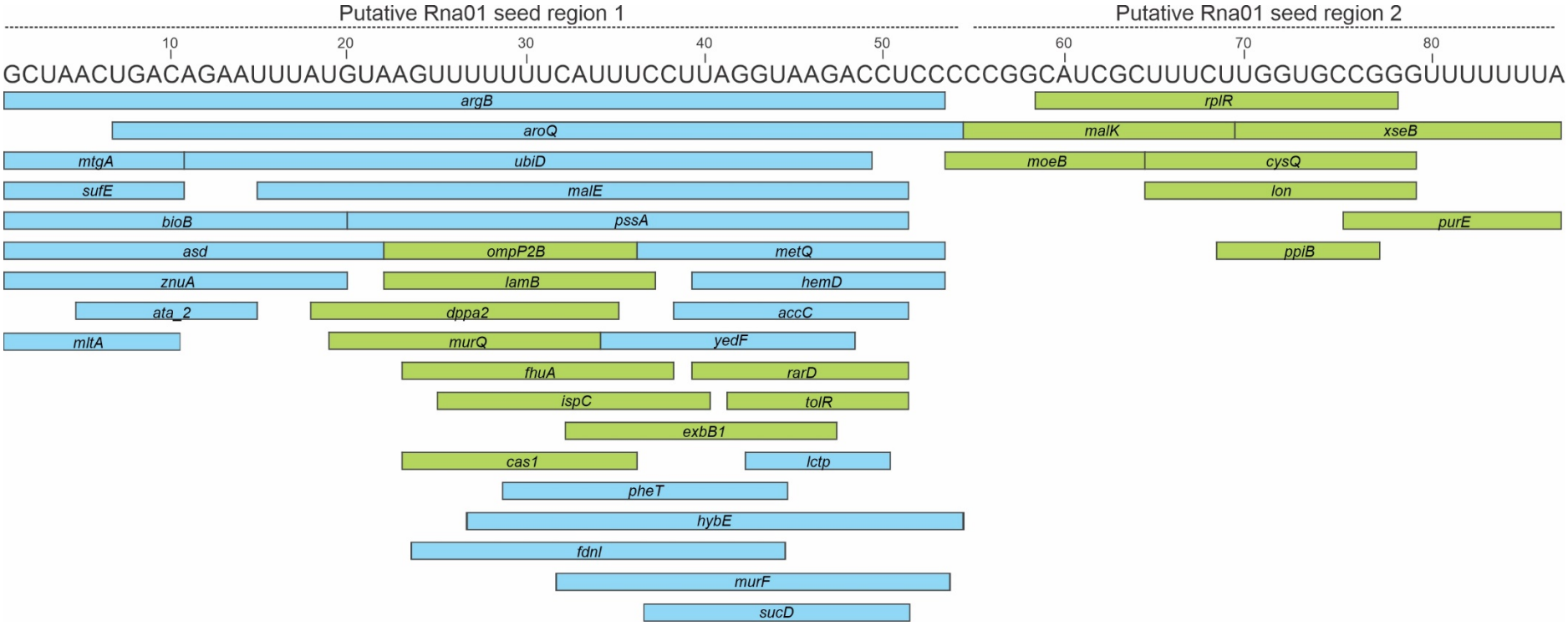

Supplementary Figure 3 | Putative "seed" region of Rna01' targets. Target prediction by TargetRNA2 and CopraRna shows the putative region of interaction between Rna01 and its targets. Targets predicted by TargetRNA2 are shown in green and targets predicted by CopraRna, in blue.

Supplementary Figure 4 | RNA-RNA interaction between Rna01 and respective targets. Putative region of interaction of the seed region 1 (A) and seed region 2 (B) of the Rna01 and the mRNAs targets. Targets predicted by TargetRNA2 are shown in green and targets predicted by CopraRna, in blue.

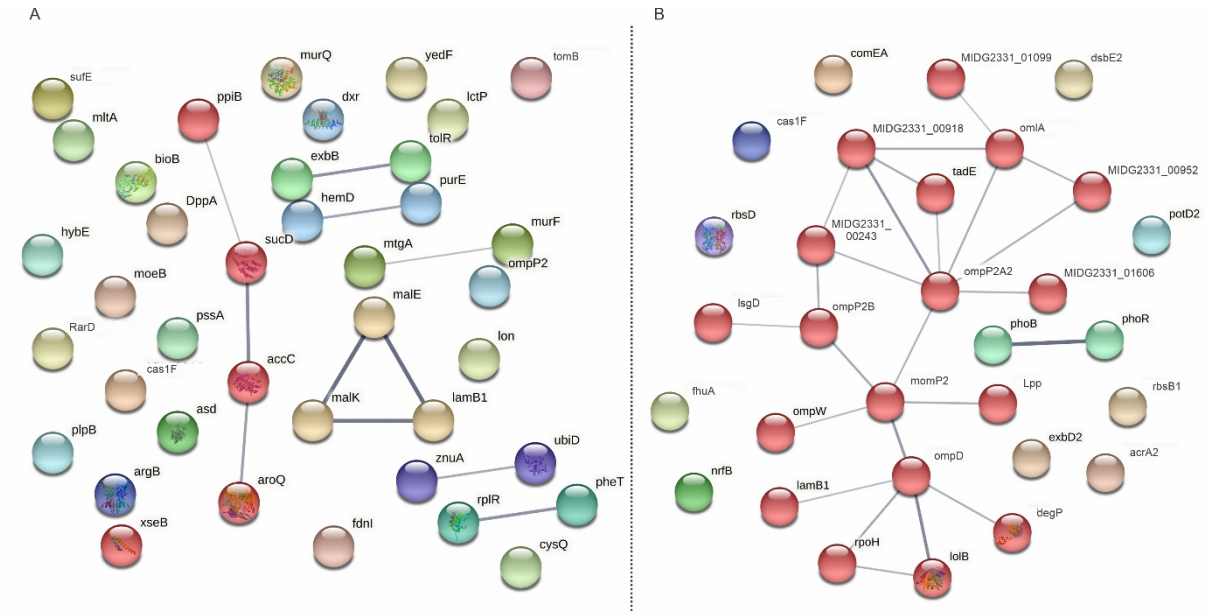

Supplementary Figure 5 | Protein-protein associations predicted by STRING for the Rna01 targets. (A) Software predicted targets of Rna01. (B) Manually predicted targets for the Rna01. Grey lines represent protein-protein associations, and their thickness indicates the strength of data support. Associations are meant to be specific and meaningful, for example, proteins that jointly contribute to a shared function. Genes were analyzed with a moderate confidence 0.400 and Markov clustering method (MCL) with inflation parameter 1.1. Associated proteins share color of the network.

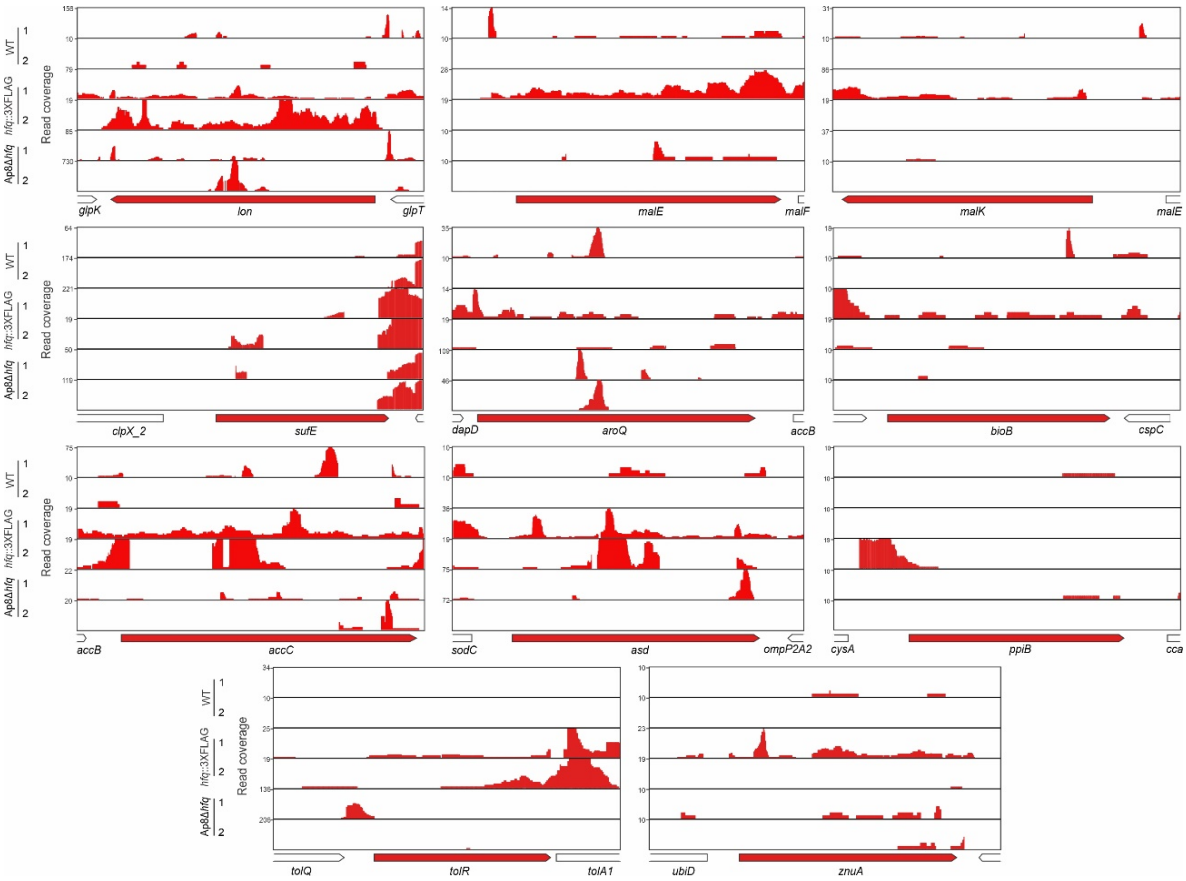

Supplementary Figure 6 | Identification of the mRNA targets of Rna01 in the RNAseq data. Mapping regions of the targets of Rna01 associated with phenotype results obtained in the phenotypic analysis. Reads for the genes *lon*, *malE*, *malK, sufE, aroQ, bioB, accC, asd, ppiB, tolR* and *znuA* genes are shown for the WT, Ap8*hfq*::3XFLAG and Ap8Δ*hfq* strains in aerobiosis (1) and anaerobiosis (2).

Supplementary table 3 | Pairwise comparisons of the log-hank test of *G. mellonella* infection assay with *A. pleuropneumoniae* strains

Comparisons	P-Value	Significant?
Ap8WT vs. PBS	0,000000409	Yes
Ap8WT vs. Ap8Δ*hfq*	0,00000409	Yes
Ap8WT vs. Ap8Δ*hfq*Δ*rna*01	0,0000915	Yes
Ap8WT vs. Ap8Δ*rna*01	0,0136	Yes
Ap8Δ*rna*01 vs. PBS	0,0153	Yes
Ap8Δ*rna*01 vs. Ap8Δ*hfq*	0,0667	No
Ap8Δ*hfq*Δ*rna*01 vs. PBS	0,277	No
Ap8Δ*rna*01 vs. Ap8Δ*hfq*Δ*rna*01	0,288	No
Ap8Δ*hfq* vs. Ap8Δ*hfq*Δ*rna*01	0,520	No
Ap8Δ*hfq* vs. PBS	0,317	No

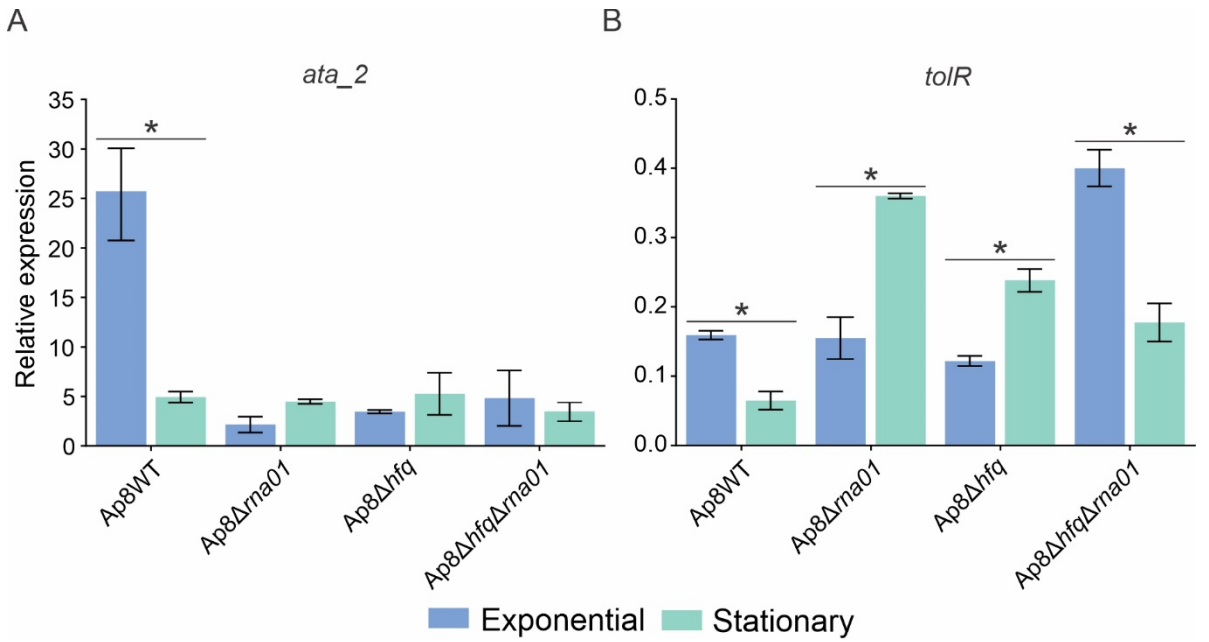

Supplementary Figure 7 | Targets expression are affected by Rna01. qPCR of *ata_2* (A) and *tolR* (B) targets in exponential and stationary phase among the strains. Significative difference between Cells and BEVs is represented by "*" by t-test ($p<0.1$).

Supplementary table 4 | Pairwise comparisons of the log-hank test of *G. mellonella* infection assay with BEVs from *A. pleuropneumoniae* strains

Comparisons	P-Value	Significant?
Ap8Δ*rna*01 vs. Ap8Δ*hfq*	0,00000495	Yes
Ap8WT vs. Ap8Δ*rna*01	0,0000175	Yes
Ap8Δ*rna*01 vs. Ap8Δ*hfq*Δ*rna*01	0,000305	Yes
Ap8Δ*rna*01 vs. PBS	0,000839	Yes
Ap8Δ*hfq*Δ*rna*01 vs. PBS	0,619	No
Ap8Δ*hfq* vs. Ap8Δ*hfq*Δ*rna*01	0,592	No
Ap8WT vs. PBS	0,777	No
Ap8WT vs. Ap8Δ*hfq*Δ*rna*01	0,765	No
Ap8Δ*hfq* vs. PBS	0,729	No
Ap8WT vs. Ap8Δ*hfq*	0,559	No

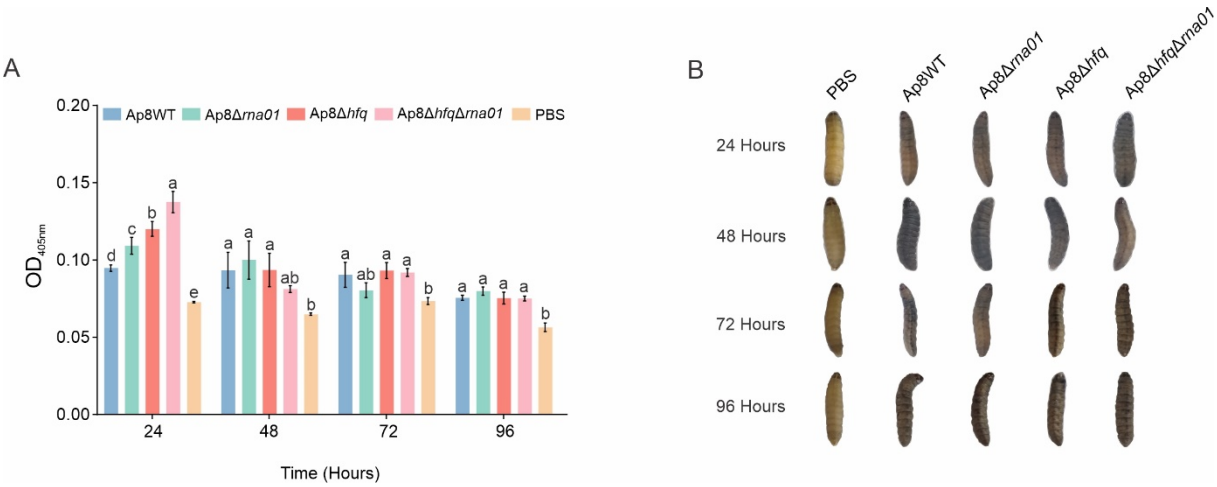

Supplementary Figure 8 | Extracellular vesicles cause strong melanization in *G. mellonella*. (A) optical density of larval hemolymph post-infection. (B) visual observation of larval melanization through the course of the experiment. Means with different letters are significantly different by Tuckey's test ($p<0.05$).

Final conclusions

In this work, we revealed the importance of mobile genetic elements in the dissemination of resistance genes in Pasteurellaceae, in addition we reinforced that bioinformatics analyses aimed at investigating resistance genes can help to the better understanding of AMR evolution and dissemination in the Pasteurellaceae. Also, we characterized the BEVs produced by *A. pleuropneumoniae*, bringing new information about some aspects so far not investigated and expanding what is already known about these vesicles, providing a new perspective on its importance and function in *A. pleuropneumoniae*. Furthermore, we described, for the first time, the RNA content of extracellular vesicles produced by *A. pleuropneumoniae* and we expanded the possibilities in the knowledge regarding the host-pathogen interaction for the specie. Moreover, we characterized, for the first time, the function of a small RNA to *A. pleuropneumoniae*, which showed to be associated with stress response and extracellular vesicles production. These findings reinforced how diverse the mobile elements can be in Pasteurellaceae in addition to their great importance regarding the transported gene content. This study also revealed the potential of functions of the vesicles produced by *A. pleuropneumoniae*, bringing a new perspective on the behavior of this specie in the environment and in the host.